



Fakulta rybnářství
a ochrany vod
Faculty of Fisheries
and Protection
of Waters

Jihočeská univerzita
v Českých Budějovicích
University of South Bohemia
in České Budějovice



Fakulta rybnářství
a ochrany vod
Faculty of Fisheries
and Protection
of Waters

Jihočeská univerzita
v Českých Budějovicích
University of South Bohemia
in České Budějovice

2022

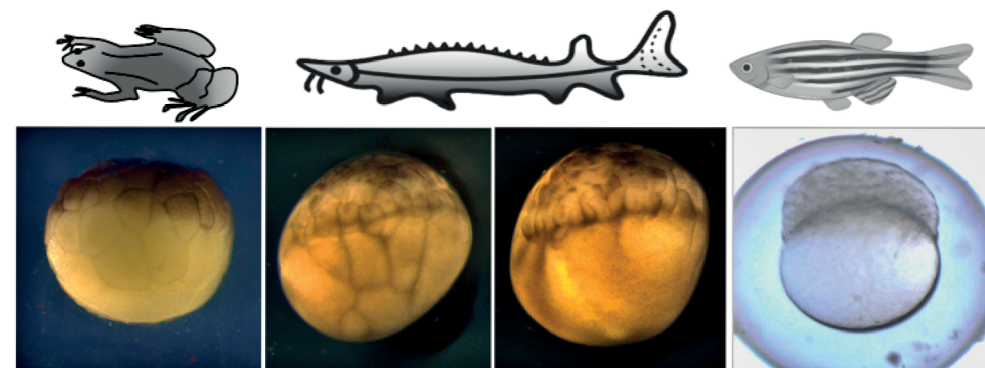


Doctoral thesis

Sturgeon (*Acipenser*) represents the evolutionary transition from the holoblastic to meroblastic cleavage pattern and unique gut development

Jeseter (*Acipenser*) představuje evoluční přechod od holoblastického k meroblastickému rýhování a unikátní způsob vývoje střeva.

Sturgeon (*Acipenser*) represents the evolutionary transition from the holoblastic to meroblastic cleavage pattern and unique gut development



Doctoral thesis by
Mujahid Ali Shah

Mujahid Ali Shah



Fakulta rybnářství
a ochrany vod
Faculty of Fisheries
and Protection
of Waters

Jihočeská univerzita
v Českých Budějovicích
University of South Bohemia
in České Budějovice

Sturgeon (*Acipenser*) represents the evolutionary transition from the holoblastic to meroblastic cleavage pattern and unique gut development

Jeseter (*Acipenser*) představuje evoluční přechod od holoblastického k meroblastickému rýhování a unikátní způsob vývoje střeva

Doctoral thesis by Mujahid Ali Shah

I, Mujahid Ali Shah, thereby declare that I wrote the Ph.D. thesis myself using results of my own work or collaborative work of me and colleagues and with help of other publication resources which are properly cited.

I hereby declare that, in accordance with the § 47b Act No. 111/1998 Coll., as amended, I agree with publicizing of my Ph.D. thesis in full version electronically in a publicly accessible part of the STAG database operated by the University of South Bohemia in České Budějovice on its web sites, with keeping my copyright to the submitted text of this Ph.D. thesis. I also agree so that the same electronic way, in accordance with above mentioned provision of the Act No. 111/1998 Coll., was used for publicizing reviews of supervisor and reviewers of the thesis as well as record about the progress and result of the thesis defence. I also agree with compering the text of my Ph.D. thesis with a database of theses "Theses.cz" operated by National Register of university theses and system for detecting of plagiarisms.

In Vodňany 2nd May, 2022

Supervisor:

Assoc. Prof. Martin Pšenička
University of South Bohemia in České Budějovice (USB)
Faculty of Fisheries and Protection of Waters (FFPW)
Research Institute of Fish Culture and Hydrobiology (RIFCH)
Zátiší 728/II, 389 25 Vodňany, Czech Republic

Consultant:

Xuan Xie, Ph.D.
University of South Bohemia in České Budějovice (USB)
Faculty of Fisheries and Protection of Waters (FFPW)
Research Institute of Fish Culture and Hydrobiology (RIFCH)
Zátiší 728/II, 389 25 Vodňany, Czech Republic

Head of Laboratory of Germ Cells:

Assoc. Prof. Martin Pšenička

Dean of Faculty of Fisheries and Protection of Waters:

Prof. Pavel Kozák

Board of doctorate study defence with reviewers:

Prof. Lukáš Kalous – head of the board
Prof. Petr Ráb – board member
Assoc. Prof. Pavel Horký – board member
Assoc. Prof. Jiří Patoka – board member
Assoc. Prof. Martin Kocour – board member
Assoc. Prof. Tomáš Polícar – board member
Assoc. Prof. Zdeněk Adámek – board member

Prof. Etsuro Yamaha, Field Science Center for Northern Biosphere, Hokkaido University, Japan – thesis reviewer
Assoc. Prof. Vladimír Krylov, Charles University, Praha – thesis reviewer

Date, hour and place of Ph.D. defence:

15th September 2022 at 10.15 a.m. in USB, FFPW, RIFCH, Vodňany, Czech Republic

Name: Mujahid Ali Shah

Title of thesis:

Sturgeon (*Acipenser*) represents the evolutionary transition from the holoblastic to meroblastic cleavage pattern and unique gut development

Jeseter (*Acipenser*) představuje evoluční přechod od holoblastického k meroblastickému rýhování a unikátní způsob vývoje střeva

Ph.D. thesis, USB FFPW, RIFCH, Vodňany, 2022, 104 pages, with the summary in English and Czech.

ISBN 978-80-7514-160-6

Graphic design & technical realisation: Tiskárna Brázda, www.TiskarnaBrazda.cz

CONTENT

CHAPTER 1

5

General introduction

CHAPTER 2

31

Novel technique for definite blastomere inhibition and distribution of maternal RNA in sterlet *Acipenser ruthenus* embryo

CHAPTER 3

47

Blastomeres derived from the vegetal pole provide extra-embryonic nutrition to sturgeon (*Acipenser*) embryos: transition from holoblastic to meroblastic cleavage

CHAPTER 4

65

The gut development of sturgeon is unique among vertebrates: A comparative study

CHAPTER 5

85

General discussion

87

English summary

97

Czech summary

99

Acknowledgements

101

List of publications

102

Training and supervision plan during study

103

Curriculum vitae

104

CHAPTER 1

GENERAL INTRODUCTION

1. Introduction

1.1. Embryo cleavage

The first developmental axis formed during the oogenesis is called animal-vegetal and can be distinguished in every animal species. The animal part of the oocyte contains a germinal vesicle (oocyte nucleus), whereas the vegetal region stores yolk. The zygote – a fertilized biological cell – is formed by the fusion of oocyte and sperm pronuclei, which undergoes a series of synchronized mitotic cell divisions in which the massive amount of cytoplasm in an egg is divided into many smaller nucleated cells, a process known as cleavage (Gilbert, 2010).

For vertebrate developmental events such as gastrulation, organogenesis, and overall body plan formation, early divisions of embryonic cells are very critical. Therefore, studying vertebrate development requires understanding these early cell divisions and the mechanisms that produce them. There are two main types of cleavage patterns, which are determined primarily by the concentration of yolk in the egg: 1) holoblastic (complete) cleavage, which occurs mostly in amphibians, mammals, and chondrosteans and is thought to be ancestral for vertebrates; and 2) meroblastic (incomplete/partial) cleavage, which evolved in birds, reptiles, and teleost fishes (Hasley et al., 2017).

1.1.1. Holoblastic cleavage

The entire egg is cellularized through holoblastic cleavage, and yolk platelets are either absent (as in mammals) or present as cytoplasmic inclusions that partition across cells (as in amphibians and chondrosteans). Cleavage covers an area of the embryo, from the animal pole (AP) to the vegetal pole (VP) (Hasley et al., 2017). Currently, the embryos of the African clawed frog – *Xenopus laevis* (amphibian) – are regarded as a model to study the holoblastic cleavage pattern. The embryos of *X. laevis* have certain specific characteristics, including the following 1) The AP of the egg generally contains determinants for ectoderm formation, while mesoderm is developed in the equatorial position and endoderm from the VP (Horb and Slack, 2001; Yasuo and Lemaire, 2001). The VP stores the majority of fate determinants, such as mesendodermal and germplasm, during early embryogenesis, indicating its importance. 2) Because of the unequal distribution of yolk, cleavage produces blastomeres with increased yolk volume towards the VP. 3) During blastulation, the embryo forms the blastocoels, which separate the ectoderm from the endoderm and allow cell migration during gastrulation; 3) the formation of morphologically “bottle cells” that initiate cell involution via the blastopore dorsal lip; 4) the formation of the archenteron (primary gut) caused by the said cell involution; and 5) an increase in the amount of yolk stored in the VP and used intracellularly (Collazo et al., 1994; Gilbert, 2010) (Figure 1).

1.1.2. Meroblastic cleavage

In meroblastic cleavage, cell division does not divide the embryo completely. Instead, embryonic cells divide in the AP without the vegetally located yolk, with cells typically remaining syncytial to the yolk cell for a period of time that varies by species (Hasley et al., 2017). For example, in teleost (e.g., in zebrafish), eggs have an uncleaved yolk mass. Although yolk mass provides the nutrition and some maternally deposited determinants for embryonic patterning and primordial germ cells (PGCs), however, it does not form any embryonic layer.

During the early cleavage phase, the embryo develops the yolk streams to transport the maternal determinants from the yolk to the AP. The AP of the embryo is the only one that divides and produces a cluster of blastoderm-blastomeres (Mizuno et al., 1996; Maegawa et al., 1999). The blastoderm consists of a middle layer of deep cells and a multinucleate yolk syncytial layer (YSL) between the middle layer and the yolk. An external enveloping layer covers the blastoderm. The YSL is very important for embryonic patterning, morphogenetic movements, and metabolic/nutrient transportation (Chen and Kimelman, 2000; D'Amico and Cooper, 2001). Epiboly, or the spread of a cell sheet over the yolk, is the first critical morphogenetic process during gastrulation. Deep cells accumulate at the front edge of the vegetally expanding blastoderm as gastrulation progresses, causing the germ ring to thicken – the germ ring's deep cells form two layers of involution: epiblast and hypoblast. The epiblast leads to ectodermal cell lines, while the hypoblast contributes to the further development of the embryonic endoderm of the digestive tract (Gilbert, 2010) (Figure 2).

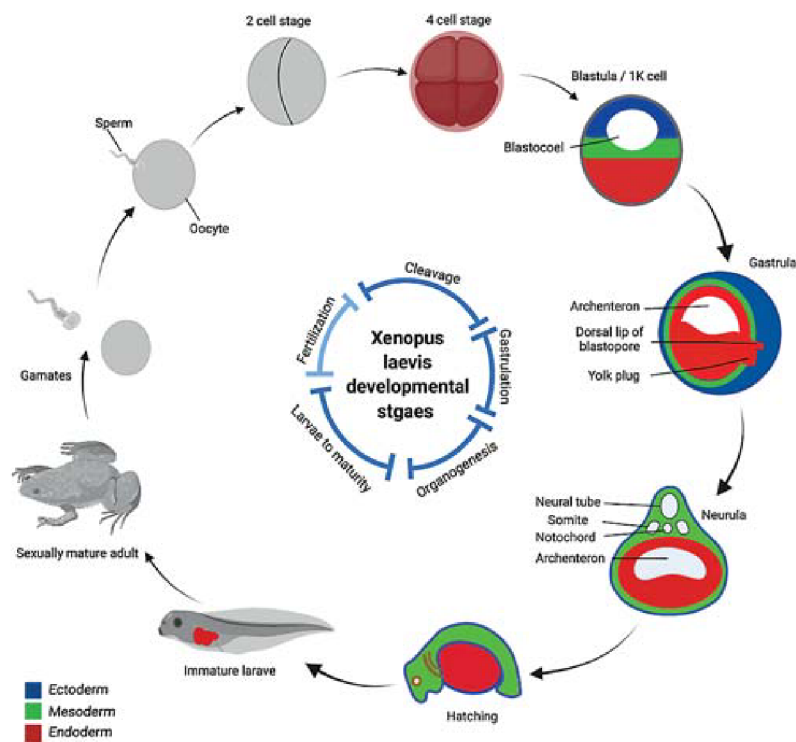


Figure 1. Pictorial diagram of *Xenopus laevis* (holoblastic) development pattern.

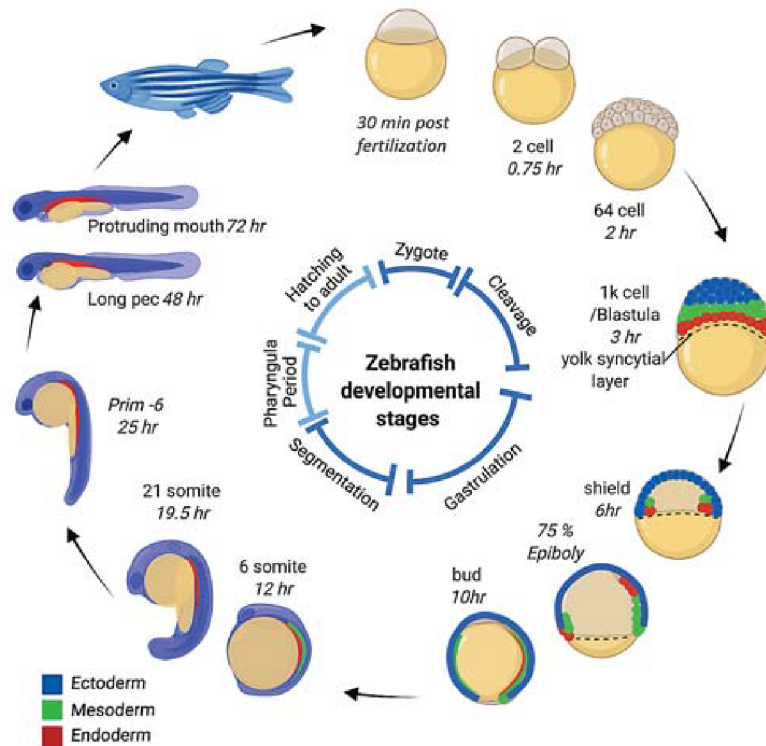


Figure 2. Pictorial diagram of zebrafish (meroblastic) development pattern.

1.2. Evolution of meroblastic cleavage and sturgeon (*Acipenser*)

The evolution of meroblastic cleavage has occurred at least five times within the lineages of vertebrates, including hagfish, elasmobranchs, coelacanth, amniotes and teleosts. The bony fish (*Osteichthyes*) are classified into two major classes: Ray-finned fish (*Actinopterygii*) and lobe-finned fish (*Sarcopterygii*). Tetrapods (including amphibians, birds, reptiles and mammals) are presumed to have evolved from the *Sarcopterygii* lineage. Amphibians and mammals (except monotremes) have holoblastic cleavage, whereas birds and reptiles embryos have meroblastic cleavage (Figure 3) (Collazo et al., 1994; Elinson, 2009). After it diverged, the actinopterygian lineage (e.g., teleost taxon 33,000 species) developed meroblastic cleavage. Whole-genome duplication occurs in teleosts, and as a result, their genomes have been altered (Chiu et al., 2004; Ravi and Venkatesh, 2008; Glasauer and Neuhauss, 2014; Pasquier et al., 2016).

Non-teleost fishes like bichir (*Polypterus*), sturgeon (*Acipenser*), gar (*Lepisosteus*), and bowfin (*Amia*) diverged from the teleost lineage before WGD because their embryogenesis retained some archaic characteristics. Unlike the teleost, bichir and sturgeon retained the holoblastic cleavage pattern as amphibians (*X. laevis*) (Bolker, 1993, 1994; Inoue et al., 2003; Kikugawa et al., 2004; Hurley et al., 2007; Takeuchi et al., 2009a, b). On the other hand, closely related groups such as bowfin and gar retained intermediated morphologies between holoblastic and meroblastic cleavage patterns {Figure 3; (Ballard, 1986a,b; Long and Ballard, 2001)}. Once the meroblastic cleavage has evolved, it is very conserved in the group. The only exception is a reversal within the Amniota, a transition from meroblastic to holoblastic cleavage in therian mammals (Collazo et al., 1994). So far, several studies have accumulated numerous insights about the stem vertebrates of each lineage that had developed meroblastic cleavage. However, the role of non-teleost fishes (including bichir, sturgeon, gar, and bowfin) in the evolution of meroblastic cleavage in ray-finned fishes is still under investigation.

Sturgeons, also known as living fossils, are famous for their highly-valued caviar and meat (Friedrich, 2018). These archaic giants also received considerable attention in studying the origin and evolution of the species (Duong et al., 2013; Narum et al., 2013; Saito et al., 2014). For example, sturgeons belong to the chondrosteian species of the ray-finned-fish lineage and have existed for ~200 million years (mya) (Bemis et al., 1997). It has been reported that sturgeons share many aspects of development with Sarcopterygii lineage, e.g., *X. laevis* (Friedrich, 2018), For example, i) embryonic cleavage pattern (holoblastic) (Bolker, 1993), ii) germplasm specification (Saito et al., 2014), iii) morphogenesis during gastrulation (Bolker, 1993, 1994) and iv) distribution of some maternal mRNAs (Pocherniaieva et al., 2018). Importantly, sturgeons are phylogenetically placed between *X. laevis* and gar – closely related species that show transition towards meroblastic cleavage (Figure 3) (Long and Ballard, 2001; Takeuchi et al., 2009b).

This thesis chapter reviewed the several anuran and fish taxa representing the cleavage pattern transition (holoblastic to meroblastic). Here, our special attention has been paid to the embryogenesis of *X. laevis* – holoblastic and zebrafish – meroblastic, as well as their comparison with sturgeon – holoblastic, to better comprehend the following goals: 1) How does an increase in egg size or yolk content (symmetry of yolk deposition in relation to oocyte polarity, from AP to VP) influence cleavage pattern (Dettlaff et al., 1993; Buchholz et al., 2007; Takeuchi et al., 2009b)? 2) What the consequences of an increase in egg size and yolk volume were during the evolution, such as maternally supplied mRNA localization, 3) how PGCs' localized and migrated during the evolution of the cleavage pattern, and 4) whether the vegetal blastomeres of sturgeon (holoblastic) contributed the development as seen in *X. laevis*. 5) Furthermore, whether the sturgeon's gut development and use of the yolk are conserved to any vertebrate.

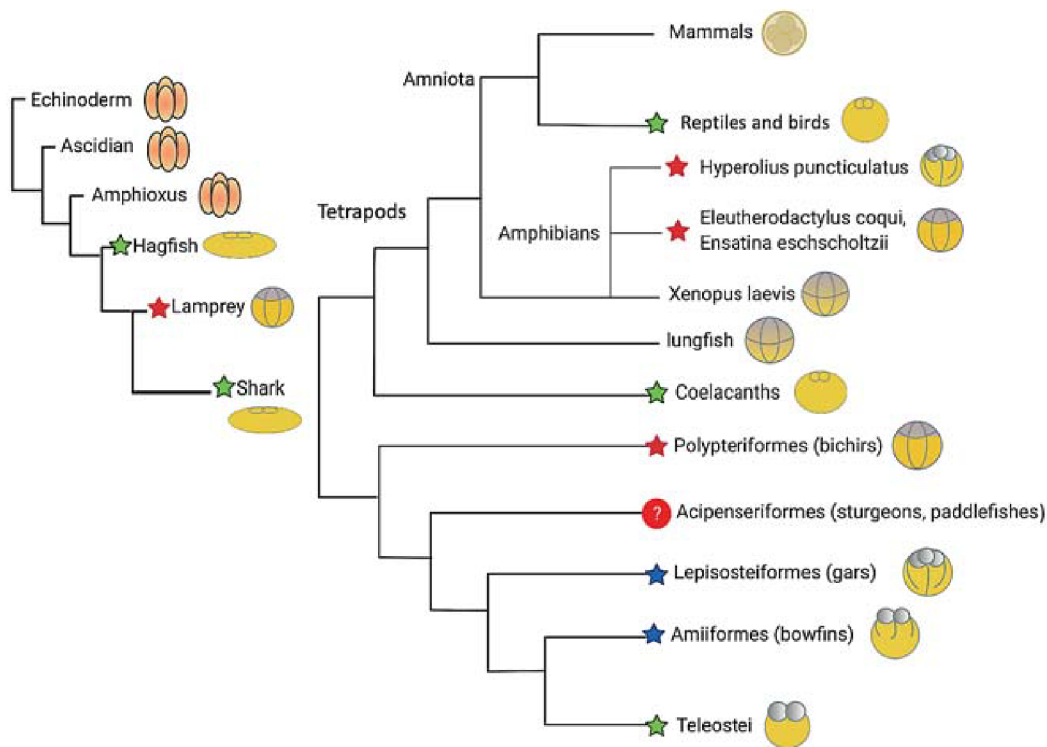


Figure 3. Evolution of meroblastic cleavage in vertebrate lineages.

Figure 3 illustrates the evolution of meroblastic cleavage according to the phylogenetic relationship of vertebrates. The groups without stars retained the ancient mode of cleavage pattern (holoblastic). Meroblastic cleavage evolved in vertebrates' lineages, indicated by the green stars. Blue stars show the transition phase between the holoblastic and meroblastic cleavage in ray-finned fishes. The red stars denote lineages retained holoblastic cleavage; however, their vegetal blastomeres are extra-embryonic as yolk sac of meroblastic cleaved embryos. Hypothetically, they represent the specific transition towards meroblastic cleavage. The question mark indicates the research gap – the vegetal blastomeres fate mapping in sturgeon embryos remains unknown, which may also show the specific transition phase as seen in *Eleutherodactylus coqui*, *Ensatina eschscholtzii*, bichir, and lamprey.

1.3. Egg size, yolk volume and the transition from holoblastic to meroblastic cleavage pattern

Based on previous studies, the distribution of yolk or egg size and has been identified as a crucial element in the transition of the egg cleavage pattern among tetrapods (Dettlaff et al., 1993; Elinson and Beckham, 2002; Buchholz et al., 2007; Elinson, 2009; Hasley et al., 2017). For example, in *X. laevis* embryos, the first and second cleavage plans are meridional. The first furrow appears at the AP and reaches VP, divides the egg into two complete portions (2-cell stage), followed by a second cleavage (4-cell stage). Subsequently, the third cleavage furrow is latitudinal/horizontal above the equator nearer the AP (8-cell stage). The latitudinal furrow affects all blastomeres uniformly. Eight blastomeres are formed as a result of this process. Four are in the VP (macromeres), and four are in AP (micromeres). Micromeres are much smaller than macromeres. The influence of yolk concentration in the VP causes for such macromeres (Klein, 1987; Gilbert, 2010). As cleavage progresses, the animal region becomes densely packed with numerous small cells. On the other hand, the vegetal region contains only a small number of large, yolk-laden macromeres, namely endodermal cells (yolky endoderm cells) (Gilbert, 2010).

In comparison, eggs of *Eleutherodactylus coqui* and *Ensatina eschscholtzii* have a diameter of 3.5 mm and 6 ± 0.43 mm, respectively, which are significantly larger than that of *X. laevis* (~1.0–1.3 mm) (Buchholz et al., 2007; Collazo and Keller, 2010). Owing to the yolk-rich vegetal region, the first few cleavage furrows in *E. coqui* and *E. eschscholtzii* appear to be different from *X. laevis*, such as cleavage initially occurs only in the AP, and limited number of furrows visible in the VP – 40-cell and 16-cell stage in *E. Coqui* and *E. eschscholtzii*, respectively. However, it is a holoblastic cleavage pattern and produces larger vegetal cells, namely nutritional yolk cells; YCs, rather than endodermal cells like *X. laevis*, (see heading 1.5) (Fang et al., 2000; Elinson and Beckham, 2002; Collazo and Keller, 2010). Following that, the first few cleavage furrows of *Hyperolius puncticulatus*' eggs (1.5–1.8 mm) do not reach the vegetal area, and cleavage mostly occurs at AP, resulting in the so-called pseudo meroblastic cleavage pattern. Thus, an increase in yolk volume (comprises approximately 75% of the area of a section through the embryo's A–V axis and is composed of significantly larger cells) is an appropriate example for such kind of cleavage pattern (Chipman et al., 1999).

Furthermore, the early development of *E. coqui* and *X. laevis* differs in several ways due to the volume of yolk. The fertilization in *X. laevis* is usually monospermic, whereas it can be polyspermic in *E. coqui*. Polyspermy is tolerated in large yolky eggs, such as those of birds (Elinson, 1986, 1987). In *E. coqui*, the blastopore lip arises closer to the AP than in *X. laevis* (Elinson and Fang, 1998; Ninomiya et al., 2001). The nutritional YCs derived from the VP of *E. coqui* do not contribute any germ layer formation, implying that the vegetal half is less active (see heading 1.5) (Buchholz et al., 2007).

The last common ancestor of amphibians and amniotes is thought to have had holoblastic cleavage (Figure 3). According to Elinson (2009), there could be two possibilities concerning the transition of holoblastic (amphibians) to meroblastic (amniotes) cleavage pattern: 1) They could have directly evolved meroblastic cleavage; or 2) two transitions were developing meroblastic cleavage among amniotes, one leading to the turtle-lizard-bird clade and another comprising monotreme (Collazo et al., 1994; Elinson, 2009). It has been suggested that the second possibility is improbable. On the other hand, increased egg yolk is usually linked to the evolution of the extra-embryonic membranes that define amniotes, and it could be an essential factor in their evolution (Collazo et al., 1994; Buchholz et al., 2007; Elinson, 2009).

In the case of fishes, it has been anticipated that an increased egg size and yolk content in the non-teleost fish eggs (bichir, sturgeon, gar, and bowfin) has altered the cleavage pattern and gastrulation (Dettlaff et al., 1993; Takeuchi 2009b). For example, compared to *X. laevis* (~1.0–1.3 mm), the eggs of bichir and sturgeon (2–3 mm) are significantly larger. Despite the varying size, fate mapping in *X. laevis*, bichir, sturgeon, and zebrafish embryos suggested those of bichir, sturgeon, and *X. laevis* share many similarities regard to cleavage pattern, blastulation and gastrulation {for details, see heading below 1.5 below; (Bolker, 1993, 1994; Pocherniaieva et al., 2018; Takeuchi et al., 2009a,b)}. However, due to the increased yolk mass toward the VP, the early cleavage patterns in sturgeon and bichir embryos are different from those of *X. laevis*.

For example, in bichir and sturgeon, the first cleavage divides the cytoplasm into two halves. The second cleavage furrow runs perpendicular to the first, across the center of the AP, and divides the egg into four roughly equal parts. Two clefts of the third division run parallel to the first, and eight blastomeres develop in the AP. The clefts have a limited depth. Because there is more yolk in the VP than in the AP, the separation depth in this part of the egg is lower. The fourth division produces an equatorial cleft that is irregular and located near the AP. A difference is caused by the concentration of the yolk and the delay in divisions of the VP (Diedhiou and Bartsch, 2009; Ostaszewska and Dabrowski, 2009). According to Dettlaff et al (1993), the AP of the egg contains a low concentration of small deutoplasmic inclusions, whereas the VP is densely packed with large yolk granules and lipid inclusions. Division of the vegetal blastomeres is much slower than that of the animal blastomeres, but it is completed in this region as well by the end of the cleavage period, owing to the abundance of yolk inclusions. As a result, the cleavage in sturgeon can be considered complete unequal cleavage (Dettlaff et al., 1993). Furthermore, similar to *E. coqui*, sturgeon fertilization can be polyspermic (Igorova et al., 2018; Elinson, 1987). Comparatively, sturgeon and bichir vegetal blastomeres' division produces massive amounts of YCs as in *E. coqui* (Buchholz et al., 2007; Takeuchi et al., 2009b). It was recently discovered that YCs of bichir are extra-embryonic, similar to *E. coqui*. However, it is unknown whether sturgeon YCs contribute to embryonic development or are extra-embryonic like bichir and *E. coqui* {see heading below 1.5 (Takeuchi et al., 2009b)}.

Following that, in closely related fishes, such as the egg size of gar (~3 mm) and bowfin (2.0 mm) is almost similar to bichir and sturgeon (2–3 mm). Gar and bowfin, on the hand, have a limited number of furrows towards VP – 2-cells and 12-cells in the VP of gar and bowfin, respectively. Bowfin has a holoblastic egg cleavage pattern, however, due to yolk-rich vegetal region, embryo produce about a dozen large yolky blastomeres (giant blastomeres that support the blastoderm's smaller cells), similar to *E. coqui*. Detailed fate mapping of the vegetal region in bowfin embryos, as well as comparisons with other taxa, have yet to be described. The cleavage in gars is meroblastic, which means that the furrows divide the blastoderm in a pattern similar to that of the teleost (Dean, 1895; Jaroszewska and Dabrowski, 2009; Long and Ballard, 2001). The majority of the yolk in the teleost egg, on

the other hand, remains uncleaved from the start, which is a significant difference between the early blastula of the gars and the teleosts {see heading 1.5; Figure 3–5 (Collazo et al., 1994; Kunz, 2004)}.

It has been reported that a likely derived form of holoblastic cleavage can be seen in the eggs of bichir and sturgeon. Select traits, such as varying degrees of reliance on egg nutrient stores, may link cleavage type and egg size in such cases (Buchholz et al., 2007; Collazo, 1996). Nevertheless, despite this enormous size, they still retain a holoblastic cleavage. We, therefore, speculate that increased yolk inclusions towards the VP led to the evolution of meroblastic cleavage in ray-finned fishes, as seen in the amphibian – *H. puncticulatus*’ and non-teleost fishes – gar and bowfin eggs (Chipman et al., 1999). Here, we raise one doubt: Can such nutritional YCs in these species (*E. eschscholtzii*, *E. coqui* and *H. puncticulatus*) represent a step toward the transition phase (holoblastic to meroblastic) towards the amniotes? If so, then theoretically, the transition would be in this way in fishes e, g., bichir > sturgeon > bowfin > gar > zebrafish (Figure 3–5). The current study was designed to investigate the fate of sturgeon vegetal blastomeres/YCs, which represent the transition of cleavage pattern from holoblastic to meroblastic in rays-finned fishes.

1.4. Egg size, yolk volume and RNA localization

The specification of the germ layer is one of the earliest developmental stages in metazoan, occurring before the development of the organ and tissue primordia that eventually become the complex adult organism. As the embryonic organism develops, the cells in the three basic germ layers – the ectoderm, mesoderm, and endoderm – differentiate into various lineages. The epidermis and nervous system are both produced by ectodermal cells. Blood, muscle, kidneys, notochord, and connective tissue are all developed by mesodermal cells. The gastrointestinal and respiratory tracts are formed by endodermal cells (Gilbert, 2010).

The development of fish and amphibian embryos occurs externally, and their rapid rate of early development ensures the rapid formation of independent larvae. Because yolk is a form of energy and maternal determinants (i.e., maternal protein) mediate the development of these embryos until the mid-blastula stage. Once zygotic transcription has been activated, many zygotic genes are incorporated into signal transduction pathways for germ layer patterning (Heasman et al., 1984; Kane and Kimmel, 1993; Rodaway et al., 1999). Recent comparative studies have documented widespread conservation of developmental genes between amphibians and fish. However, their expression patterns, functions, and epigenetic regulation have evolved despite preserving the genes. The same or closely related genes may have different functions in different contexts, either within the organism or between the species. The relative contribution and regulation of the zygotic and maternal genome vary between vertebrates, particularly the speed and pattern of early cleavages formation and, therefore, the morphology of the blastula (Solnica-Krezel, 2005; Pocherniaieva et al., 2018; Naraine et al., 2022). In this part, we have reviewed the function and localization pattern of maternally supplied mRNAs (including germplasm, endoderm and mesoderm genes) in *X. laevis* and zebrafish, as well as their comparison with sturgeon.

1.4.1. Localization of germplasm and migration of primordial germ cells

The germplasm contains maternal mRNAs from germline-specific genes. The asymmetric preservation of germplasm in the localized region of oocytes and the migration of PGCs differ between vertebrates (Gross-Thebing et al., 2017; Starz-Gaiano and Lehmann, 2001).

For example, in *X. laevis*, the yolk is unequally distributed – slightly increased toward the VP. The maternally supplied germplasm – *dnd*, *vas*, *grip2*, *dzl*, and *nanos1*, localized in a VP and specifying the fate of the PGCs. Compared with *X. laevis*-holoblastic, the germplasm of teleost-meroblastic, i.e., *vas*, *nanos1*, and *dnd*, is located in the animal hemisphere at the distal ends of the blastodisc's first and second cleavages. Moreover, DZL and *grip2* gradients are localized toward the oocyte vegetal region and migrate toward the AP via yolk streams {(Whittington and Dixon, 1975; Houston et al., 1998; Braat et al., 1999; Knaut et al., 2000; Köprunner et al., 2001; Miyake et al., 2006; Herpin et al., 2007; Kirilenko et al., 2008; Sindelka et al., 2010; Kitauchi et al., 2012; Lai et al., 2012; Pocherniaieva et al., 2018; Naraine et al., 2022) see Figure 4}. The early localization of DZL is conserved with *X. laevis* and involved in the PGCs' development. The localization of *grip2* occurs in the VP of *X. laevis* and sturgeon eggs, and it is considered a potential marker for PGCs development (Naraine et al., 2022). On the other hand, the same gene in zebrafish is also localized in the VP. It plays a crucial role in bundling microtubules at the vegetal cortex of embryos (Kirilenko et al., 2008).

Regarding PGCs' migration in holoblastic cleavage pattern (e.g., in *X. laevis*), the specified PGCs at the VP region are passively translocated to the endoderm's center, after which they begin active migration dorsally within the gut endoderm's ventral part, eventually reaching the dorsal wall of the body cavity and the gonadal ridge via the dorsal mesentery (Whittington and Dixon, 1975). Comparatively, in meroblastic cleavage pattern (e.g., in teleost), PGCs migrate from the marginal region of the blastodisc, the YSL in close proximity, and the presumed mesendodermal region at the blastula stage; these cells then migrate dorsally as the embryo develops (Köprunner et al., 2001; Saito et al., 2014). These cells migrate along the trunk mesoderm's border toward the region where the genital ridge will form during early somitogenesis (Braat et al., 1999; Theusch et al., 2006).

In comparison, the embryo of sturgeons is intermediated between zebrafish and *X. laevis* due to the increase in egg size and yolk volume (Miyake et al., 2006; Saito et al., 2014). For example, the localization of the germplasm in sturgeon embryos (e.g., *dnd*, *vas*, *grip2*, *dzl*, and *nanos*) occurs in the vegetal region as in *X. laevis* (amphibian); however, their migration pattern is conserved to that of teleost (Saito et al., 2014; Pocherniaieva et al., 2018; Naraine et al., 2022). It is thus interspecific between teleost and *X. laevis* embryos in terms of PGCs' localization and migration (Figure 4).

In sturgeon and *E. coqui*, it seems that the holoblastic cleavage remains unchanged due to germplasm localization in the VP and its inability to migrate to the AP during the cleavage phase (Elinson et al., 2011; Saito et al., 2014, 2018) (Figure 4). Comparatively, in *gar* – a closely related species – the VP does not undergo normal cleavage (Long and Ballard, 2001). Thus, *gar* has already overcome this problem, and there can be three possibilities: a) all the determinants moved to the AP already during oocyte maturation before embryogenesis; b) the determinants are in the vegetal hemisphere, then they have to be transported to the animal hemisphere by a mechanism similar to the yolk streams of teleost species; c) the PGC determination is controlled epigenetically like in mammals. The analysis of PGCs determinants in *gar* is expected to assess this hypothesis's feasibility further. Moreover, on the other hand, it is also possible to develop a potential technique for inhibiting vegetal blastomeres in sturgeon (shifting holoblastic to meroblastic cleavage pattern – mimic *gar* cleavage pattern) and investigate the detailed fate mapping of vegetal blastomeres such as analyzing the yolk stream and germplasm movement, and PGCs migration after inhibition of said blastomeres (Heading 1.6). Thus, we have investigated these goals in our present study.

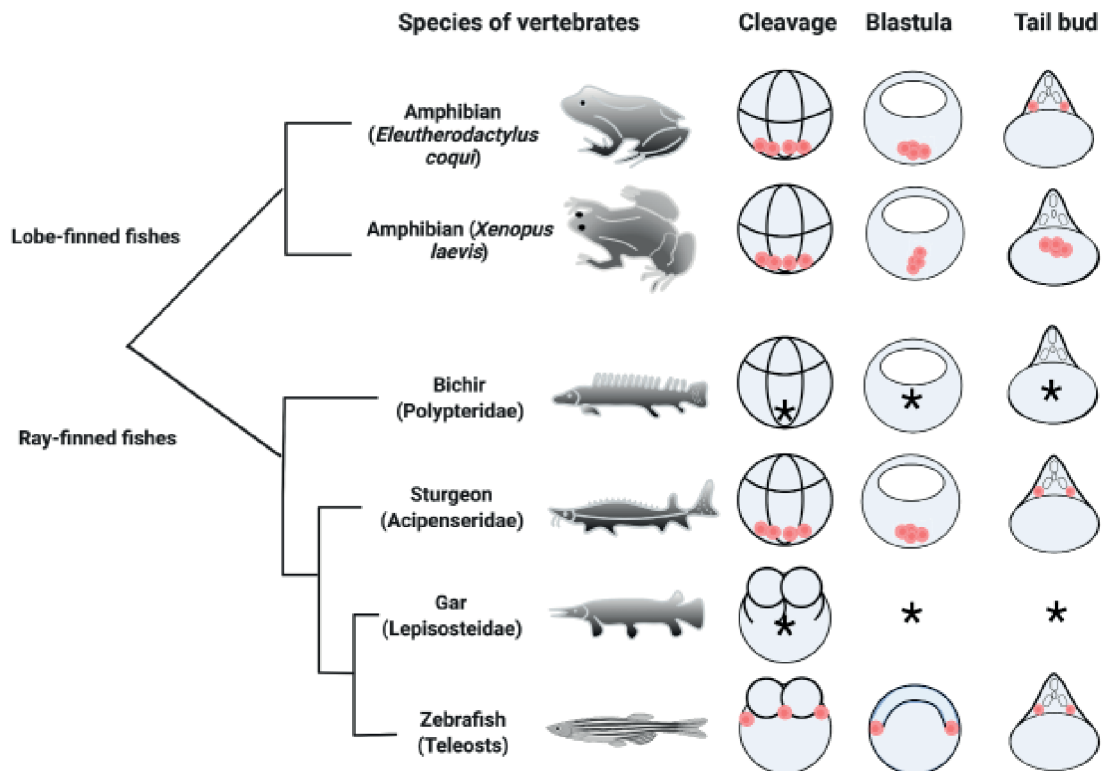


Figure 4. The transition of cleavage pattern and the migration of germplasm between Sarcopterygii (Lobe-finned fishes) and Actinopterygii (ray-finned fishes).

Figure 4 shows the localization and migration of PGCs regarding the evolution of the cleavage pattern. The orange dots are PGCs and indicate their localization and migration information. Star marks denote the research gap.

1.4.2. Germ layer – mesendodermal determinants

Endoderm and mesoderm determinants are conserved in all vertebrates in terms of patterning; however, their RNA localization pattern and time of expression differ by species (Feldman et al., 1998; Kofron et al., 1999; Rodaway et al., 1999; Stainier, 2002; Afouda et al., 2005; Agius et al., 2008). For example, in *X. laevis* (holoblastic), all germ layer precursors are arranged in a gradient along the animal-vegetal (top-bottom) axis. In zebrafish eggs (meroblastic), all germ layer precursors are localized in AP (Gilbert, 2010). Furthermore, because gastrulation in zebrafish begins less than two hours after full activation of Nodal signaling, most genes regulated by Nodal signaling at the start of gastrulation are thought to be immediate-early targets (Erter et al., 1998; Feldman et al., 1998; Rebagliati et al., 1998; Gritsman et al., 2000). In contrast, Nodal signaling does not begin in *X. laevis* until the mid-blastula stage (Fagotto, 2007). This section has reviewed the localization and functions of selected genes for endoderm and mesoderm development. Particular emphasis is given to endoderm determinants since they localized in the VP of holoblastic cleaved embryos (e.g., *X. laevis*), and the AP in meroblastic cleaved embryos (e.g., zebrafish). We summarized the localization and conservation and their regulatory connections between *X. laevis*, sturgeon, and zebrafish. In addition, we also have reviewed how the increasing egg size and yolk volume in closely related species interrupts the localization of maternally supplied mRNA for endoderm development (Buchholz et al., 2007; Takeuchi et al., 2009b).

In *X. laevis* (e.g., amphibian), the maternally supplied VegT, Vg1, and wnt/ -catenin are critical players in the activation of nodal pathways for mesendodermal formation, and they are localized in the vegetal cortex of the oocyte (Deshler et al., 1997; Clements et al., 1999; Kofron et al., 1999; Stennard et al., 1999; Zhang et al., 2005, 1998; Montague and Schier, 2017). VegT is essential for the direct activation of core mesendodermal genes; the transcription factors Sox17a, Sox7, and gsc are bona fide VegT direct targets, and Sox17b, mixer, mix1, hhex, and ventx1 are additional putative direct targets; for details, see (Howard et al., 2007; Charney et al., 2018). In addition, Eomesodermin's (eomes) also play a role in the expression of the mesendodermal genes mix1, xbra, wnt8, sox17a, foxa4, and gsc (Ryan et al., 1996; Conlon et al., 2001).

Compared with *X. laevis* embryos, the *E. coqui* (an amphibian) has enough yolk to develop without feeding the tadpole. Interestingly, due to an increase in the yolk volume towards VP, the maternal RNA gradient, including EcVegT and EcVg1 move and are localized mainly near the oocyte's AP, which is quite similar to that of sturgeon (Beckham et al., 2003; Pocherniaieva et al., 2018). Compared to sturgeon and amphibians, the endodermal marker in bichir is eomes but not VegT; orthologs have the same maternal expression in bichir and zebrafish embryos, suggesting that VegT is only required for amphibians (*X. laevis* and *E. coqui*) and sturgeon (Zhang et al., 1998; Takeuchi et al., 2009b; Pocherniaieva et al., 2018) endoderm development. In bichir embryos, eomes transcripts were found in animal blastomeres and marginal at the zone 4-8 cell and gastrula stage, respectively (Takeuchi et al., 2009b). Although in *X. laevis* embryos, eomes has been implicated in stimulating mesoderm development, in zebrafish and humans, eomes play a role similar to *X. laevis* maternal VegT in activating the endodermal gene regulatory program (Ryan et al., 1996; Bjornson et al., 2005).

The Wnt signaling pathway is responsible for axis patterning, cell fate specification, proliferation, and migration (Wessely and De Robertis, 2000; Claussen and Pieler, 2004; Zearfoss et al., 2004). Most of the studies about the Wnt pathway have been done on *X. laevis* and zebrafish models. Recently, study has reported that the key ligands are WNT11 (including WNT11r and WNT11b paralogs), WNT5A and WNT8B (Naraine et al., 2022). Authors have identified WNT11b in the VP of *X. laevis*, while WNT8B and WNT5A have been found in the VP of sturgeon (Naraine et al., 2022). Moreover, many critical genes in wnt pathways for sturgeons are still unknown.

Maternal Forkhead box protein H1 (Foxh1) is an essential factor for endoderm development. For example, in *X. laevis*, VegT has a significant role in the regulation of nodal gene expression by activating transcription in the blastula through Smad2/3; the Nodal signaling cascade promotes cell division in the embryo (along with the maternal partner to all R-Smad signaling, Smad4) (Osada and Wright, 1999; Tan et al., 2013). The activated Smad2/3-Smad4 complex regulates target genes in collaboration with co-transcription factors, including Foxh1, Eomes, Foxh1.2, Gtf2i, Gtf2ird1, Mixer, Tcf3 (also known as E2a), and Tp53. Maternal Foxh1 is involved in transcriptional regulation via Smad2/3 interactions (Chen et al., 1996; Kee et al., 2011; Yoon et al., 2011). To the best of our knowledge, the function and localization of crucial maternal Foxh1 have been extensively investigated in *X. laevis* (Kofron, 2004; Chiu et al., 2014) and zebrafish (Pogoda et al., 2000; Pei et al., 2007), except sturgeon.

Sox7 is also involved in endoderm development. In zebrafish, sox7 is localized in the AP. The divergent F-type Sox casanova acts downstream of the Nodal signaling pathway (Dickmeis et al., 2001). In contrast, no casanova orthologs have been identified in tetrapods. The F-type Sox and Sox7 are supplied maternally in *X. laevis* and localized in the vegetal region of the embryo (Zhang et al., 2005). The T-box transcription factor VegT, which initiates mesendodermal differentiation, directly regulates Sox7 expression. Sox7 induces the expression of the Nodal-related genes Xnr1, Xnr2, Xnr4, Xnr5, and Xnr6, the homeodomain transcription factor Mixer, and

the endodermal marker Sox17b; both Sox7 and Sox17 induce the expression of endodermin. Sox7 induction of Xnr expression in animal caps is independent of Mixer and Nodal signaling. In animal caps, VegT's ability to induce Mixer and Edd depends on Sox7 activity (Zhang et al., 2005). The functional study of the Sox7 gene in sturgeon embryos is yet to be undertaken.

Maternally supplied determinants control the development of embryos until the blastula stage (1 k cell). When animal embryos reach the mid-blastula stage, developmental control is transferred from maternally provided to zygotic genome synthesized gene products. In model organisms such as echinoderms, nematodes, insects, fish, amphibians, and mammals, the maternal-to-zygotic transition has been extensively studied {for detail, see (Tadros and Lipshitz, 2009)}. However, little is known about sturgeons (chondrosteans) (Pocherniaieva et al., 2019).

In all vertebrates, Sox17 is a highly conserved endodermal transcription factor. The Sox17 plays a crucial role in the endoderm formation in *X. laevis* and zebrafish. Compared to *X. laevis*, Sox17 and Sox7 are localized in the AP of zebrafish embryos (Bjornson et al., 2005; Zhang et al., 2005; Takenaka et al., 2007; Haworth et al., 2008). In sturgeon, Sox factors (sox7 and sox17) are localized in the AP of oocytes (unpublished data from our laboratory). The fate-mapping of pre-oral gut development among non-teleost fishes, including sturgeon, bichir, and gar, showed that Sox17 plays a crucial role in the development of sturgeon's pre-oral gut (Minarik et al., 2017). However, the role of Sox17 in the development of actual gut (gastrointestinal tract) in sturgeon has not yet been investigated.

Furthermore, Gata, a transcription factor that regulates endoderm formation in metazoan model systems, is a highly conserved regulator. The Gata4/5/6 subfamily of Gata factors is involved in the formation of *X. laevis* (Weber et al., 2000; Afouda et al., 2005) and zebrafish (Afouda et al., 2005; Lou et al., 2011) endoderm. Besides the functional conservation, their location is different in zebrafish and *X. laevis*. Interestingly, the role of GATA factors in sturgeon also remains unknown (Weber et al., 2000; Haworth et al., 2008).

Forkhead (Foxa), zygotic transcription factors are critical for endoderm development across diverse organisms (Friedman and Kaestner, 2006; De-Leon, 2014). Of the three Foxa transcription factors in mice (Foxa1, Foxa2, and Foxa3), Foxa2 is required for early development (Weinstein et al., 1994; Gualdi et al., 1996). So far, the role of Foxa3 is unclear, while Foxa2 and Foxa1 serve a crucial role in the development of mesendoderm of *X. laevis* and zebrafish, respectively. Moreover, the localization of these transcription factors is different between *X. laevis* and zebrafish (Bjornson et al., 2005; Chen et al., 2005; Tomomi Haremaki1, 2009; Dalpra et al., 2011). Compared to *X. laevis* and zebrafish, the function and localization of Foxa1, Foxa2, and Foxa3, have yet to be described. Moreover, many other essential genes (such as mixer, mezzo, (znr or xnr), bon, and cas) are also still unknown in the case of sturgeon (Erter et al., 1998; Whitman, 2001; Poulain and Lepage, 2002; Rebagliati et al., 2002; Bjornson et al., 2005; Agius et al., 2008; Haworth et al., 2008).

We can deduce that the majority of the germ layer determines localization to the AP in meroblastic cleaved embryos during oogenesis. On the other hand, some maternal determinants are limited to the VP and move toward the AP via yolk streams during the formation of the first and second cleavage furrows. In the case of holoblastic cleavage, the germ layer determinant is localized from the animal to the vegetal region of the embryo, and all blastomeres contribute equally to embryo development. However, the germ layer gradient changes ambiguously because of the increased amount of yolk towards the vegetal area (Takeuchi et al., 2009b; Buchholz et al., 2007; Pocherniaieva et al., 2018). Thus, it will be interesting to know whether inhibition of vegetal blastomeres (shifting holoblastic to meroblastic cleavage pattern) affect the asymmetry preservation of RNA gradient. Furthermore, many endodermal markers in sturgeon are unknown, and future studies on fate mapping of gut-endoderm development can be conducted by selecting potential marker genes, as mentioned above.

1.5. Gut development and the utilization of yolk

As previously stated, the evolution of meroblastic cleavage in vertebrates is caused by an increase in egg size and yolk volume (heading 1.2 and 1.3). However, compared to other vertebrates (including holoblastic and meroblastic representatives), it is also essential to know how the yolk distribution (increased towards VP) affects the gastrulation in sturgeon embryos, and how their gut develops to utilize the yolk.

In *X. laevis* (holoblastic), the endoderm originates from the VP of the embryo and yolk is stored in cellular form (yolky endoderm cells). During early gastrulation, the “bottle cells” formed on the dorsal side, which marks the onset of blastopore formation and involute the surface material that makes the mesodermal and endodermal lining of the gastrocoel, leads to the development of the archenteron (primary gut) (Figure 1 and 5) (Bolker, 1994). The ventral part of the archenteron is composed of a yolky cell mass (yolky endodermal cells) that is fated to be gut-endoderm (Agius et al., 2008; Gilbert, 2010) (Figure 1 and 5). The yolk, namely yolk platelets, is utilized intracellularly via endodermal cells.

In zebrafish (meroblastic), on the other hand, have no gastrocoel during the gastrulation period. Neither blastopores nor archenteron are present. The blastoderm’s deep enveloping layer cells involute at the blastoderm margin, thus playing a blastopore’s role. Involution causes the blastoderm to fold back on itself, forming the germ ring. As a result, the germ ring is divided into two layers: The upper epiblast feeds cells to the lower hypoblast throughout gastrulation (Collazo et al., 1994; Kimmel et al., 1995). The entire gut is developed from the hypoblast cells and lied on the yolk sac, and the yolk is substantially used up via YSL, and feeding commences, allowing for nutritional intake to be processed in the gut (Ober et al., 2003; Gilbert, 2010) (Figure 2 and 5).

Similarly, reptiles and birds’ embryos have a flattened blastodisc on yolk mass and a gastrulation pattern that differs significantly from that of amphibians due to their large yolk volume. On the other hand, placental mammals have the same gastrulation pattern as reptiles and birds, despite having significantly less/no yolk (Takeuchi et al., 2009b). Amniotes include mammals, reptiles, and birds (i.e., they produce eggs that develop extra-embryonic membranes). Gastrulation in chicks and mice begins in the epiblast, a type of epithelial layer. The epiblast’s cells transition from epithelial to mesenchymal, migrate through the primitive streak, and integrate into the middle (mesoderm) or outer (endoderm) layer. The presumptive definitive endoderm cells invade and displace an outer layer of extra-embryonic tissue cells (hypoblast in chicks and visceral endoderm in mice), which form supporting structures like the yolk sac (Zorn and Wells, 2009). Endoderm has revealed how a two-dimensional sheet of cells forms the primitive gut tube during the late gastrula stage (E7.5 in mouse, HH4 in chicken) (Rosenquist, 1971; Lawson et al., 1986; Lawson and Schoenwolf, 2003; Tremblay and Zaret, 2005; Kimura et al., 2007; Tam et al., 2007). The vascular yolk sac develops in amniotes and serves as an extra-embryonic gut, digesting, absorbing, and delivering nutrients to the embryo (Jorgensen, 2008; Sheng and Foley, 2012; Incardona and Scholz, 2016).

Analogously to *X. laevis*, the embryos of other amphibians – *E. coqui* and *E. eschscholtzii*, and non-teleost fishes – bichir and sturgeon retained the blastocoel, bottle cell, blastophore, gastrocoel, archenteron and stored their yolk in a cellularized form; YCs (Bolker, 1993, 1994; Collazo et al., 1994; Ninomiya et al., 2001; Buchholz et al., 2007; Takeuchi et al., 2009a,b; Collazo and Keller, 2010). Interestingly, the ventral part of archenteron in the embryos of *E. coqui* and bichir is extra-embryonic YCs, do not contribute to gut development. The presence of cellularized yolk; YCs (nutritional endoderm) in *E. coqui* may correspond to changes in the evolution of the amniote egg 360 million years ago. Furthermore, in these species, the entire gut is established as a tubular structure covered in mesenchymal cells, and the YCs mass is

located on the anterior-ventral side of the embryo; the mass is not covered in mesenchymal cells but is directly surrounded by surface ectoderm, indicating that it is extra-embryonic (Buchholz et al., 2007; Takeuchi et al., 2009b), Figure 5).

Aside from jawed fishes, lamprey – an ancient extant lineage of jawless fish – belongs to the order Petromyzontiformes – is an ancestor of all above holoblastic representative vertebrates. Recently, it has been reported that vegetal blastomeres of lamprey embryos produce extra-embryonic YCs (Takeuchi et al., 2009b). Interestingly, morphoanatomical studies have indicated that the archenteron of lamprey embryos extended towards the blastopore position; however, due to colossal yolk mass, archenteron showed delayed epithelization and from the secondary gut structure. From our point of view, precise fate mapping is required in order to understand the gut development and utilization of yolk in lamprey embryos (Shiple, 1885; Kupffer, 1890; Damas, 1943; Piavis, 1971; Li et al., 2019; Richardson et al., 2010).

Numerous previous studies have demonstrated that gut-endoderm of sturgeon develops from the YCs/vegetal blastomeres, as seen in *X. laevis* (Ballard and Ginsburg, 1980; Ginsburg and Dettlaff, 1991; Gawlicka et al., 1996). On the other hand, few recent studies have reported VP only stored germplasm, and YCs facilitate the PGCs migration from the vegetal region to the genital ridge (Linhartová et al., 2015; Saito and Psenicka, 2015; Pocherniaieva et al., 2018; Saito et al., 2014, 2018). Until now, observations related to sturgeon YCs have been dispersed throughout several articles, with little emphasis on their precise role in development. To the best of our knowledge, the fate mapping of vegetal blastomeres/YCs and gut-endoderm of sturgeon have not been thoroughly investigated (Figure 5). Thus, the present study was conducted to know 1) whether the YCs in sturgeon embryos contribute to the embryonic body or serve to provide extra-embryonic nutrition as in *E. coqui*, *E. eschscholtzii*, and bichir. 2) Can sturgeon embryo develop the YSL/YSL-like-structure. 3) Is the sturgeon's gut developmental pattern conserved to any vertebrate (mentioned above), or is it unique? 4) Can sturgeon utilize their yolk in an acellular form instead YCs after inhibition of vegetal blastomeres (Ballard and Ginsburg, 1980; Buchholz et al., 2007; Elinson, 2009; Takeuchi et al., 2009b; Saito et al., 2018).

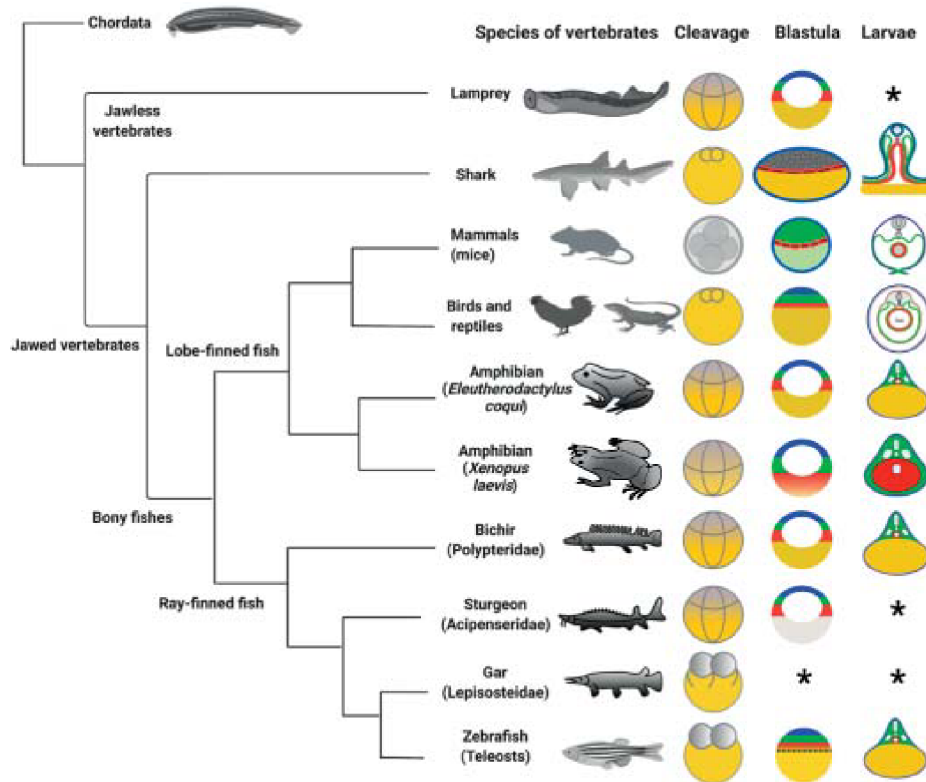


Figure 5. Transition of the egg cleavage pattern and gut development among vertebrates. The figure shows the evolution of the cleavage pattern, germ layer determinants during blastula, and gut structure during hatched larvae in vertebrates. Blue, green, and red color indicates the ectoderm, mesoderm, and endoderm, respectively. The stars indicate research gaps regarding gut development.

1.6. Inhibition of blastomeres cleavage

As mentioned in the above heading 1.3 – 1.5, it is essential to have a robust technique for inhibiting definite blastomeres for further studies (Buchholz et al., 2007). Wilhelm Roux came up with the idea of blastomere inhibition in 1888 by poking a heated needle into one of two blastomeres of *X. laevis* embryo to examine early embryonic development by blocking blastomere cleavage. However, due to incorrect needle placement in the blastomere, this method may either entirely stop the embryo's development, or a slightly wounded blastomere may continue to develop. In 1892, Driesch removed two blastomeres from a sea urchin embryo by shaking instead of killing it; nevertheless, this approach had a low success rate because the embryos were shaken at an inopportune time (Sander, 1997a,b).

Following that, the use of cytochalasin (mycotoxin) as a microfilaments inhibitor was evaluated in the embryos of the mouse (Karasiewicz and Sottyfiska, 1986), *X. laevis* (de Laat et al., 1973) and ascidian (Okado and Takahashi, 1988). The cytochalasin-B microinjection is not ideal for big embryos due to its delayed distribution. Furthermore, owing to cell permeability and high toxicity, its activity can be problematic (de Laat et al., 1973). Additionally, the injection with an optimal concentration of cytostatic factor (c-mos), mitogen-activated protein kinase (MAPK), and p21-activated protein kinase (PAK1) have been reported to cause blastomere cleavage arrest in frog embryos (Sagata et al., 1989; Haccard et al., 1993; Rooney et al., 1996; Buchholz et al., 2007). Because of the complex mechanisms involved, microinjection of cytostatic factor and kinase proteins is not a viable strategy for non-model species (Haccard et al., 1993; Rooney et al., 1996; Buchholz et al., 2007).

Diatoms are the groups of unicellular microalgae that contribute approximately 20% carbon

fixation by photosynthesis annually and contribute as a fundamental food source for small crustacean copepods (Mann, 1999). Nonetheless, due to the production of some biotoxins, such as oxylipins and polyunsaturated aldehydes (PUAs), 30% of diatoms have been reported as antiproliferative representatives (Cutignano et al., 2006; Fontana et al., 2007; Miralto et al., 1999; Pohnert, 2000; Romano et al., 2014). These PUAs, including decadienal (DD—a model aldehyde used in many experimental studies), have been reported to decrease fertilization processes in a sea urchin by inhibiting sperm motility and pronuclear fusion (Caldwell et al., 2004, 2002). Moreover, cleavage arrest of cells in the embryos of *Paracentrotus lividus* and *Sphaerechinus granularis* have already been reported (Poulet et al., 2007; Romano et al., 2014). DD inhibits tubulin polymerization, DNA synthesis, and cyclin B/Cdk1 kinase activity in copepod and sea urchin embryos and induces apoptosis via caspase-3-like protease activity, resulting in cell cycle arrest (Castellano et al., 2015; Hansen et al., 2004; Romano, 2003). Most previous studies focused on the lethal and sub-lethal effect DD had on the development of embryos when they were immersed in different concentrations of DD. However, whether this biotoxin can affect a specific portion of embryos in any species remains undetermined. It thus interests to explore the effects of DD in a localized part of sturgeon embryos and optimize it for definite blastomeres inhibition.

The findings of our study comprise on two published articles and one unpublished manuscript (Chapter 2–4). Based on our review of extant literature, we concluded that: Evolution of meroblastic cleavage pattern in amniotes and fishes is related to the distribution of yolk i.e., increased in volume towards the VP of egg. Amphibians such as *X. laevis* > *E. Coqui* > *E. eschscholtzii* show the transition phase toward amniotes (birds and reptiles). Similarly, non-teleost fishes such as bichir > sturgeon > gar > bowfin illustrate the teleost transition phase. Sturgeon PGCs are produced in the VP, and the rest of the cells are thought to be extra-embryonic, as in *E. Coqui* and bichir. Therefore, in Chapter two, we developed a robust technique for inhibiting specific blastomere and investigated its effect on RNA localization. Then, in Chapter three, we continued our research on the detailed fate mapping of sturgeon vegetal blastomeres; YCs and their comparison with other taxa (Chapter 2–3). Moreover, we also concluded that maternally supplied mRNA moved to the AP and gut-endoderm development evolved drastically as yolk volume increased in the eggs. For example, *E. Coqui*, bichir, and sturgeon embryos cleave holoblastically like *X. laevis*. However, their endoderm precursors localized in the AP, which is not conserved to *X. laevis*. Furthermore, *E. Coqui* and bichir develop the gut on the dorsal position of the yolk and utilize their yolk in a cellular form. Therefore, in Chapter four, we investigated the fate of gut development in sturgeon and their comparison with other taxa (Chapter 3–4).

1.7. Objectives of the thesis

The main aim of this study was to use sturgeon as a great model for the description of a) evolutionary transition from the holoblastic to meroblastic cleavage pattern and b) unique archaic mode of gut development. The thesis has been written based on three following objectives:

- O1 – Development of a novel technique for inhibition of the specific blastomere cleavage and its impact on maternal mRNA localization of sturgeon embryos.
- O2 – Developmental and functional studies of the sturgeon vegetal blastomeres/yolk cells and PGCs; and its comparison with *X. laevis* and zebrafish.
- O3 – The gut development of sturgeon and its comparison with other taxa.

References

- Afouda, B.A., Ciau-uitz, A., Patient, R., 2005. GATA4, 5 and 6 mediate TGF maintenance of endodermal gene expression in *Xenopus* embryos. *Development* 132, 763–774.
- Agius, E., Oelgeschläger, M., Wessely, O., Kemp, C., Robertis, E.M. De, 2008. Endodermal Nodal-related signals and mesoderm induction in *Xenopus*. *Development* 127, 1173–1183.
- Ballard, W.W., 1986a. Morphogenetic movements and a provisional fate map of development in the holostean fish *Amia calva*. *Journal of Experimental Zoology* 238, 355–372.
- Ballard, W.W., 1986b. Stages and rates of normal development in the holostean fish, *Amia calva*. *Journal of Experimental Zoology* 238, 337–354.
- Ballard, W.W., Ginsburg, A.S., 1980. Morphogenetic movements in acipenserid embryos. *Journal of Experimental Zoology* 213, 69–103.
- Beckham, Y.M., Nath, K., Elinson, R.P., 2003. Localization of RNAs in oocytes of *Eleutherodactylus coqui*, a direct developing frog, differs from *Xenopus laevis*. *Evolution and Development* 5, 562–571.
- Bemis, W.E., Birstein, V.J., Waldman, J.R., 1997. Sturgeon biodiversity and conservation: An introduction. *Environmental Biology of Fishes* 8, 13–14.
- Bjornson, C.R.R., Griffin, K.J.P., Farr, G.H., Terashima, A., Himeda, C., Kikuchi, Y., Kimelman, D., 2005. Eomesodermin is a localized maternal determinant required for endoderm induction in zebrafish. *Developmental Cell* 9, 523–533.
- Bolker, J.A., 1993. Gastrulation and mesoderm morphogenesis in the white sturgeon. *Journal of Experimental Zoology* 266, 116–131.
- Bolker, J.A., 1994. Comparison of gastrulation in frogs and fish. *Integrative and Comparative Biology* 34, 313–322.
- Braat, A.K., Zandbergen, T., Van De Water, S., Goos, H.J.T.H., Zivkovic, D., 1999. Characterization of zebrafish primordial germ cells: Morphology and early distribution of vasa RNA. *Developmental Dynamics* 216, 153–167.
- Buchholz, D.R., Singamsetty, S., Karadge, U., Williamson, S., Langer, C.E., Elinson, R.P., 2007. Nutritional endoderm in a direct developing frog: A potential parallel to the evolution of the amniote egg. *Developmental Dynamics* 236, 1259–1272.
- Caldwell, G.S., Bentley, M.G., Olive, P.J.W., 2004. First evidence of sperm motility inhibition by the diatom aldehyde 2 E , 4 E -decadienal. *Marine Ecology Progress Series* 273, 96–108.
- Caldwell, G.S., Olive, P.J.W.W., Bentley, M.G., 2002. Inhibition of embryonic development and fertilization in broadcast spawning marine invertebrates by water soluble diatom extracts and the diatom toxin 2-trans,4-trans decadienal. *Aquatic Toxicology* 60, 123–137.
- Castellano, I., Ercolesi, E., Romano, G., Ianora, A., Palumbo, A., Palumbo, A., 2015. The diatom-derived aldehyde decadienal affects life cycle transition in the ascidian *Ciona intestinalis* through nitric oxide / ERK signalling. *Open Biology* 5, 1–10.
- Charney, R.M., Paraiso, K.D., Blitz, I.L., Cho, K.W.Y., Biology, C., 2018. A gene regulatory program controlling early *Xenopus* mesendoderm formation: network conservation and motifs. *Seminars in Cell and Developmental Biology* 66, 12–24.
- Chen, J.A., Voigt, J., Gilchrist, M., Papalopulu, N., Amaya, E., 2005. Identification of novel genes affecting mesoderm formation and morphogenesis through an enhanced large scale functional screen in *Xenopus*. *Mechanisms of Development* 122, 307–331.

- Chen, S., Kimelman, D., 2000. The role of the yolk syncytial layer in germ layer patterning in zebrafish. *Development* 127, 4681–4689.
- Chen, X., Rubock, M.J., Whitman, M., 1996. A transcriptional partner for mad proteins in TGF-signalling. *Nature* 383, 691–696.
- Chipman, A.D., Haas, A., Khaner, O., 1999. Variations in anuran embryogenesis: Yolk-rich embryos of *Hyperolius puncticulatus* (Hyperoliidae). *Evolution and Development* 1, 49–61.
- Chiu, C.H., Dewar, K., Wagner, G.P., Takahashi, K., Ruddle, F., Ledje, C., Bartsch, P., Scemama, J.L., Stellwag, E., Fried, C., Prohaska, S.J., Stadler, P.F., Amemiya, C.T., 2004. Bichir HoxA cluster sequence reveals surprising trends in ray-finned fish genomic evolution. *Genome Research* 14, 11–17.
- Chiu, W.T., Le, R.C., Blitz, I.L., Fish, M.B., Li, Y., Biesinger, J., Xie, X., Cho, K.W.Y., 2014. Genome-wide view of TGF /Foxh1 regulation of the early mesendoderm program. *Development (Cambridge)* 141, 4537–4547.
- Claussen, M., Pieler, T., 2004. Xvelo1 uses a novel 75-nucleotide signal sequence that drives vegetal localization along the late pathway in *Xenopus oocytes*. *Developmental Biology* 266, 270–284.
- Clements, D., Friday, R.V., Woodland, H.R., 1999. Mode of action of VegT in mesoderm and endoderm formation. *Development* 126, 4903–4911.
- Collazo, A., 1996. Evolutionary correlations between early development and life history in plethodontid salamanders and teleost fishes. *Integrative and Comparative Biology* 36, 116–131.
- Collazo, A., Bolker, J.A., Keller, R., 1994. A phylogenetic perspective on teleost gastrulation. *The American Naturalist* 144, 133–152.
- Collazo, A., Keller, R., 2010. Early development of *Ensatina eschscholtzii*: an amphibian with a large, yolky egg. *EvoDevo* 1, 6. <http://www.evodevojournal.com/content/1/1/6>
- Conlon, F.L., Fairclough, L., Price, B.M.J., Casey, E.S., Smith, J.C., 2001. Determinants of T box protein specificity. *Development* 128, 3749–3758.
- Cutignano, A., D'Ippolito, G., Romano, G., Lamari, N., Cimino, G., Febbraio, F., Nucci, R., Fontana, A., 2006. Chloroplastic glycolipids fuel aldehyde biosynthesis in the marine diatom *Thalassiosira rotula*. *ChemBioChem* 7, 450–456.
- D'Amico, L.A., Cooper, M.S., 2001. Morphogenetic domains in the yolk syncytial layer of axiating zebrafish embryos. *Developmental Dynamics* 222, 611–624.
- Dal-pra, S., Thisse, C., Thisse, B., 2011. FoxA transcription factors are essential for the development of dorsal axial structures. *Developmental Biology* 350, 484–495.
- Damas, H., 1943. Recherches sur le développement de "*Lampetra fluviatilis*" I: ., contribution à l'étude de la céphalogenèse des vertébrés. Liège: H. Vaillant-Carmanne (impr. de H. Vaillant-Carmanne). *Archives of Biology* 55, 284. (in French)
- De-Leon, S.B.-T., 2014. The conserved role and divergent regulation of foxa, a pan- eumetazoan developmental regulatory gene. *Developmental Biology* 357, 21–26.
- Dean, B., 1895. The early development of *Amia*. *Journal of Cell Science* 38, 413–411.
- Deshler, J.O., Highett, M.I., Schnapp, B.J., 1997. Localization of *Xenopus* Vg1 mRNA by Vera protein and the endoplasmic reticulum. *Science* 276, 1128–1131.
- Dettlaff, T.A., Ginsburg, A.S., Schmalhausen, O.I., 1993. Sturgeon fishes: Developmental biology and aquaculture. Springer, NewYork, pp. 92–100.
- de Laat, S.W., Luchtel, D., Bluemink, J.G., 1973. The action of cytochalasin B during egg cleavage in *Xenopus laevis*: Dependence on cell membrane permeability. *Developmental Biology* 31, 163–177.

- Dickmeis, T., Mourrain, P., Saint-Etienne, L., Fischer, N., Aanstad, P., Clark, M., Strähle, U., Rosa, F., 2001. A crucial component of the endoderm formation pathway, *casanova*, is encoded by a novel *sox*-related gene. *Genes and Development*, 15:487–1492.
- Diedhiou, S., Bartsch, P., 2009. Staging of the early development of *Polypterus* (Cladistia: Actinopterygii). *Development of Non-teleost Fishes*, pp. 104–169.
- Duong, T.Y., Scribner, K.T., Forsythe, P.S., Crossman, J.A., Baker, E.A., 2013. Interannual variation in effective number of breeders and estimation of effective population size in long-lived iteroparous lake sturgeon (*Acipenser fulvescens*). *Molecular Ecology*, 22, 1282–1294.
- Elinson, R.P., 1986. Fertilization in amphibians: the ancestry of the block to polyspermy. *International Review of Cytology* 101, 59–100.
- Elinson, R.P., 1987. Fertilization and aqueous development of the puerto rican terrestrial breeding frog, *Eleutherodactylus coqui*. *Journal of Morphology* 193, 217–224.
- Elinson, R.P., 2009. Nutritional endoderm: A way to breach the holoblastic-meroblastic barrier in tetrapods. *Journal of Experimental Zoology Part B: Molecular and Developmental Evolution* 312B, 526–532.
- Elinson, R.P., Fang, H., 1998. Secondary coverage of the yolk by the body wall in the direct developing frog, *Eleutherodactylus coqui*: an unusual process for amphibian embryos. *Development Genes and Evolution* 208, 457–466.
- Elinson, R.P., Beckham, Y., 2002. Development in frogs with large eggs and the origin of amniotes. *Zoology* 105, 105–117.
- Elinson, R.P., Sabo, M.C., Fisher, C., Yamaguchi, T., Orii, H., Nath, K., 2011. Germ plasm in *Eleutherodactylus coqui*, a direct developing frog with large eggs. *EvoDevo* 2, 20. <http://www.evodevojournal.com/content/2/1/20>
- Erter, C.E., Solnica-Krezel, L., Wright, C.V.E.E., 1998. Zebrafish nodal-related 2 encodes an early mesendodermal inducer signaling from the extraembryonic yolk syncytial layer. *Developmental Biology* 204, 361–372.
- Fagotto, A.S., Fagotto, F., 2007. Beta-catenin, MAPK and Smad signaling during early *Xenopus* development. *Development* 129, 37–52.
- Fang, H.Y., Marikawa, Elinson, R.P., 2000. Ectopic expression of *Xenopus* noggin RNA induces complete secondary body axes in embryos of the direct developing frog of *Eleutherodactylus coqui*. *Development Genes and Evolution* 210, 21–27.
- Feldman, B., Gates, M.A., Egan, E.S., Dougan, S.T., Rennebeck, G., Sirotkin, H.I., Schier, A.F., Talbot, W.S., 1998. Zebrafish organizer development and germ-layer formation require nodal-related signals. *Nature* 395, 81–185.
- Fontana, A., D'Ippolito, G., Cutignano, A., Romano, G., Lamari, N., Gallucci, A.M., Cimino, G., Miralto, A., Lanora, A., 2007. LOX-induced lipid peroxidation mechanism responsible for the detrimental effect of marine diatoms on zooplankton grazers. *ChemBioChem* 8, 1810–1818.
- Friedman, J.R., Kaestner, K.H., 2006. The Foxa family of transcription factors in development and metabolism. *Cellular and Molecular Life Sciences* 63, 2317–2328.
- Friedrich, T., 2018. Danube sturgeons: Past and future in: riverine ecosystem management, pp. 507–518. Cham: Springer International Publishing. https://doi.org/10.1007/978-3-319-73250-3_26
- Gawlicka, A., McLaughlin, L., Hung, S.S.O., De La Noüe, J., 1996. Limitations of carrageenan microbound diets for feeding white sturgeon, *Acipenser transmontanus*, larvae. *Aquaculture* 141, 245–265.

- Gilbert, S.F., 2010. *Developmental Biology*, Ninth ed. Sinauer Associates, Oxford University Press.
- Ginsburg, A.S., Dettlaff, T.A., 1991. The Russian sturgeon *Acipenser Güldenstädti*. Part I. Gametes and Early Development up to Time of Hatching. In: Dettlaff, T.A., Vassetzky, S.G. (Eds), *Animal Species for Developmental Studies* Springer, Boston, pp. 15–65.
- Glasauer, S.M.K., Neuhauss, S.C.F., 2014. Whole-genome duplication in teleost fishes and its evolutionary consequences. *Molecular Genetics & Genomics* 289, 1045–1060.
- Gritsman, K., Talbot, W.S., Schier, A.F., 2000. Nodal signaling patterns the organizer. *Development* 127, 921–932.
- Gross-Thebing, T., Yigit, S., Pfeiffer, J., Reichman-Fried, M., Bandemer, J., Ruckert, C., Rathmer, C., Goudarzi, M., Stehling, M., Tarbashevich, K., Seggewiss, J., Raz, E., 2017. The vertebrate protein dead end maintains primordial germ cell fate by inhibiting somatic differentiation. *Developmental Cell* 43, 704–715.
- Gualdi, R., Bossard, P., Zheng, M., Hamada, Y., Coleman, J.R., Zaret, K.S., 1996. Hepatic specification of the gut endoderm *in vitro*: Cell signaling and transcriptional control. *Genes and Development* 10, 1670–1682.
- Haccard, O., Sarcevic, B., Lewellyn, A., Hartley, R., Roy, L., Izumi, T., Erikson, E., Maller, J.L., 1993. Induction of metaphase arrest in cleaving *Xenopus* embryos by MAP kinase. *Science* 262, 1262–1265.
- Hansen, E., Even, Y., Genevière, A.M., 2004. The $\alpha,\beta,\gamma,\delta$ -unsaturated aldehyde 2-trans-4-trans-decadienal disturbs DNA replication and mitotic events in early sea urchin embryos. *Toxicological Sciences* 81, 190–197.
- Hasley, A., Chavez, S., Danilchik, M., Wühr, M., Pelegri, F., 2017. Vertebrate embryonic cleavage pattern determination. *Advances in Experimental Medicine and Biology* 953, 117–171.
- Haworth, K.E., Kotecha, S., Mohun, T.J., Latinkic, B.V., 2008. GATA4 and GATA5 are essential for heart and liver development in *Xenopus* embryos. *BMC Developmental Biology* 8, 1–15. <https://doi.org/10.1186/1471-213X-8-74>
- Heasman, J., Wylie, C.C., Hausen, P., Smith, J.C., 1984. Fates and states of determination of single vegetal pole blastomeres of *X. laevis*. *Cell* 37, 185–194.
- Herpin, A., Rohr, S., Riedel, D., Kluever, N., Raz, E., Scharl, M., 2007. Specification of primordial germ cells in medaka (*Oryzias latipes*). *BMC Developmental Biology*, 10.1186/1471-213X-7-3.
- Horb, M.E., Slack, J.M.W., 2001. Endoderm specification and differentiation in *Xenopus* embryos. *Developmental Biology* 236, 330–343.
- Houston, D.W., Zhang, J., Maines, J.Z., Wasserman, S.A., King, M.L., 1998. A *Xenopus* DAZ-like gene encodes an RNA component of germ plasm and is a functional homologue of *Drosophila boule*. *Development* 125, 171–180.
- Howard, L., Rex, M., Clements, D., Woodland, H.R., 2007. Regulation of the *Xenopus* Xsox17 1 promoter by co-operating VegT and Sox17 sites. *Developmental Biology* 310, 402–415
- Hurley, I.A., Mueller, R.L., Dunn, K.A., Schmidt, E.J., Friedman, M., Ho, R.K., Prince, V.E., Yang, Z., Thomas, M.G., Coates, M.I., 2007. A new time-scale for ray-finned fish evolution. *Proceedings of the Royal Society B: Biological Sciences* 274, 489–498.
- Incardona, J.P., Scholz, N.L., 2016. The influence of heart developmental anatomy on cardiotoxicity-based adverse outcome pathways in fish. *Aquatic Toxicology* 177, 515–525.
- Inoue, J.G., Miya, M., Tsukamoto, K., Nishida, M., 2003. Basal actinopterygian relationships: A mitogenomic perspective on the phylogeny of the “ancient fish.” *Molecular Phylogenetics and Evolution* 26, 110–120.

- Jaroszewska, M., Dabrowski, K., 2009. Early ontogeny of semionotiformes and *Amiiformes* (*Neopterygii*). In: Kunz, Y.W., Luer, C.A., Kapoor, B.G. (Eds), *Development of Non-teleost Fishes*, Science Publishers, pp. 230–274. <https://doi.org/101201/b10184-5>.
- Jorgensen, P., 2008. Yolk. *Current Biology* 18, 103–104.
- Kane, D.A., Kimmel, C.B., 1993. The zebrafish midblastula transition. *Development* 119, 447–456.
- Karasiewicz, J., Sottyfiska, M.S., 1986. Effects of cytochalasin B on the cleavage furrow in mouse blastomeres. *Roux's Archives of Developmental Biology* 194, 137–141.
- Kee, A., Teo, K., Arnold, S.J., Trotter, M.W.B., Brown, S., Ang, L.T., Chng, Z., Robertson, E.J., Dunn, N.R., Vallier, L., 2011. Eomes Chip-Seq 2, 238–250.
- Kikugawa, K., Katoh, K., Kuraku, S., Sakurai, H., Ishida, O., Iwabe, N., Miyata, T., 2004. Basal jawed vertebrate phylogeny inferred from multiple nuclear DNA-coded genes. *BMC Biology* 11, 1–11.
- Kimmel, C.B., Ballard, W.W., Kimmel, S.R., Ullmann, B., Schilling, T.F., 1995. Stages of embryonic development of the zebrafish. *Developmental Dynamics* 203, 255–310.
- Kimura, W., Yasugi, S., Fukuda, K., 2007. Regional specification of the endoderm in the early chick embryo. *Development Growth and Differentiation* 49, 365–372.
- Kirilenko, P., Weierud, F.K., Zorn, A.M., Woodland, H.R., 2008. The efficiency of *Xenopus* primordial germ cell migration depends on the germplasm mRNA encoding the PDZ domain protein Grip2. *Differentiation* 76, 392–403.
- Kitauchi, T., Saito, T., Motomura, T., Arai, K., Yamaha, E., 2012. Distribution and function of germ plasm in cytoplasmic fragments from centrifuged eggs of the goldfish, *Carassius auratus*. *Journal of Applied Ichthyology* 28, 998–1005.
- Klein, S.L., 1987. The first cleavage furrow demarcates the dorsal-ventral axis in *Xenopus* embryos. *Developmental Biology* 120, 299–304.
- Knaut, H., Pelegri, F., Bohmann, K., Schwarz, H., Nüsslein-Volhard, C., 2000. Zebrafish vasa RNA but not its protein is a component of the germ plasm and segregates asymmetrically before germline specification. *Journal of Cell Biology* 149, 875–888.
- Kofron, M., 2004. New roles for FoxH1 in patterning the early embryo. *Development* 131, 5065–5078.
- Kofron, M., Demel, T., Xanthos, J., Lohr, J., Sun, B., Sive, H., Osada, S., Wright, C., Wylie, C., Heasman, J., 1999. Mesoderm induction in *Xenopus* is a zygotic event regulated by maternal VegT via TGFbeta growth factors. *Development* 126, 5759–5770.
- Köprunner, M., Thisse, C., Thisse, B., Raz, E., 2001. A zebrafish nanos-related gene is essential for the development of primordial germ cells. *Genes and Development* 15, 2877–2885.
- Kunz, Y., 2004. *Development Biology of Teleost Fishes*. Springer the Netherlands. DOI: 10.1007/978-1-4020-2997-4.
- Kupffer, C. von, 1890. Die Entwicklung von *Petromyzon planeri*. *Archiv für Mikroskopische Anatomie* 35, 469–558. (in German)
- Lai, F., Singh, A., King, M. Lou, 2012. *Xenopus* nanos1 is required to prevent endoderm gene expression and apoptosis in primordial germ cells. *Development* 139, 1476–1486.
- Lawson, A., Schoenwolf, G.C., 2003. Epiblast and primitive-streak origins of the endoderm in the gastrulating chick embryo. *Development* 130, 3491–3501.
- Lawson, K.A., Meneses, J.J., Pedersen, R.A., 1986. Cell fate and cell lineage in the endoderm of the presomite mouse embryo, studied with an intracellular tracer. *Developmental Biology* 115, 325–339.

- Igorova, V., Psenicka, M., Lebeda, I., Rodina, M., Saito, T., 2018. Polyspermy produces viable haploid/diploid mosaics in sturgeon. *Biology of Reproduction* 99, 695–706.
- Li, J., Han, Y., Ma, Q., Liu, H., Pang, Y., Li, Q., 2019. Early development of Lamprey *Lampetra japonica* (Martens, 1868). *Aquaculture Research* 50, 1501–1514.
- Linhartová, Z., Saito, T., Kašpar, V., Rodina, M., Prášková, E., Hagihara, S., Pšenička, M., 2015. Sterilization of sterlet *Acipenser ruthenus* by using knockdown agent, antisense morpholino oligonucleotide, against dead end gene. *Theriogenology* 84, 1246–1255.
- Long, W.L., Ballard, W.W., 2001. Normal embryonic stages of the longnose gar, *Lepisosteus osseus*. *BMC Developmental Biology* 1: <http://www.biomedcentral.com/1471-213X/1/6>.
- Lou, X., Deshwar, A.R., Crump, J.G., Scott, I.C., 2011. Smarcd3b and Gata5 promote a cardiac progenitor fate in the zebrafish embryo. *Development* 15, 3113–3123.
- Maegawa, S., Yasuda, K., Inoue, K., 1999. Maternal mRNA localization of zebrafish DAZ-like gene. *Mechanisms of Development* 81, 223–226.
- Mann, D.G., 1999. The species concept in diatoms. *Phycologia* 38, 437–495.
- Minarik, M., Stundl, J., Fabian, P., Jandzik, D., Metscher, B.D., Psenicka, M., Gela, D., Osorio-Pérez, A., Arias-Rodríguez, L., Horáček, I., Cerny, R., 2017. Pre-oral gut contributes to facial structures in non-teleost fishes. *Nature* 547, 209–212.
- Miralto, A., Barone, G., Romano, G., Poulet, S.A., Ianora, A., Russo, G.L., Buttino, I., Mazzarella, G., Laablr, M., Cabrini, M., Glacobbe, M.G., 1999. The insidious effect of diatoms on copepod reproduction. *Nature* 402, 173–176.
- Miyake, A., Saito, T., Kashiwagi, T., Ando, D., Yamamoto, A., Suzuki, T., Nakatsuji, N., Nakatsuji, T., 2006. Cloning and pattern of expression of the shiro-uo vasa gene during embryogenesis and its roles in PGC development. *International Journal of Developmental Biology* 50, 619–625.
- Mizuno, T., Yamaha, E., Wakahara, M., Kuroiwa, A., Takeda, H., 1996. Mesoderm induction in zebrafish. *Nature* 383, 131–132.
- Montague, T.G., Schier, A.F., 2017. Vg1-nodal heterodimers are the endogenous inducers of mesendoderm. *eLife* 6, e28183.
- Naraine, R., Igorova, V., Abaffy, P., Franek, R., Soukup, V., Sindelka, R., 2022. Evolutionary conservation of maternal RNA localization in fishes and amphibians revealed by TOMO-Seq. *Developmental Biology* 489, 146–160.
- Narum, S.R., Buerkle, C.A., Davey, J.W., Miller, M.R., Hohenlohe, P.A., 2013. Genotyping-by-sequencing in ecological and conservation genomics. *Molecular Ecology* 22, 2841–2847.
- Ninomiya, H., Zhang, Q., Elinson, R.P., 2001. Mesoderm formation in *Eleutherodactylus coqui*: Body patterning in a frog with a large egg. *Developmental Biology* 236, 109–123.
- Ober, E.A., Field, H.A., Stainier, D.Y.R., 2003. From endoderm formation to liver and pancreas development in zebrafish. *Mechanisms of Development* 120, 5–18.
- Okado, H., Takahashi, K., 1988. A simple “neural induction” model with two interacting cleavage-arrested ascidian blastomeres. *Proceedings of the National Academy of Sciences* 85, 6197–6201.
- Osada, S.I., Wright, C.V.E., 1999. *Xenopus* nodal-related signaling is essential for mesendodermal patterning during early embryogenesis. *Development* 126, 3229–3240.
- Ostaszewska, T., Dabrowski, K., 2009. Early development of *Acipenseriformes* (Chondrostei: Actinopterygii). *Development of non-teleost fishes*. Science Publishers, Enfield, NH, pp. 170–229.

- Pasquier, J., Cabau, C., Nguyen, T., Jouanno, E., Severac, D., Braasch, I., Bobe, J., 2016. Gene evolution and gene expression after whole genome duplication in fish: the PhyloFish database. *BMC Genomics* 17, 368. <https://doi.org/10.1186/s12864-016-2709-z>.
- Pei, W., Noushmehr, H., Costa, J., Ouspenskaia, M.V., Elkahloun, A.G., Feldman, B., 2007. An early requirement for maternal FoxH1 during zebrafish gastrulation. *Developmental Biology* 310, 10–22.
- Piavis, G.W., 1971. London, Academic Press. Embryology In: Hardisty, M.W., Potter, I.C. *The Biology of Lampreys*, 361–400.
- Pocherniaieva, K., Güralp, H., Saito, T., Pšenička, M., Tichopád, T., Janko, K., Kašpar, V., 2019. The timing and characterization of maternal to zygote transition and mid-blastula transition in sterlet *Acipenser ruthenus* and *A. Ruthenus* x *Acipenser gueldenstaedtii* hybrid. *Turkish Journal of Fisheries and Aquatic Sciences*, 19:77–84.
- Pocherniaieva, K., Psenicka, M., Sidova, M., Havelka, M., Saito, T., Sindelka, R., Kaspar, V., 2018. Comparison of oocyte mRNA localization patterns in sterlet *Acipenser ruthenus* and African clawed frog *Xenopus laevis*. *Journal of Experimental Zoology Part B, Molecular and Developmental Evolution* 330, 181–187.
- Pogoda, H.M., Solnica-Krezel, L., Driever, W., Meyer, D., 2000. The zebrafish forkhead transcription factor FoxH1/Fast1 is a modulator of Nodal signaling required for organizer formation. *Current Biology* 10, 1041–1049.
- Pohnert, G., 2000. Wound-activated chemical defense in unicellular planktonic algae. *Angewandte Chemie – International Edition* 39, 4352–4354.
- Poulain, M., Lepage, T., 2002. Mezzo, a paired-like homeobox protein is an immediate target of Nodal signalling and regulates endoderm specification in zebrafish. *Development* 129, 4901–4914.
- Poulet, S., Lange, M., Cordevant, C., Adolph, S., Cueff, A., Pohnert, G., Lumineau, O., 2007. Are volatile unsaturated aldehydes from diatoms the main line of chemical defence against copepods? *Marine Ecology Progress Series* 245, 33–45.
- Ravi, V., Venkatesh, B., 2008. Rapidly evolving fish genomes and teleost diversity. *Current Opinion in Genetics and Development* 18, 544–550.
- Rebagliati, M.R., Toyama, R., Fricke, C., Haffter, P., Dawid, I.B., 1998. Zebrafish nodal-related genes are implicated in axial patterning and establishing left-right asymmetry. *Developmental Biology* 199, 261–272.
- Rebagliati, M.R., Toyama, R., Haffter, P., Dawid, I.B., 2002. Cyclops encodes a nodal-related factor involved in midline signaling. *Proceedings of the National Academy of Sciences* 95, 9932–9937.
- Richardson, M.K., Admiraal, J., Wright, G.M., 2010. Developmental anatomy of lampreys. *Biological Reviews* 85, 1–33.
- Rodaway, A., Takeda, H., Koshida, S., Broadbent, J., Price, B., Smith, J.C., Patient, R., Holder, N., 1999. Induction of the mesendoderm in the zebrafish germ ring by yolk cell-derived TGF-beta family signals and discrimination of mesoderm and endoderm by FGF. *Development* 126, 3067–3078.
- Romano, G., 2003. A marine diatom-derived aldehyde induces apoptosis in copepod and sea urchin embryos. *Journal of Experimental Biology* 206, 3487–3494.
- Romano, G., Zoologica, S., Dohrn, A., Ianora, A., Zoologica, S., Dohrn, A., Russo, G.L., Buttino, I., 2014. The insidious effect of diatoms on copepod reproduction. *Nature*, DOI: 10.1038/46023.
- Rooney, R.D., Tuazon, P.T., Meek, W.E., Carroll, E.J., Hagen, J.J., Gump, E.L., Monnig, C.A., Lugo, T., Traugh, J.A., 1996. Mitogen-activated protein kinase. *Journal of Biological Chemistry* 271, 21498–21504.

- Rosenquist, G.C., 1971. The location of the pre-gut endoderm in the chick embryo at the primitive streak stage as determined by radioautographic mapping. *Developmental Biology* 26, 323–335.
- Ryan, K., Garrett, N., Mitchell, A., Gurdon, J.B., 1996. Eomesodermin, a key early gene in *Xenopus* mesoderm differentiation. *Cell* 87, 989–1000.
- Sagata, N., Watanabe, N., Vande Woude, G.F., Ikawa, Y., 1989. The c-mos proto-oncogene product is a cytostatic factor responsible for meiotic arrest in vertebrate eggs. *Nature* 342, 512–518.
- Saito, T., Psenicka, M., 2015. Novel technique for visualizing primordial germ cells in sturgeons (*Acipenser ruthenus*, *A. gueldenstaedtii*, *A. baerii*, and *Huso huso*). *Biology of Reproduction* 93, 1–7.
- Saito, T., Psěnička, M., Goto, R., Adachi, S., Inoue, K., Arai, K., Yamaha, E., Psěnička, M., 2014. The origin and migration of primordial germ cells in sturgeons. *PLoS ONE* 9, e86861.
- Saito, T., Guralp, H., Iegorova, V., Rodina, M., Psenicka, M., 2018. Elimination of primordial germ cells in sturgeon embryos by ultraviolet irradiation. *Biology of Reproduction* 99, 556–564.
- Sander, K., 1997a. “Mosaic work” and “assimilating effects” in embryogenesis: Wilhelm Roux’s conclusions after disabling frog blastomeres. In: Sander, K., et al. (Eds), *Landmarks in Developmental Biology 1883–1924: Historical Essays from Roux’s Archives*. Springer, Berlin Heidelberg, pp. 13–15. https://doi.org/10.1007/978-3-642-60492-8_5
- Sander, K., 1997b. Shaking a concept: Hans Driesch and the varied fates of sea urchin blastomeres. In: Sander, K. et al. (Eds), *Landmarks in Developmental Biology 1883–1924: Historical Essays from Roux’s Archives*. Springer, Berlin Heidelberg, pp 29–31. https://doi.org/10.1007/978-3-642-60492-8_10
- Sheng, G., Foley, A.C., 2012. Diversification and conservation of the extraembryonic tissues in mediating nutrient uptake during amniote development. *Annals of the New York Academy of Sciences* 1271: 97–103.
- Shiple, A.E., 1885. On the formation of the mesoblast, and the persistence of the blastopore in the lamprey. *Proceedings of the Royal Society of London* 39, 244–248.
- Sindelka, R., Sidova, M., Svec, D., Kubista, M., 2010. Spatial expression profiles in the *Xenopus laevis* oocytes measured with qPCR tomography. *Methods* 51, 87–91.
- Solnica-Krezel, L., 2005. Conserved patterns of cell movements during vertebrate gastrulation. *Current Biology* 15, 213–228.
- Stainier, D.Y.R., 2002. A glimpse into the molecular entrails of endoderm formation. *Genes and Development* 16, 893–907.
- Starz-Gaiano, M., Lehmann, R., 2001. Moving towards the next generation. *Mechanisms of Development* 10, 5–18.
- Stennard, F., Zorn, A.M., Ryan, K., Garrett, N., Gurdon, J.B., 1999. Differential expression of VegT and Antipodean protein isoforms in *Xenopus*. *Mechanisms of Development* 86, 87–98.
- Tadros, W., Lipshitz, H.D., 2009. The maternal-to-zygotic transition: a play in two acts. *Development* 136, 3033–3042.
- Takenaka, M., Horiuchi, T., Yanagimachi, R., 2007. Effects of light on development of mammalian zygotes. *Sciences-New York* 104, 14289–14293.
- Takeuchi, M., Okabe, M., Aizawa, S., 2009a. The genus *Polypterus* (Bichirs): a fish group diverged at the stem of ray-finned fishes (Actinopterygii). *CSH Protocols* 1, 1–12. doi:10.1101/pdb.emo117.

- Takeuchi, M., Takahashi, M., Okabe, M., Aizawa, S., 2009b. Germ layer patterning in bichir and lamprey; an insight into its evolution in vertebrates. *Developmental Biology* 332, 90–102.
- Tam, P.P.L., Khoo, P.L., Lewis, S.L., Bildsoe, H., Wong, N., Tsang, T.E., Gad, J.M., Robb, L., 2007. Sequential allocation and global pattern of movement of the definitive endoderm in the mouse embryo during gastrulation. *Development* 134, 251–260.
- Tan, M.H., Au, K.F., Yablonovitch, A.L., Wills, A.E., Chuang, J., Baker, J.C., Wong, W.H., Li, J.B., 2013. RNA sequencing reveals a diverse and dynamic repertoire of the *Xenopus tropicalis* transcriptome over development. *Genome Research* 23, 201–216.
- Theusch, E.V., Brown, K.J., Pelegri, F., 2006. Separate pathways of RNA recruitment lead to the compartmentalization of the zebrafish germ plasm. *Developmental Biology* 292, 129–141.
- Tomomi Haremake1 and DCWCS, 2009. Inhibition of mesodermal fate by *Xenopus* HNF3 /FoxA2 Crystal. *Developmental Biology* 265, 90–104.
- Tremblay, K.D., Zaret, K.S., 2005. Distinct populations of endoderm cells converge to generate the embryonic liver bud and ventral foregut tissues. *Developmental Biology* 280, 87–99.
- Weber, H., Symes, C.E., Walmsley, M.E., Rodaway, A.R.F., Patient, R.K., 2000. A role for GATA5 in *Xenopus* endoderm specification. *Development* 127, 4345–4360.
- Weinstein, D.C., Ruiz i Altaba, A., Chen, W.S., Hoodless, P., Prezioso, V.R., Jessell, T.M., Darnell, J.E., 1994. The winged-helix transcription factor HNF-3 is required for notochord development in the mouse embryo. *Cell* 78, 575–588.
- Wessely, O., De Robertis, E.M., 2000. The *Xenopus* homologue of Bicaudal-C is a localized maternal mRNA that can induce endoderm formation. *Development* 127, 2053–2062.
- Whittington, P.M., Dixon, K.E., 1975. Quantitative studies of germ plasm and germ cells during early embryogenesis of *Xenopus laevis*. *Journal of Embryology and Experimental Morphology* 33, 57–74.
- Whitman, M., 2001. Nodal signaling in early vertebrate embryos: Themes and Variations. *Developmental Cell* 1, 605–617.
- Yasuo, H., Lemaire, P., 2001. Generation of the germ layers along the animal-vegetal axis in *Xenopus laevis*. *International Journal of Developmental Biology* 45, 229–235.
- Yoon, S.J., Wills, A.E., Chuong, E., Gupta, R., Baker, J.C., 2011. HEB and E2A function as SMAD/FOXH1 cofactors. *Genes and Development* 25, 1654–1661.
- Zearfoss, N.R., Chan, A.P., Wu, C.F., Kloc, M., Etkin, L.D., 2004. Hermes is a localized factor regulating cleavage of vegetal blastomeres in *Xenopus laevis*. *Developmental Biology* 267, 60–71.
- Zhang, C., Basta, T., Fawcett, S.R., Klymkowsky, M.W., 2005. SOX7 is an immediate-early target of VegT and regulates Nodal-related gene expression in *Xenopus*. *Developmental Biology* 278, 526–541.
- Zhang, J., Houston, D.W., King, M. Lou, Payne, C., Wylie, C., Heasman, J., 1998. The role of maternal VegT in establishing the primary germ layers in *Xenopus* embryos. *Cell* 94, 515–524.
- Zorn, A.M., Wells, J.M., 2009. Vertebrate endoderm development and organ formation. *Annual Review of Cell and Developmental Biology* 25, 221–251.

CHAPTER 2

NOVEL TECHNIQUE FOR DEFINITE BLASTOMERE INHIBITION AND DISTRIBUTION OF MATERNAL RNA IN STERLET *Acipenser ruthenus* EMBRYO

Shah, M.A., Saito, T., Šindelka, R., Iegorova, V., Rodina, M., Baloch, A.R., Franěk, R., Tichopád, T., Pšenička, M., 2021. Novel technique for definite blastomere inhibition and distribution of maternal RNA in sterlet *Acipenser ruthenus* embryo. *Fisheries Science* 87, 71–83.

According to the publishing agreement between the authors and publisher (Springer Nature) on Mar 02, 2022 (licence no. 5260931476530), the article is reprinted by permission from Springer Nature, *Fisheries Science*, Novel technique for definite blastomere inhibition and distribution of maternal RNA in sterlet *Acipenser ruthenus* embryo, Mujahid Ali Shah et al, Copyright © 2021 Japanese Society of Fisheries Science, 4 Jan 2021 HYPERLINK "<https://doi.org/10.1007/s12562-020-01481-7>" doi.org/10.1007/s12562-020-01481-7. *Fish Sci.*

My share on this work was about 60%.



Novel technique for definite blastomere inhibition and distribution of maternal RNA in sterlet *Acipenser ruthenus* embryo

Mujahid Ali Shah¹ · Taiju Saito² · Radek Šindelka³ · Viktoriia Iegorova³ · Marek Rodina¹ · Abdul Rasheed Baloch¹ · Roman Franěk¹ · Tomáš Tichopád¹ · Martin Pšenička¹

Received: 10 August 2020 / Accepted: 26 October 2020 / Published online: 4 January 2021
© Japanese Society of Fisheries Science 2020

Abstract

The cleavage pattern of a vertebrate's embryo is either holoblastic (complete) or meroblastic (partial). Sturgeon and other basal bony fishes represent a transition of the cleavage pattern. To understand the transition, it is essential to develop an effective technique for the inhibition of specific blastomere cleavage. So far, various studies have demonstrated that diatom-derived polyunsaturated aldehyde (PUA), 2,4-decadienal (DD)—a model aldehyde for experimental studies—adversely affects the developing embryos of several aquatic species. In this study, we employed DD for inhibition of cleavage of a definite blastomere in sturgeon embryos under various conditions. The effective treatment was found to be a combination of DD injection (0.01 v/v) and visible light (44.86–91.15 W m⁻²). Notably, DD injection or light irradiation alone cannot inhibit cleavage. Furthermore, spatial RNA localization analysis using quantitative polymerase chain reaction (qPCR)-tomography revealed that the localized pattern of selected maternal messenger ribonucleic acids (mRNAs) remained constant along the animal–vegetal (A–V) axis, which suggests that RNA localization is completed by the end of oogenesis and that early embryonic cleavage is not required for A–V asymmetry preservation.

Keywords Cleavage pattern inhibition · 2,4-Decadienal · Light irradiation · qPCR /tomography · RNA localization · Sterlet *Acipenser ruthenus*

Electronic supplementary material The online version of this article (<https://doi.org/10.1007/s12562-020-01481-7>) contains supplementary material, which is available to authorized users.

✉ Mujahid Ali Shah
mshah@frov.jcu.cz

Taiju Saito
taiju76@gmail.com

Radek Šindelka
Radek.Sindelka@ibt.cas.cz

Viktoriia Iegorova
Viktoriia.Iegorova@ibt.cas.cz

Marek Rodina
rodina@frov.jcu.cz

Abdul Rasheed Baloch
baloch.rasheed@hotmail.com

Roman Franěk
franek@frov.jcu.cz

Introduction

Vertebrate egg cleavage patterns can be divided into two broad categories: (1) holoblastic (complete) cleavage and (2) meroblastic (partial) cleavage. Bony fishes (Osteichthyes)

Tomáš Tichopád
tichopad@frov.jcu.cz

Martin Pšenička
psenicka@frov.jcu.cz

- ¹ Faculty of Fisheries and Protection of Waters, South Bohemian Research Center of Aquaculture and Biodiversity of Hydrocenoses, University of South Bohemia in Ceske Budejovice, Zatisi 728/II, 389 25 Vodnany, Czech Republic
- ² South Ehime Fisheries Research Center, Ehime University, Ainan, Ehime 798-4206, Japan
- ³ Laboratory of Gene Expression, Institute of Biotechnology of the Czech Academy of Sciences, Vestec, Czech Republic

include ~30,000 species and divaricated into two lineages, (1) ray-finned—Actinopterygii and (2) lobe-finned fish—Sarcopterygii, about 476 million years ago (mya) (Takeuchi et al. 2009a). In sarcopterygian lineage, amphibians and lungfish underwent holoblastic cleavage, while reptile and avian species evolved meroblastic cleavage due to increased yolk volume. Ultimately, embryos of mammals lost yolk and regained a size of around 100 μm diameter to develop in the uterus and undergo holoblastic cleavage. At the crown of actinopterygian evolution, approximately 27,000 species of the teleost taxon constituted more than half of all extant vertebrates. They develop by meroblastic cleavage; the vegetal half of the embryo is the nutritive yolk cell, and only the animal region of the embryo undergoes cleavage, generating all three primary germ layers. The animals of the teleost taxon underwent whole-genome duplication (WGD) and subsequent changes in their genome (Ravi and Venkatesh 2008; Amores et al. 1998; Chiu et al. 2004). Prior to the WGD event, four clads of actinopterygian lineage including bichir *Polypterus* (370 mya; polypterids), sturgeon *Acipenser* and paddlefish *Polyodon* (200 mya; chondrosteans), gar *Lepisosteus* (65–100 mya; lepisosteids), and bowfin *Amia* (100 mya; amiids) also diverged from teleost lineage after divarication from Sarcopterygii and retained some archaic characteristics in their embryogenesis. As in bichir and sturgeon, holoblastic cleavage is preserved—a situation similar to the hypothesized ancestral state for vertebrates (e.g., *Xenopus laevis* 400 mya) rather than that of teleosts (Bartsch et al. 1997; Cooper and Virta 2007; Hurley et al. 2007). In addition to cleavage, their embryonic development is highly similar to that of *Xenopus laevis*, for instance, (i) formation of blastocoel during blastulation, (ii) formation of morphologically distinct “bottle cells” initiating cell involution via the dorsal lip of the blastopore, and (iii) formation of the archenteron (primary gut) (Bolker 1993, 1994; Takeuchi et al. 2009a, 2009b).

Conversely, closely related species, i.e., gar *Lepisosteus* and bowfin *Amia*, possess intermediate morphologies that lie between the chondrosteans and teleosts. For example, they generate giant yolky blastomeres (2 cells in gar, 12 cells in bowfin) in the vegetal pole (VP), and cleavage takes place mostly in the animal pole (AP) (Long and Ballard 2001; Ballard 1986). Embryogenesis of gar *Lepisosteus* and bowfin *Amia* indicates that meroblastic cleavage supposedly evolved by two major changes: (1) loss of bottle cells during gastrulation and (2) fusion of vegetal blastomeres into a single cell to store their yolk in the form of yolk platelets and development of the yolk syncytial layer (YSL) to separate the yolk from the blastoderm (Cooper and Virta 2007; Long and Ballard 2001; Ballard 1986).

Additionally, the egg cleavage pattern of the Puerto Rican tree frog *Eleutherodactylus coqui* (*E. coqui*) represents a similar kind of transition as bowfin *Amia*. For example, eggs

of *E. coqui* are 20 times as large as those of *Xenopus laevis* (~1.0–1.3 mm), and their VP produce yolk-rich vegetal cells which do not eventually become part of the embryo. When cleavage of vegetal blastomeres of *E. coqui* embryos at the 60- to 100-cell stage was inhibited, embryogenesis continued, indicating that these cells are extraembryonic (Buchholz et al. 2007). Similarly, sturgeon eggs (~3.5 mm) are larger than those of their ancestor (*Xenopus laevis*), and VP produce a massive amount of yolk cells that serve only as nutrition. The presence of such nutritional cells may represent an important step in the evolutionary transition from holoblastic to meroblastic cleavage (Buchholz et al. 2007; Saito et al. 2018). Consequently, the sterlet *Acipenser ruthenus* is a great model in which to study the transition between cleavage patterns among actinopterygians (1) because of their phylogenetic relationship between vertebrates, i.e., between amphibian *Xenopus laevis* and gar *Lepisosteus*, and (2) because the whole embryo divides during early development, representing holoblastic cleavage; however, its vegetal cells mimic the *E. coqui* and *Amia* by dividing more slowly than animal cells (Buchholz et al. 2007; Takeuchi et al. 2009a). Therefore, to understand the evolution (holoblastic–meroblastic) of the cleavage patterns and their mechanisms, the development of effective applications is needed for inhibition of blastomere cleavage in sturgeon embryos.

With regard to the study of early embryonic development by inhibiting blastomere cleavage, Wilhelm Roux first introduced the blastomere inhibition concept in 1888 by poking a hot needle into one of two blastomeres of the *Xenopus laevis* embryo. However, this technique may completely block the development of the embryo through improper positioning of the needle in the blastomere, or a slightly injured blastomere may continue to develop. Therefore, in 1892, Driesch separated two blastomeres from a sea urchin embryo using shaking instead of killing; however, owing to the shaking of embryos at the wrong moment, this technique has a low success rate (for reference see Sander 1997a, b). Subsequently, the use of cytochalasin (mycotoxin) as a microfilament inhibitor was tested for inhibition of blastomere cleavage in the embryo of *Halocynthia roretzi* (Okado and Takahashi 1988), *Xenopus laevis* (Siegfried et al. 1973), and *Mus musculus* (Karasiewicz and Sottyfiska 1986). However, because of its slow spread into cells, cytochalasin-B (CB) microinjection is not suitable for large embryos. Furthermore, its action can be problematic because of cell permeability and high toxicity (Siegfried et al. 1973). Additionally, the microinjection of cytotostatic factor (*c-mos*) (Sagata et al. 1989; Buchholz et al. 2007), mitogen-activated protein kinase (MAPK) (Haccard et al. 1993) and p21-activated protein kinase (PAK1) has also been reported to cause the arrest of blastomere cleavage in *Xenopus laevis* embryos (Haccard et al. 1993; Rooney et al. 1996; Sagata et al. 1989). However, owing to the complicated processes involved, microinjection

of the cytostatic factor and kinase proteins is not a practical technique for non-model species (Daniel R. Buchholz et al. 2007; Haccard et al. 1993; Rooney et al. 1996). It is clear from the overview that, to date, there has not been an effective technique for controlled blastomere inhibition applicable during sturgeon development.

Diatoms are a group of unicellular microalgae that are responsible for approximately 20% of the world's carbon fixation by photosynthesis and are a fundamental source of food for small crustacean copepods (Mann 1999). Nevertheless, approximately 30% of diatoms have been reported as antiproliferative representatives owing to the production of biotoxins including oxylipins and polyunsaturated aldehydes (2,4-decadienal) (Cutignano et al. 2006; Fontana et al. 2007; Miralto et al. 1999; Pohnert 2000). 2,4-Decadienal (DD) has been observed to induce changes in the membrane lipid structure of the plasma membrane and decrease permeability to various external low molecular weight solutes when culture of *Phaeodactylum tricorutum* was treated with sublethal DD concentrations (Sabharwal et al. 2017). The cleavage arrest of cells by DD has already been reported in the embryos of *Paracentrotus lividus* and *Sphaerechinus granularis* (Miralto et al. 1999; Poulet et al. 2007). Several studies have shown that DD inhibits tubulin polymerization, deoxyribonucleic acid (DNA) synthesis and cyclin B/cyclin-dependent kinase 1 (cdk1) activity; it also induces apoptosis via caspase-3-like protease activity that ultimately leads to cell cycle arrest in copepod and sea urchin embryos (Hansen et al. 2004; Romano 2003; Castellano et al. 2015). The study showed that DD induces the reduction of endogenous nitric oxide (NO) levels likely owing to glutathione (GSH) depletion. A reduction in NO levels leads to early upregulation of *mkp1* with consequent extracellular signal-regulated kinase (ERK) inactivation and changes in the downstream transcription of the metabolic enzyme dehydrogenase *dhg* and the key developmental genes *ets* and *mx*, leading to a delay in the metamorphosis of *Ciona intestinalis* (Castellano et al. 2015). This stress can generally cause hypersensitivity to UV-B light (Li et al. 2017). So far, DD has not yet been investigated in definite blastomeres/cells of embryos in any species. It is therefore in our interest to investigate the specification of DD treatment for definite blastomere inhibition under different conditions, such as dark/light irradiation.

In our previous studies, we showed robust fate-mapping techniques for sturgeon embryos including fate mapping of vegetal blastomere including primordial germ cells (PGCs) by labeling with fluorescein isothiocyanate (FITC)-dextran of 500,000 molecular weight (MW) (Saito and Psenicka 2015) or delivering the iron oxide nanoparticles into sturgeon germ cells (Baloch et al. 2019). Minarik et al. have also shown labeling of endodermal cells of a sturgeon embryo which are involved in facial structure and represent the ancestral developmental module among actinopterygians

(Minarik et al. 2017). Moreover, we demonstrated elimination of PGCs using UV irradiation at the VP of sturgeon embryos (Saito et al. 2018). It is suggested that the vegetal blastomere only gives rise to PGCs and generates a massive amount of yolk cells that only serve as endogenous nutrients. To date, enough information is available on the contribution of blastomeres or cells to the development of embryos (Ballard and Ginsburg 1980; Ginsburg and Dettlaff 1991; Minarik et al. 2017; Saito et al. 2014). However, no research has been conducted to inhibit the specific blastomere cleavage and its effect on the development of sturgeon embryos.

In this work, we show the inhibition of specific blastomere cleavage in sturgeon embryos by utilizing the optimal DD concentration and visible light irradiation. The distribution of mRNAs along the A-V axis in sturgeon oocytes is critical for successful development (Pocherniaieva et al. 2018). Thus, we have speculated that RNA localization along the A-V axis will directly reflect the inhibition of cleavage patterns. We employed quantitative polymerase chain reaction (qPCR)-tomography to examine whether the blastomere cleavage inhibition influences the localization of maternal mRNA. We proposed that the development of the present methodology will lay the foundation for further research on the transition of cleavage patterns and for the purpose of fate mapping in sturgeon and their comparison with other taxa, such as amphibia and teleosts.

Materials and methods

Ethics statement

All animal experiments were conducted in accordance with the Animal Research Committee of the Faculty of Fisheries and Protection of Waters in Vodnany, University of South Bohemia in Ceske Budejovice, Czech Republic.

Preparation of embryos, working solutions and microinjection

During the spawning season from 2019 to 2020, the adult sterlet males and females were kept in recirculating aquaculture systems (RAS) at 15 °C. For spermiation, the male sterlet was injected with a single intramuscular injection [4 mg/kg body weight (BW)] of carp pituitary extract (CPE) at 0.9% NaCl. Milt was collected 48 h after hormonal injection and was kept at 4 °C until fertilization. The milt exhibiting > 80% motility was used for fertilization. For ovulation, CPE was administered by intramuscular injection in two doses spread 12 h apart at 0.5 mg/kg BW and 4.5 mg/kg BW, respectively. Ovulated eggs were collected from six females 18–20 h after the second injection, and the eggs were inseminated with sperm at 15 °C in dechlorinated

water. To remove the stickiness, embryos were washed three times for 3 min with 0.04% tannic acid dissolved in tap water. The chorion membranes were removed using fine forceps, and the dechorionated embryos were kept at 15 °C (Fig. 1). Embryos with a 95% fertilization rate were used, and samples were collected in triplicate for all experiments.

2,4-trans,trans-Decadienal \geq 89% (DD) is a very hydrophobic molecule that is practically insoluble in water (Wishart et al. 2007). A stock solution of DD was prepared by dissolving 10 μ l of DD into 90 μ l of absolute methanol with subsequent dilution in 9900 μ l of 0.2 M KCl. To evaluate the general effect of DD by immersion, subsequently, five more working solutions were prepared by making 10 \times serial dilution into dechlorinated tap water to give the required experimental concentrations of DD. Consequently, dechorionated embryos at 0 h post-fertilization (hpf) were transferred to six-well plates containing 0–10⁻⁶ % of DD for ~2 h at 18 °C. Methanol had no effect up to 0.09% v/v on the cleavage pattern. For the microinjection of DD, 1% of FITC-biotin-dextran (MW = 500,000, Sigma-Aldrich, Germany) dissolved in 0.2 M KCl was utilized as a co-injection with the working solution. The FITC ensured microinjection control and tracing of injected blastomere as described previously (Saito and Psenicka 2015). For microinjection of CB, serial 10 \times dilutions of the stock solution (10 mg/ml DMSO) were performed in 0.2 KCL to acquire 1 mg > 100 μ g > and 10 μ g. DMSO had no effect (up to 10% v/v)—same percentage as 1 mg/ml of CB. All working solutions were centrifuged at 10,000 g for 5 min to prevent the blockage of the glass capillary. A glass micropipette was drawn from a glass needle (Drummond, Tokyo, Japan) using a needle puller

(PC-10; Narishige, Tokyo, Japan). Microinjection was conducted under a Leica M165 FC fluorescence stereomicroscope, (Leica, Wetzlar, Germany) using an automatic micro-injector (FemtoJet, Eppendorf) with a pressure of 100 hPa for ~1 s.

Optimization of treatment for the inhibition of definite blastomere cleavage

The working concentrations of DD (0.0001–0.1%) tested under irradiance of a halogen light source (the KL 2500 LCD emits high-intensity light and is mainly used for laboratory applications) and dark/without irradiance were experimentally selected through preliminary experiments. Based on the three replicates for DD concentration under halogen light that were tested, they were then considered for optimization of light conditions. To optimize the intensity and wavelength of light, embryos were injected with 0.0001–0.01% DD into one blastomere at the two-cell stage and were irradiated using a halogen light source along with bandpass and longpass color glass filters with selective wavelengths (Knight Optical UK Ltd). The glass filters separated light into ultraviolet B and A (UV, B–A) and visible light (245–390 nm, 335–445 nm, and 395–700 nm), respectively. The light intensity was measured by the Blak-Ray[®] UV intensity meter (Analytik Jena US) and LI-250A light meter (LI-COR GmbH, Germany). The final optimal concentration of DD and lighting conditions were chosen based on the proportion of cleavage inhibition of treated blastomeres until the 1000-cell stage. Thereafter, all partially cleaved A-V embryos lost their viability, except vegetal blastomere-inhibited embryos.

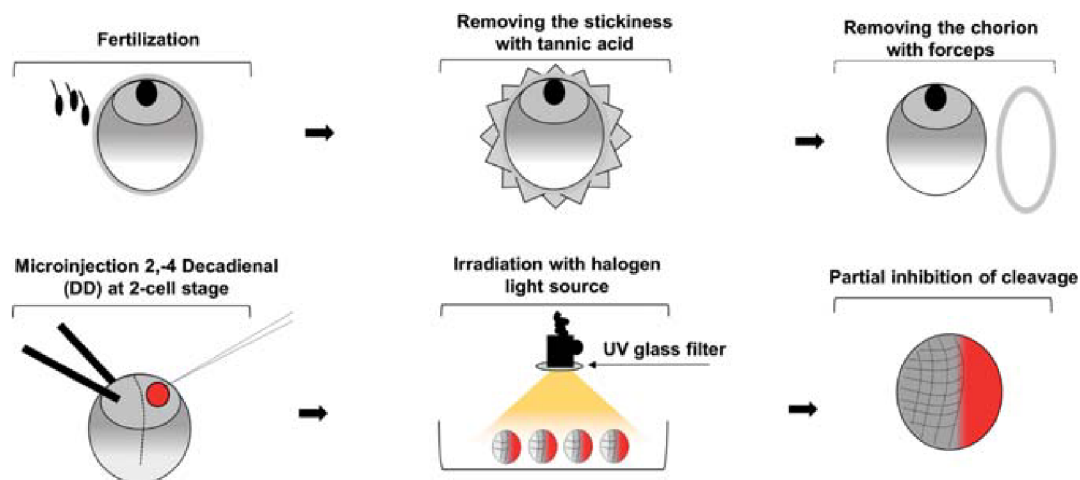


Fig. 1 Schematic of definite blastomere inhibition by DD injection and light irradiation

Irradiance-dependent inhibition of specific blastomeres

Revealing the inhibition of cleavage patterns in DD-injected embryo depends on irradiation. Thus, we used three more approaches: Firstly, the embryos were injected with 0.01% DD into one blastomere at the two-cell stage and were kept in a dark incubator at 16 °C. Subsequently, embryos from each consecutive developmental stage 5–11 were irradiated under optimized light for the next two cell cycles [we followed the description of the developmental stages as described previously by Ginsburg and Dettlaff (1991)]. Secondly, to inhibit the targeted blastomere only by using the point light irrigation, the visible light intensity was adjusted at 44.86–91.15 W m⁻². Aluminum foil was wrapped around the halogen light source, and a paper pin was used to poke a hole in the foil. The embryos were injected with 0.01% DD at the one-cell stage/0 hpf and were placed on an agar-coated (1%) petri dish filled with dechlorinated tap water. To fix the movement of the embryo, a hole of about 2 mm² was made on the agar with a forceps, and the embryo was placed on it. Thirdly, embryos injected with 0.01% DD into one blastomere and uninjected embryos were placed on a hole in an agar-coated (1%) petri dish, so that the injected blastomere could face upwards. For light irradiation, all other laboratory lights were switched off, and the embryos were exposed to 44.86–91.15 W m⁻². All irradiance-dependent experiments were conducted at an adjusted temperature of ~ 16 °C in the absence of external light.

Embryo imaging and evaluation

After irradiation and non-irradiation treatment, all injected embryos were rechecked based on FITC signal, and inadequately injected embryos were discarded. The images were captured using a Leica M205 FCA stereomicroscope. For the

irradiance-dependent experiment, time-lapse imaging was captured at 30 s intervals for 10 h at 18 °C.

Total RNA extraction and qPCR tomography

Embryos in triplicate from control and treated groups at four-cell (inhibited vegetal blastomere), 256-cell (inhibited A-V blastomeres) and 1000-cell stages (inhibited vegetal blastomeres) were separately embedded in a drop of Tissue-Tek® O.C.T.™ compound at an optimal temperature of the compound on a precooled dissection block. The blocks were kept in a cryostat chamber at a temperature of –18 °C for 10 min to acclimatize to the temperature. All embryos were sectioned into five segments along the A-V axis following the protocol previously used by Sindelka et al. (2010). Total RNA was extracted by using a TRIzol reagent (Invitrogen) according to the manufacturer's instructions and LiCl precipitation. The concentration of RNA was determined with the NanoDrop®ND1000 quantification system (Thermo Scientific). Complementary DNA (cDNA) synthesis was performed using the SuperScript™ III Reverse Transcriptase kit (Invitrogen) and 50 ng of total RNA. cDNA was diluted to a final volume of 100 µl (Pocherniaieva et al. 2018) and stored at –20 °C.

The complete nucleotide sequences of animal localized (axis inhibition protein 1—*axin1*; hyaluronidase 4—*hyal4*) and potentially ubiquitous (cyclin-dependent kinase 1-B—*cdk1b*, caspase-3—*casp3*) genes were identified from a de novo assembled sterlet oocyte transcriptome (Laboratory of Germ Cells, unpublished data). Gene searches were carried out with BLAST using the NCBI/GenBank database based on the highest pairwise identity, the highest bit score, and the lowest e-value. Primer sequences were designed using Primer3 (<http://bioinfo.ut.ee/primer3-0.4.0/>). Primer for vegetal localized (dead end protein 1—*dnd1*; DEAD-box helicase—*vasa*) genes were obtained from Pocherniaieva et al. (2018) (Table 1). qPCR reaction of total volume of 7 µl

Table 1 Primers sequences for RT-qPCR

Gene	Sequence 5'-3'	PCR product (bp)	Accession number/Reference
<i>axin1</i>	AGGCCAAACAGAGGCATAGA CTTCGCGAACCTCTTCAAAC	228	XM_034926901.1
<i>hyal4</i>	GGATGACTGCATCCGAAAGT CACCGATGGTGTGAATCAAG	164	XM_034019743.2
<i>casp3</i>	TTTTGTGTGTGCACTGCTGA TCTGGGGAGAGCTGCTCACTT	215	XM_034014535.2
<i>cdk1b</i>	CAATGATGTTGGCCAGATG TGGTTAAGGGATTGCTTTGC	180	XM_034025100.2
<i>dnd1</i>	GGACTCAGAAAATGGGGATCTCCCTGG AAACCTCACAGCCAGAGGAAGGGGG	108	Pocherniaieva et al. (2018)
<i>vasa</i>	CAAGAATATCAGTAAATCGGGG GATCTGGTTTATTAGCTCTCTTGTT	244	Pocherniaieva et al. (2018)

contained 2 μ l of cDNA, 0.29 μ l of the forward and reverse primers (10 μ M), 3.5 μ l of TATAA SYBR GrandMaster Mix (TATAA Biocenter) and deionized water. The cycling conditions of the PCR real-time CFX384 cycler system (Bio-Rad) were as follows: 3 min at 95 °C, 45 cycles of 95 °C for 15 s, 60 °C for 20 s, and 72 °C for 20 s. The melting curve was recorded from 65 to 95 °C at 0.5 °C intervals.

Statistical analysis

The percentage of embryos arrested after different treatments; the working concentrations of DD (set as a continuous variable) and the light irradiance (set as a discrete variable) were analyzed using logistic regression and the post hoc Tukey test in R (v. 3.6.2.). Subsequently, the percentage of maternal mRNA localization in treated vs. control embryos from the A-V axis were calculated as described by Sindelka et al. (2010), and then data were transformed using centered

log ratio transformation and analyzed by ANOVA and Tukey test in R (v. 3.6.2.).

Results

Effect of 2,4-trans,trans-decadienal on sturgeon embryo cleavage

The aim of this study was to reveal whether DD adversely affects the cleavage of sturgeon embryos. The one-cell embryos immersed in 0.001–0.1% DD solution under dark conditions (without irradiance) showed adverse effects on cleavage, whereas 0.000001–0.0001% DD was unable to exert an adverse effect on the cleavage pattern (Fig. 2 and Table 2). Conversely, two-cell embryos injected with 0.01% DD into one blastomere and incubated in the dark showed a normal cleavage pattern as compared to uninjected ones.

Fig. 2 General (immersion) effect of DD on the cleavage pattern of sturgeon embryo shows the animal view of embryos that were immersed in DD 10^{-6} –0.1% (a–f)

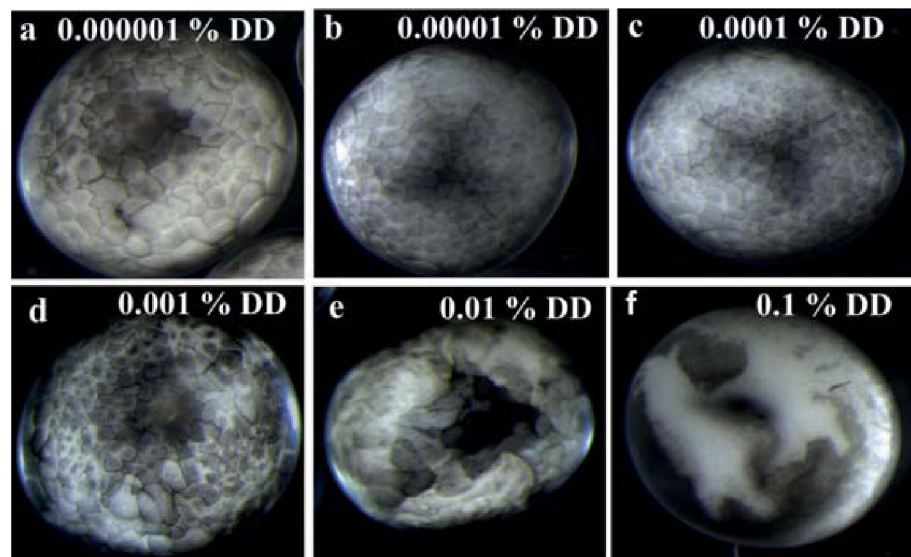


Table 2 General/immersion effect of DD on cleavage pattern

No. of embryos in triplicate	Concentration of DD v/v (%)	Number (%) of abnormal cleaved embryos	Number (%) of normal cleaved embryos
20	0.000001	0 (0%)	20 (100%)
17	0.00001	0 (0%)	17 (100%)
23	0.0001	0 (0%)	23 (100%)
23	0.001	23 (100%)	0 (0%)
21	0.01	21 (100%)	0 (0%)
21	0.1	21 (100%)	0 (0%)
24	Methanol control (0.09)	0 (0%)	24 (100%)
40	Dechlorinated water	0 (0%)	40 (100%)

Table shows that embryos that were immersed in DD up to 0.001% cleaved abnormally (see Fig. 2), whereas embryos immersed in methanol up to 0.09 cleaved normally, as in dechlorinated water

Embryos injected with 0.01% DD and irradiated using a halogen lamp ($\sim 91.15 \text{ W m}^{-2}$) for the next two cell cycles showed 100% cleavage inhibition in treated blastomeres (Figs. 3, 4).

Optimal DD concentration and light conditions for inhibition of definite blastomere cleavage

The embryos injected with 0.01% DD and irradiated under UV light with intensity and wavelength of $20 \mu\text{W/cm}^2$ and 245–390 nm, and 335–445 nm, respectively, did not show any effect on the cleavage (Fig. 4). Comparatively, embryos injected with 0.01% DD and irradiated by light with intensity and wavelength $44.86\text{--}91.15 \text{ W m}^{-2}$ and 395–700 nm, respectively, were found to be significantly more efficient

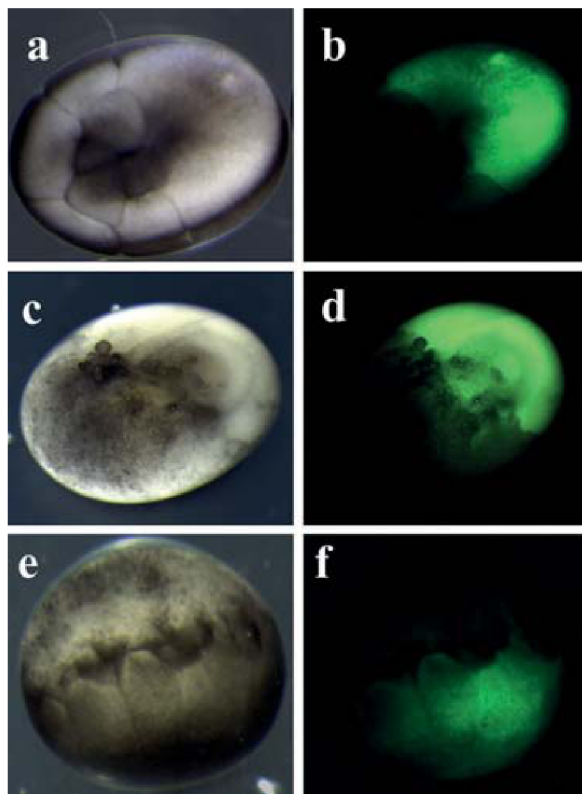


Fig. 3 Inhibition of cleavage in definite blastomere of sturgeon embryos. **a–d** Animal view of embryos with blastomere cleavage inhibition; the blastomere was injected with 0.01% DD into the animal pole blastomere at the two-cell stage and irradiated by visible light (395–700 nm) with intensity of $44.86\text{--}91.15 \text{ W m}^{-2}$ for the next two cell cycles: bright and fluorescent view at 16-cell stage (**a–b**), bright and fluorescent view at 1000-cell stage (**c–d**). **e–f** Shows lateral (A–V) view of embryos with inhibition of cleavage at the VP; the embryos were injected with 0.01% DD into the VP at the two-cell stage and irradiated by visible light (395–700 nm) with intensity of $44.86\text{--}91.15 \text{ W m}^{-2}$ for the next four cell cycles: bright and fluorescent view at 1000-cell stage

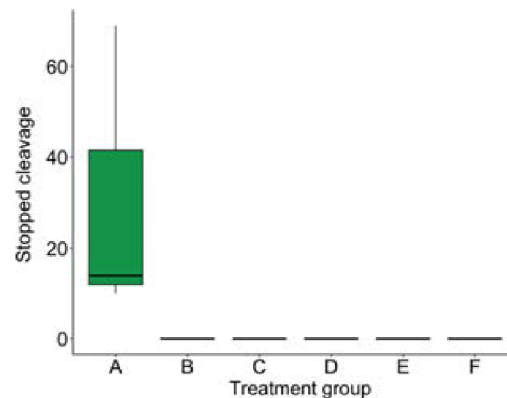


Fig. 4 Optimization of light type for irradiation. Represents the working condition of cleavage inhibition: the Y-axis represents the number of embryos with inhibited cleavages, and the X-axis represents different condition for inhibition of blastomere cleavage. **a**=injected with 0.01% DD and irradiated by halogen light ($\sim 91.15 \text{ W m}^{-2}$), **b**=injected with 0.01% DD and irradiated by UV-B ($20 \mu\text{W/cm}^2$ and 245–390 nm), **c**=injected with 0.01% DD and irradiated by UV-A ($20 \mu\text{W/cm}^2$ and 335–445 nm), **d**=injected with DD (0.01%) and unirradiated, and **e**, **f**=uninjected control, irradiated ($44.86\text{--}91.15 \text{ W m}^{-2}$ and 395–700 nm) and unirradiated, respectively

as compared to irradiance at 18.65 W m^{-2} and 395–700 nm and injection with 0.0001–0.001% DD and irradiance at $18.65\text{--}91.15 \text{ W m}^{-2}$ and 395–700 nm (Fig. 5). The animal pole blastomere remained uncleaved after irradiation for the next two cell cycles. However, the vegetal blastomeres were larger than the animal blastomeres; therefore, for complete inhibition, vegetal blastomeres were irradiated for the next four cell cycles. The embryos with inhibited cleavage in the animal blastomere died before gastrulation; however, embryos with inhibited cleavage in the vegetal blastomere developed as usual (Fig. 3).

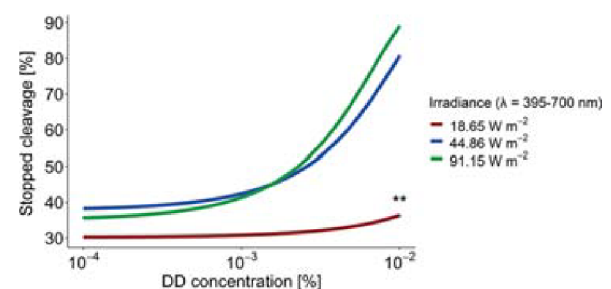


Fig. 5 Optimization of DD concentration under different visible light conditions. Shows resulting light conditions after using different concentrations of DD: the Y-axis represents the proportion of stopped cleavage, and the X-axis represents concentration of DD. Different colors represent different intensities of visible light for irradiation observed after using different concentrations of DD. The asterisks indicate the statistically significant difference between the treatments

Irradiance-dependent inhibition of specific blastomeres at different developmental stages

All irradiance-dependent experiments revealed that DD injection or light irradiation alone cannot stop the blastomere cleavage. For instance, (1) the embryos that were injected by 0.01% DD into the animal blastomere at the two-cell stage and uninjected embryos irradiated under the same visible light condition showed that only injected blastomere remained undivided, whereas irradiation itself could not harm embryos (Online Resource time-lapse recording. mpeg). (2) The embryos injected by 0.01% DD at the 2–4-cell stage into one blastomere and irradiated consecutively at the 5–11-developmental stage showed that only DD-containing blastomeres were inhibited compared to un-irradiated/control embryos (Fig. 6 and Online Resource Table S-1). (3) The embryo that was injected with 0.01% DD at the one-cell stage (whole embryo contained DD solution) and irradiated by point visible light ($44.86\text{--}91.15\text{ W m}^{-2}$) showed the inhibition of cleavage in a portion of the embryo that was only irradiated, and the rest of the embryo cleaved normally (Fig. 7). It was thus confirmed that DD injection or light irradiation alone is unable to inhibit the cleavage.

Effect of cytochalasin-B on blastomere cleavage compared to the present technique

Cytochalasin-B (CB) is a potent microfilament inhibitor, and its injection up to 1 mg/ml can harm the cleavage pattern. Compared to the present technique, the action of CB was not defined in either animal blastomere or vegetal blastomere, and more importantly, the location of the injection appears as a cyst-like structure. Also, injected embryos lost viability due to its high toxicity (Fig. 8a–b and e–f). However, the present technique using DD shows that only the treated blastomeres remained undivided, and the rest of the embryos cleaved as usual (Fig. 8c–d and g–h).

Localization of maternal mRNA

During embryo development, the pre-pattern of differentially localized mRNA and protein deposition is the basis of the precisely controlled process of cell differentiation and germ layer patterning (Pocherniaieva et al. 2018). We tested the question whether the inhibition of cleavage pattern degrades or affects the localization patterns of maternally supplied mRNA. Here, qPCR tomography revealed that treatment does not have an effect on the localization pattern and/or degradation of maternal mRNA, i.e., the pattern of RNA gradient remained equilibrated with the inhibition of cleavage from the A-V axis as compared to control groups (Fig. 9).

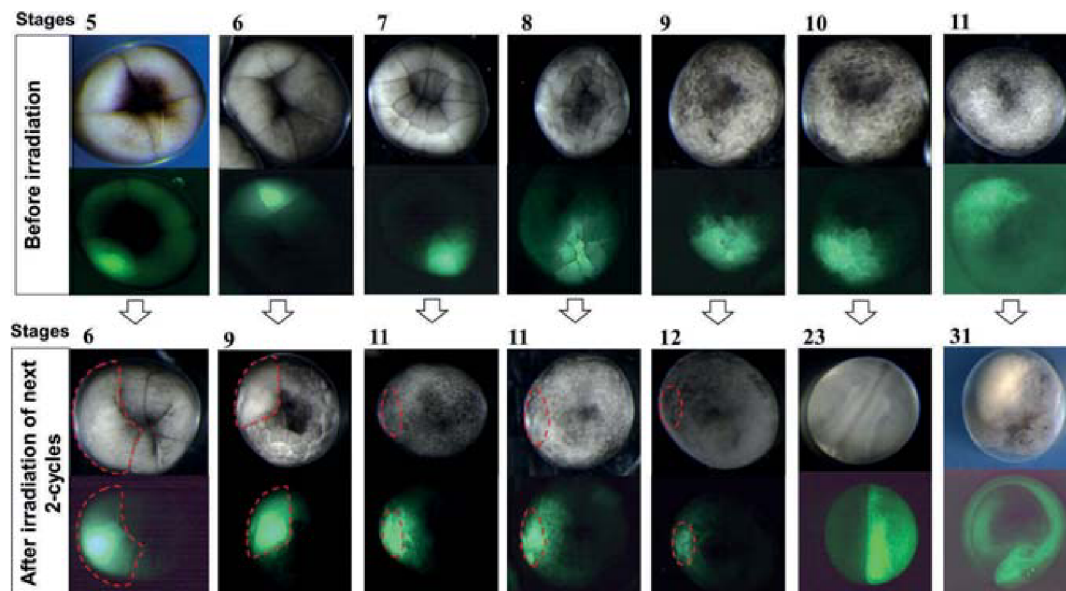


Fig. 6 Irradiation-dependent blastomere inhibition at different stages of development. Shows the effect of DD concentration in the presence and absence of light exposure. Before irradiation: all embryos injected with DD into one blastomere of the animal pole at the two-

cell stage and incubated in a dark incubator show a normal cleavage pattern from the four-cell stage to the late blastula stage. After irradiation: cleavage arrest at the blastomere from the eight-cell stage to the late blastula stage after irradiation of the next two cell cycles

Fig. 7 Cleavage inhibition at a specific blastomere in sturgeon embryos. Shows the schematic of specific blastomere inhibition by DD injection and point-light irradiation. The bright and florescent view of specific blastomeres of embryos remained uncleaved (marked with red dashed line). These embryos were injected at the one-cell stage (0-hpf) and were kept under darkness at controlled temperature. Only the specific blastomeres were irradiated, and they showed cleavage inhibition (colour figure online)

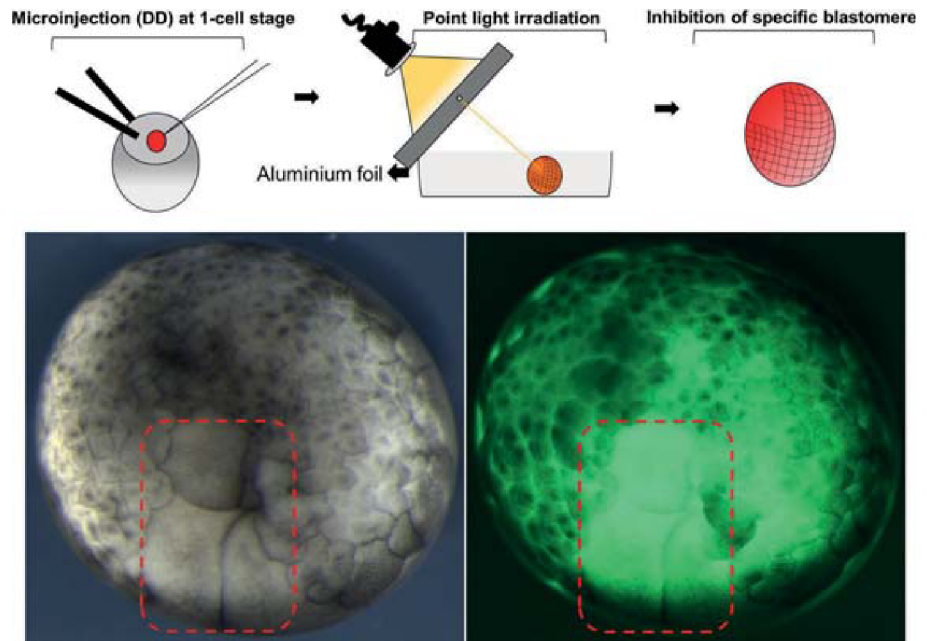
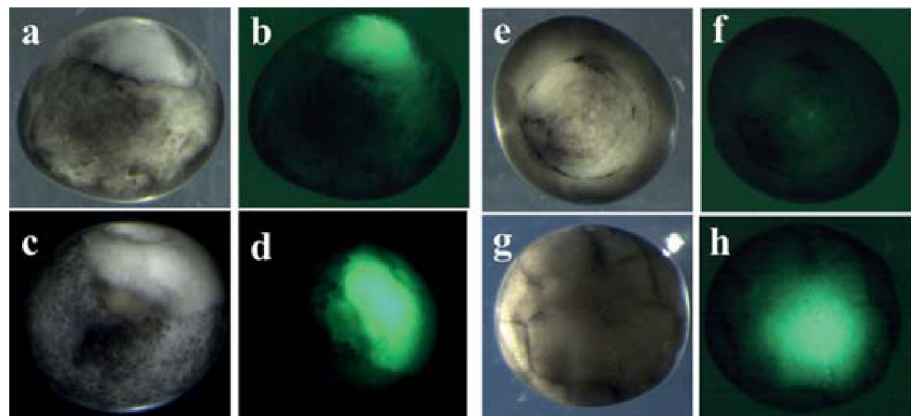


Fig. 8 Effect of cytochalasin-B on the cleavage pattern and its comparison with the current technique. Shows the comparative effect of microinjection of CB and DD plus visible light irradiation on inhibition of blastomere cleavage (a–h): Embryos injected with CB (1 mg/ml); animal view (a–b) and vegetal view (e–f). Embryos injected with 0.01% DD and irradiation by visible light (44.86–91.15 W m⁻²); animal view (c–d) and vegetal view (g–h)



Discussion

Several techniques have already been used to study the development of *Mus musculus* and *Xenopus laevis* embryogenesis by inhibition of blastomere cleavage, including strong magnetic fields, injection of mycotoxin (cytochalasin-B), cytostatic factors (*c-mos*), and kinase proteins (MAPK and PAK 1) (Haccard et al. 1993; Karasiewicz and Sottyfiska 1986; Masui 2000; Rooney et al. 1996; Siegfried et al. 1973; Valles et al. 2002; Yew et al. 1991). The strong magnetic field is a mechanical approach to alter the geometry of the first two cleavage furrows; however, it does not completely stop the cleavage (Valles et al. 2002). Microinjection of CB (10 µg/ml) has been reported to cause the regression of early cleavage furrows in *Xenopus laevis*

embryos (Siegfried et al. 1973); however, owing to its slow distribution, it does not stop the definite blastomere, and its high toxicity can damage the embryo. However, we also employed CB (1 mg > 100 µg > and 10 µg) into sturgeon embryos, and only 1 mg/ml harmed the cleavage pattern; nonetheless, the inhibition of the blastomere was not specific, and a cyst-like structure was observed at the site of injection owing to its high toxicity (Fig. 8). Moreover, the optimal amount of *c-mos* RNA (ng/blastomere) has been reported to cause the arrest of blastomere cleavage in different vertebrates (Buchholz et al. 2007; Masui 2000; Sagata et al. 1989). Despite the efficiency of *c-mos* microinjection, this technique entails a prolonged and complicated process, such as plasmid constructions for non-model species and the amount of RNA or number of injections (Buchholz et al. 2007; Yew et al. 1991).

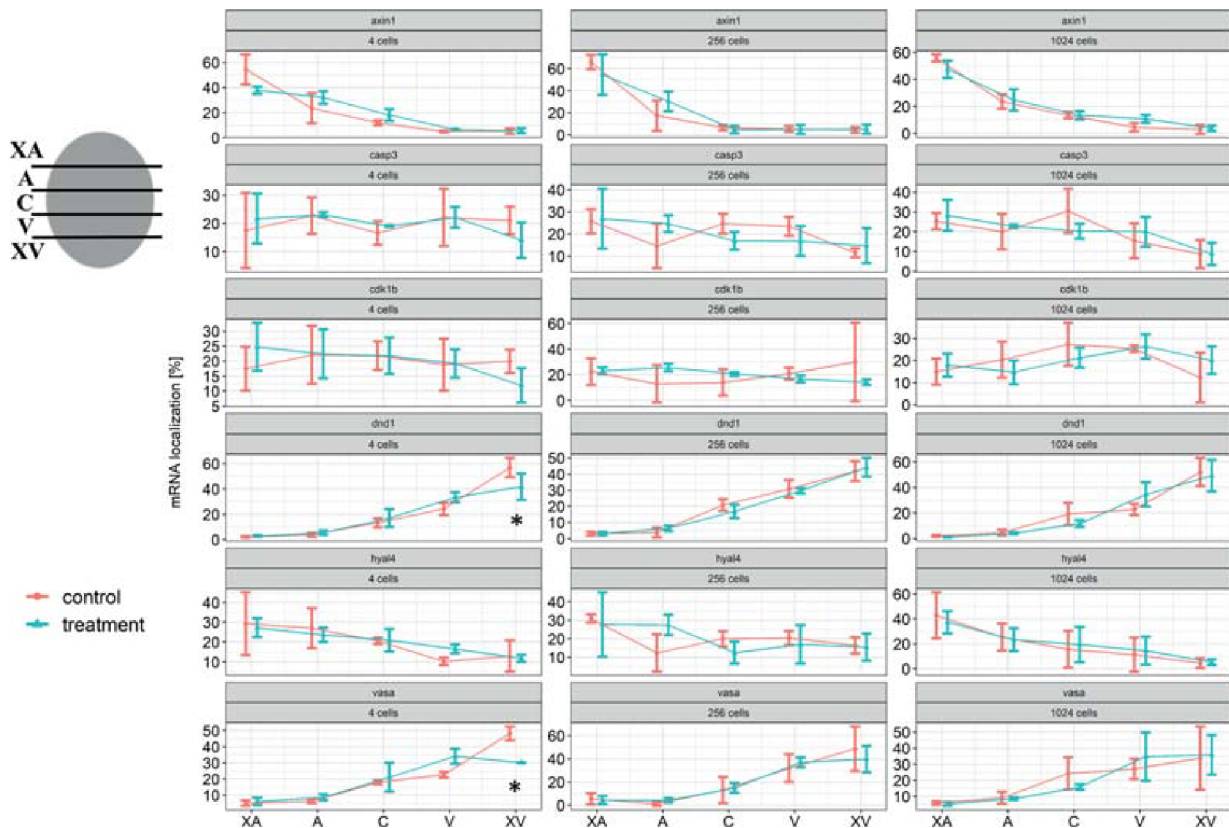


Fig. 9 Effect of cleavage inhibition on maternal RNA localization. Shows the localization pattern of maternal RNA: the Y-axis represents percentage of RNA in a specific part (complete embryo has 100%), and the X-axis represents each part of the embryo from animal to vegetal (XA—extreme animal; A—animal; C—center; V—vegetal; XV—extreme vegetal). The horizontal column shows developmental stages of embryos; 4-cell stage of embryos, 256-

cell stage of embryos and 1000-cell stage of embryos. The vertical column shows the number of selected genes in each developmental stage. Orange color=controlled (without inhibition of cleavage). Green color=treated (with inhibition of cleavage). The percentage of mRNA at specific portions of embryos before and after treatment were shown in mean and standard error, and the asterisks indicate a significant difference (colour figure online)

Additionally, PAK1 (p58) or the active catalytic domain (p37) and MAPK injection have also been reported to cause the arrest of cleavage/division of blastomeres in the *Xenopus laevis* embryo (Haccard et al. 1993; Rooney et al. 1996). In fact, the microinjection of kinase proteins also has certain limitations, such as the amount of its injection (pg or nl/blastomere), and is also not ideal for non-model species (Haccard et al. 1993; Rooney et al. 1996; Yew et al. 1991). Compared with earlier methods, we present a more convenient, economical and efficient technique to inhibit or arrest specific blastomere cleavage by utilizing a combination of the optimal amount of DD (0.01%) injection and light irradiation (44.86–91.15 W m⁻²) (Figs. 3, 5), which could be employed for other non-model fish species.

To the best of our knowledge, DD has previously been employed only by the immersion method. Several studies have reported that the embryos and gametes of several aquatic animals including ascidians (Tosti et al. 2003),

copepods (Ianora et al. 2003; Romano 2003), sea urchins (Hansen et al. 2004; Romano 2003; Romano et al. 2011, 2010), polychaetes *Arenicola marina* and *Nereis virens*, and echinoderms *Asterias rubens* and *Psammechinus miliaris* (Caldwell et al. 2004, 2002) showed delay development and malformation when they were immersed in a lethal concentration of DD. In our present study, we have also consistently observed that DD adversely impacts development of *Acipenser ruthenus* embryos incubated in DD even at very low concentrations (Fig. 2 and Table 2). Here, we also have employed DD treatment in specific blastomeres of sturgeon embryos through microinjection. However, DD (0.1%) injection alone was unable to arrest the blastomere cleavage.

Moreover, a high dosage of UV-B irradiation has been reported as dangerous for embryonic development and larval fitness of sea urchins (Bonaventura et al. 2006; Zhao et al. 2018). UV-B irradiation has also been reported to induce the activation of mitogen-activated protein kinase phosphatase

I (MKP1) and its targets MPK6 and MPK3 which interact with hydrogen peroxide and NO in UV-B guard cell signaling. In addition, DD induces the reduction of endogenous NO levels that leads to the early upregulation of MKP1 (responsible for the ERK signalling pathway) (Castellano et al. 2015; Li et al. 2017). On the one hand, Rutz et al. showed that visible light irradiation (abiotic stress) could ameliorate the anticancer effect of low-dosed curcumin (*Curcuma longa*) on several tumor types. However, curcumin or light exposure alone could not be found to alter the growth, proliferation and apoptosis of renal carcinoma cell lines (Rutz et al. 2019). On the other hand, DD has also been reported to block cell division and arrest the proliferation of human carcinoma cells (Miralto et al. 1999). However, the combined effect of DD and light irradiation has not yet been investigated in any field of biology. These findings led us to investigate the combined effect of DD injection and light irradiation in specific blastomeres of sturgeon embryos. We had previously reported the elimination of PGCs by UV (254 nm) irradiation (Saito et al. 2018). Interestingly, UV (245–395 nm) irradiation has not been found to alter the cleavage pattern in injected or uninjected embryos; only the combination of DD (0.01%) injection and light irradiation (44.86–91.15 W m⁻² + 395–700 nm) was found to be effective in inhibiting blastomere cleavage (Figs. 3, 4 and 5), which could be used to investigate the blastomere contribution to embryo development (Buchholz et al. 2007) (Figs. 3, 4 and 5). Consequently, the findings presented here may also help to establish a new therapeutic window for carcinoma cell treatment.

During oogenesis, the distribution of maternal mRNAs and proteins along the A-V axis in the oocyte is critical for successful development (Pocherniaieva et al. 2018). Therefore, it was also necessary to confirm whether DD treatment impacts the re-localization of maternal mRNA in developing embryos. The animal blastomere of the sturgeon embryos is relatively smaller than that of the vegetal blastomere and contains the germ-layer patterning determinants (Ginsburg and Dettlaff 1991; Pocherniaieva et al. 2018). Nevertheless, we found that treatment for blastomere inhibition does not influence the patterns of differentially localized mRNA in the AP (Fig. 9). The vegetal blastomeres of sturgeon embryos contain PGC determinants (e.g., *dnd1* and *vasa*) and the large portion of the yolk cells that serve only for nutrition (Saito et al. 2014; Pocherniaieva et al. 2018). qPCR tomography showed treatment for vegetal blastomere inhibition did not cause any alteration in whole mRNA gradient at the VP. Only small differences were observed in *dnd1* and *vasa* gradients at the four-cell stage, especially at the extremely vegetal portion of embryos. This small error could be assumed to be due to sectioning of embryos (Fig. 9). However, we can speculate that DD treatment may affect other molecule localizations such as proteins in normal and

inhibited blastomeres. Further research could be conducted on proteomics and transcriptomics to uncover the set of regulatory and kinases proteins and defensomes, respectively, which might be altered by biotic and abiotic stresses.

To understand the development of the sturgeon embryo, a comprehensive understanding of the contribution of early blastomeres to adult tissues is needed. So far, it is clear that sturgeon PGCs are formed in the vegetal pole; therefore, further research could also be conducted to determine (1) whether PGCs are formed after complete inhibition of VP cleavage, or (2) after VP inhibition and embryos switch to “meroblastic cleavage,” whether the embryo pattern develops yolk streams or YSL-like teleosts, which can help to understand the transition of the cleavage pattern.

Acknowledgements The authors are grateful to all lab members of the Laboratory of Germ Cells, Faculty of Fisheries and Protections of Waters, University of South Bohemia in Ceske Budejovice for their help during the experiments. The authors thank the Ministry of Education, Youth and Sports of the Czech Republic project CENAKVA (LM2018099), Biodiversity (CZ.02.1.01/0.0/0.0/16_025/0007370), Czech Science Foundation (20-23836S) and Grant Agency of the University of South Bohemia (036/2020/Z) for their financial support.

Author contributions Conceptualization: MAS, MP; methodology: MAS, VI; formal analysis and investigation: RF, MR, TT; writing—original draft preparation: MAS; writing—review and editing: MAS, TS, RŠ, ARB, MP, VI; supervision: MP.

Compliance with ethical standards

Conflict of interest All authors declare that they have no conflict of interest.

References

- Amores A, Force A, Yan YL, Joly L, Amemiya C, Fritz A, Ho RK, Langeland J, Prince V, Wang YL, Westerfield M, Ekker M, Postlethwait JH (1998) Zebrafish hox clusters and vertebrate genome evolution. *Science* 282:1711–1714
- Ballard WW (1986) Stages and rates of normal development in the holostean fish, *Amia calva*. *J Exp Zool* 238:337–354
- Ballard WW, Ginsburg AS (1980) Morphogenetic movements in acipenserid embryos. *J Exp Zool* 213:69–103
- Baloch AR, Fu M, Rodina M, Metscher B, Tichopád T, Shah MA, Fran R, Psěnička M (2019) Delivery of iron oxide nanoparticles into primordial germ cells in sturgeon. *Biomolecules* 333:1–10
- Bartsch P, Gemballa S, Piotrowski T (1997) The embryonic and larval development of *Polypterus senegalus* cvier, 1829: Its staging with reference to external and skeletal features, behaviour and locomotory habits. *Acta Zool* 78:309–328
- Bolker JA (1993) Gastrulation and mesoderm morphogenesis in the white sturgeon. *J Exp Zool* 266:116–131
- Bolker JA (1994) Comparison of gastrulation in frogs and fish. *Integr Comp Biol* 34:313–322
- Bonaventura R, Poma V, Russo R, Zito F, Matranga V (2006) Effects of UV-B radiation on development and hsp70 expression in sea urchin cleavage embryos. *Mar Biol* 149:79–86

- Buchholz DR, Singamsetty S, Karadge U, Williamson S, Langer CE, Elinson RP (2007) Nutritional endoderm in a direct developing frog: a potential parallel to the evolution of the amniote egg. *Dev Dyn* 236:1259–1272
- Caldwell GS, Olive PJWW, Bentley MG (2002) Inhibition of embryonic development and fertilization in broadcast spawning marine invertebrates by water soluble diatom extracts and the diatom toxin 2-trans,4-trans decadienal. *Aquat Toxicol* 60:123–137
- Caldwell GS, Bentley MG, Olive PJW (2004) First evidence of sperm motility inhibition by the diatom aldehyde 2 E, 4 E -decadienal. *Mar Ecol Prog Ser* 273:96–108
- Castellano I, Ercolesi E, Romano G, Ianora A, Palumbo A, Palumbo A (2015) The diatom-derived aldehyde decadienal affects life cycle transition in the ascidian *Ciona intestinalis* through nitric oxide/ERK signalling. *Open Biol* 5:1–10
- Chiu CH, Dewar K, Wagner GP, Takahashi K, Ruddle F, Ledje C, Bartsch P, Scemama JL, Stellwag E, Fried C, Prohaska SJ, Stadler PF, Amemiya CT (2004) Bichir HoxA cluster sequence reveals surprising trends in ray-finned fish genomic evolution. *Genome* 14:11–17
- Cooper MS, Virta VC (2007) Evolution of gastrulation in the ray-finned (actinopterygian) fishes. *J Exp Zool B Mol Dev Evol* 308:591–608
- Cutignano A, D'Ippolito G, Romano G, Lamari N, Cimino G, Febbraio F, Nucci R, Fontana A (2006) Chloroplastic glycolipids fuel aldehyde biosynthesis in the marine diatom *Thalassiosira rotula*. *ChemBioChem* 7:450–456
- Fontana A, D'Ippolito G, Cutignano A, Romano G, Lamari N, Gallucci AM, Cimino G, Miralto A, Ianora A (2007) LOX-induced lipid peroxidation mechanism responsible for the detrimental effect of marine diatoms on zooplankton grazers. *ChemBioChem* 8:1810–1818
- Ginsburg AS, Dettlaff TA (1991) The Russian sturgeon *Acipenser Guldenstädti*. Part I. Gametes and early development up to time of hatching. In: Dettlaff T.A., Vassetzky S.G. (eds) *Animal Species for Developmental Studies*. Springer, Boston, pp 15–65
- Haccard O, Sarcevic B, Lewellyn A, Hartley R, Roy L, Izumi T, Erikson E, Maller JL (1993) Induction of metaphase arrest in cleaving *Xenopus* embryos by MAP kinase. *Science* 262:1262–1265
- Hansen E, Even Y, Genevière AM (2004) The α , β , γ , δ -unsaturated aldehyde 2-trans-4-trans-decadienal disturbs DNA replication and mitotic events in early sea urchin embryos. *Toxicol Sci* 81:190–197
- Hurley IA, Mueller RL, Dunn KA, Schmidt EJ, Friedman M, Ho RK, Prince VE, Yang Z, Thomas MG, Coates MI (2007) A new time-scale for ray-finned fish evolution. *Proc Royal Soc B* 274:489–498
- Ianora A, Zoologica S, Dohrn A (2003) The effects of diatoms on copepod reproduction: a review. *Phycologia* 42:351–363
- Karasiewicz J, Sottifiska MS (1986) Effects of cytochalasin B on the cleavage furrow in mouse blastomeres. *Wilehm Roux Arch Dev Biol* 195:137–141
- Li FC, Wang J, Wu MM, Fan CM, Li X, He JM (2017) Mitogen-activated protein kinase phosphatases affect UV-B-induced stomatal closure via controlling NO in guard cells. *Plant Physiol* 173:760–770
- Long WL, Ballard WW (2001) Normal embryonic stages of the long-nose gar *Lepisosteus osseus*. *BMC Dev Biol* 1:6. <https://doi.org/10.1186/1471-213X-1-6>
- Mann DG (1999) The species concept in diatoms. *Phycologia* 38:437–495
- Masui Y (2000) The elusive cytostatic factor in the animal egg. *Nat Rev Mol Cell Biol* 1:228–231
- Minarik M, Stundl J, Fabian P, Jandzik D, Metscher BD, Psenicka M, Gela D, Osorio-pérez A, Arias-rodríguez L, Horáček I, Cerný R (2017) Pre-oral gut contributes to facial structures in non-teleost fishes. *Nature* 547:209–212
- Miralto A, Barone G, Romano G, Poulet SA, Ianora A, Russo GL, Buttino I, Mazzarella G, Laablr M, Cabrini M, Glacobbe MG (1999) The insidious effect of diatoms on copepod reproduction. *Nature* 402:173–176
- Okado H, Takahashi K (1988) A simple “neural induction” model with two interacting cleavage-arrested ascidian blastomeres. *Proc Natl Acad Sci U S A* 85:6197–6201
- Pocherniaieva K, Psenicka M, Sidova M, Havelka M, Saito T, Sindelka R, Kaspar V (2018) Comparison of oocyte mRNA localization patterns in sterlet *Acipenser ruthenus* and African clawed frog *Xenopus laevis*. *J Exp Zool B Mol Dev Evol* 330:181–187
- Pohnert G (2000) Wound-activated chemical defense in unicellular planktonic algae. *Angew Chem Int Ed* 39:4352–4354
- Poulet S, Lange M, Cordevant C, Adolph S, Cuffe A, Pohnert G, Lumineau O (2007) Are volatile unsaturated aldehydes from diatoms the main line of chemical defence against copepods? *Mar Ecol Prog Ser* 245:33–45
- Ravi V, Venkatesh B (2008) Rapidly evolving fish genomes and teleost diversity. *Curr Opin Genet Dev* 18:544–550
- Romano G (2003) A marine diatom-derived aldehyde induces apoptosis in copepod and sea urchin embryos. *J Exp Biol* 206:3487–3494
- Romano G, Miralto A, Ianora A (2010) Teratogenic effects of diatom metabolites on sea urchin *Paracentrotus lividus* embryos. *Mar drugs* 8:950–967
- Romano G, Costantini M, Buttino I, Ianora A, Palumbo A (2011) Nitric oxide mediates the stress response induced by diatom aldehydes in the sea urchin *Paracentrotus lividus*. *PLoS ONE* 6(10):e25980. <https://doi.org/10.1371/journal.pone.0025980>
- Rooney RD, Tuazon PT, Meek WE, Carroll EJ, Hagen JJ, Gump EL, Monnig CA, Lugo T, Traugh JA (1996) Cleavage arrest of early frog embryos by the G protein-activated protein kinase PAK I. *J Biol Chem* 271:21498–21504
- Rutz J, Maxeiner S, Juengel E, Bernd A, Kippenberger S, Zöllner N, Chun FKH, Blaheta RA (2019) Growth and proliferation of renal cell carcinoma cells is blocked by low curcumin concentrations combined with visible light irradiation. *Int J Mol Sci* 20(6):1464. <https://doi.org/10.3390/ijms20061464>
- Sabharwal T, Sathasivan K, Mehdy MC (2017) Defense related decadienal elicits membrane lipid remodeling in the diatom *Phaeodactylum tricoratum*. *PLoS ONE*. <https://doi.org/10.1371/journal.pone.0178761>
- Sagata N, Watanabe N, Vande Woude GF, Ikawa Y (1989) The c-mos proto-oncogene product is a cytostatic factor responsible for meiotic arrest in vertebrate eggs. *Nature* 342:512–518
- Saito T, Psenicka M (2015) Novel technique for visualizing primordial germ cells in sturgeons (*Acipenser ruthenus*, *A. gueldenstaedtii*, *A. baerii*, and *Huso huso*). *Biol Reprod* 93:1–7
- Saito T, Pšenička M, Goto R, Adachi S, Inoue K, Arai K, Yamaha E, Pšenička M, Goto R, Adachi S, Inoue K, Arai K, Yamaha E (2014) The origin and migration of primordial germ cells in sturgeons. *PLoS ONE* 9(2):e86861. <https://doi.org/10.1371/journal.pone.0086861>
- Saito T, Hilal G, Iegorova V, Rodina M, Psenicka M (2018) Elimination of primordial germ cells in sturgeon embryos by ultraviolet irradiation. *Biol Reprod* 99:556–564
- Sander K (1997a) “Mosaic work” and “assimilating effects” in embryogenesis: Wilhelm Roux’s conclusions after disabling frog blastomeres. In: Sander K et al (eds) *Landmarks in Developmental Biology 1883–1924: Historical Essays from Roux’s Archives*. Springer, Berlin Heidelberg, pp 13–15. https://doi.org/10.1007/978-3-642-60492-8_5
- Sander K (1997b) Shaking a concept: Hans Driesch and the varied fates of sea urchin blastomeres. In: Sander K et al (eds) *Landmarks in Developmental Biology 1883–1924: Historical Essays from Roux’s Archives*. Springer, Berlin Heidelberg, pp 29–31. https://doi.org/10.1007/978-3-642-60492-8_10

- Siegfried W, De L, Luchtel D, Bluemink JG (1973) The action of cytochalasin B during egg cleavage in *Xenopus laevis*: dependence on cell membrane permeability. *Dev Biol* 31:163–177
- Sindelka R, Sidova M, Svec D, Kubista M (2010) Spatial expression profiles in the *Xenopus laevis* oocytes measured with qPCR tomography. *Methods* 51:87–91
- Takeuchi M, Takahashi M, Okabe M, Aizawa S (2009) Germ layer patterning in bichir and lamprey; an insight into its evolution in vertebrates. *Dev Biol* 332:90–102
- Takeuchi M, Okabe M, Aizawa S (2009) The genus Polypterus (Bichir): a fish group diverged at the stem of ray-finned fishes (Actinopterygii). *Cold Spring Harb Protoc.* <https://doi.org/10.1101/pdb.em0117>
- Tosti E, Romano G, Buttino I, Cuomo A, Ianora A, Miralto A (2003) Bioactive aldehydes from diatoms block the fertilization current in ascidian oocytes. *Mol Reprod Dev* 66:72–80
- Valles JM, Jordan WB, Mowry KL, Lin K, Denegre JM (2002) Cleavage planes in frog eggs are altered by strong magnetic fields. *Proc Natl Acad Sci U S A* 95:14729–14732
- Wishart DS, Tzur D, Knox C (2007) HMDB: The Human Metabolome Database. *Nucleic Acids Res* (2012-09-11). Metabocard for (E,E)-2,4-Decadienal (HMDB0036598). <https://hmdb.ca/metabolites/HMDB0036598>
- Yew N, Oskarsson M, Daar I, Blair DG, Vande Woude GF (1991) *mos* gene transforming efficiencies correlate with oocyte maturation and cytostatic factor activities. *Mol Cell Biol* 11:604–610
- Zhao C, Zhang L, Shi D, Chi X, Yin D, Sun J, Ding J, Yang M, Chang Y (2018) Carryover effects of short-term UV-B radiation on fitness related traits of the sea urchin *Strongylocentrotus intermedius*. *Ecotoxicol Environ Saf* 164:659–664

Publisher's Note Springer Nature remains neutral with regard to jurisdictional claims in published maps and institutional affiliations.

Table S-1. Irradiation dependent Inhibition of cleavage

No. of embryos injected (n=2)	Stages prior to irradiation	Stages after irradiation	Embryos of cleavage arrest after irradiation (%)
6	4-cell	8 cells stage	6 (100%)
6	8 cells stage	16-eell	6 (100%)
6	16-cell	32-eell	6 (100%)
6	32-cell	64-eell	6 (100%)
6	64-cell	Early blastula	6 (100%)
6	Early blastula	Late blastula	0 (0%)
6	Late blastula	Early gastrula	0 (0%)
6*	4-64 cell		0 (0%)

Table S-1. Represents the light-dependent irradiation of injected embryos at different developing stages. All embryos were injected by 0.01% DD into one blastomere of AP at 2-cell stage and irradiated by (44.86–91.15 Wm² + 395–700nm). *Un-injected control.

Supplementary file2 (MPEG 14760 KB)

<https://link.springer.com/article/10.1007/s12562-020-01481-7>

CHAPTER 3

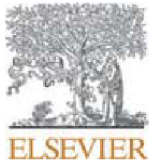
BLASTOMERES DERIVED FROM THE VEGETAL POLE PROVIDE EXTRA-EMBRYONIC NUTRITION TO STURGEON (*Acipenser*) EMBRYOS: TRANSITION FROM HOLOBLASTIC TO MEROBLASTIC CLEAVAGE

Shah, M.A., Fatira, E., Iegorova, V., Xie, X., Gela, D., Rodina, M., Franěk, R., Pšenička, M. and Saito, T., 2022. Blastomeres derived from the vegetal pole provide extra-embryonic nutrition to sturgeon (*Acipenser*) embryos: Transition from holoblastic to meroblastic cleavage. *Aquaculture* 551, 737899.

According to the publishing agreement between the authors and publisher, it is allowed to include the paper in this Ph.D. thesis.

<https://www.elsevier.com/about/company-information/policies/copyright>

My share on this work was about 60%.



Blastomeres derived from the vegetal pole provide extra-embryonic nutrition to sturgeon (*Acipenser*) embryos: Transition from holoblastic to meroblastic cleavage

Mujahid Ali Shah^{a,*}, Effrosyni Fatira^a, Viktoriia Iegorova^b, Xuan Xie^a, David Gela^a, Marek Rodina^a, Roman Franěk^a, Martin Pšenička^a, Taiju Saito^{a,c}

^a University of South Bohemia in Ceske Budejovice, Faculty of Fisheries and Protection of Waters, South Bohemian Research Center of Aquaculture and Biodiversity of Hydrocenoses, Zatisi 728/II, 389 25 Vodnary, Czech Republic

^b Laboratory of Gene Expression, Institute of Biotechnology of the Czech Academy of Sciences, Vestec, Czech Republic

^c South Ehime Fisheries Research Center, Ehime University, Ainan, Ehime 798-4206, Japan

ARTICLE INFO

Keywords:
Evolution
Fate-mapping
Vegetal blastomere
Yolk cells
Extra-embryonic nutrition

ABSTRACT

Generally, holoblastic cleavage in embryos (as in amphibians) in which all blastomeres contribute to one of the germ layers, are preserved as a stem lineage of vertebrates, and meroblastic cleavage has evolved independently in each vertebrate lineage. The increasing egg size: yolk volume is the key factor for transition from holoblastic to meroblastic cleavage patterns. Sturgeon (*Acipenser*) eggs are two times larger than those of the African clawed frog *Xenopus laevis* (amphibian); despite the varying size, sturgeon embryos retain nearly the same developmental characteristics as *X. laevis*. Comparatively, the fate of blastomeres derived from the vegetal pole (VP) of a sturgeon embryo is unspecified. Thus, the goal of this study was to determine whether the VP of the embryo contributes to embryonic development, or is simply extra-embryonic. This may also reveal whether the transition of the cleavage pattern (holoblastic to meroblastic) in the actinopterygian lineage is correlated with the egg size: yolk volume. Here, we found that sturgeon vegetal blastomeres formed only primordial germ cells, and the rest were made up of cellular yolk (yolk cells; YCs). Morphological and phenotypic characteristics revealed that after the 1 k-cell / mid-blastula transition, YCs became transcriptionally inactive and served only to provide nutrition to larvae as they developed. Furthermore, inhibition of vegetal blastomeres revealed that sturgeon can utilize their yolk in an acellular form, similar to teleosts, implying that meroblastic cleavage in the actinopterygians, like teleosts, might have evolved by the fusion of the vegetal blastomeres.

1. Introduction

Developmental processes of vertebrates, such as gastrulation, organogenesis, and overall body plan formation depend on the early division of embryonic cells. It is therefore crucial for the study of vertebrate development to understand these early cleavage patterns and the mechanisms that create them. In all vertebrates, the early embryonic cell division patterns can be divided into two broad categories: 1) holoblastic, complete cleavage which mostly occurs in amphibians, mammals and chondrosteans, and considered as ancestral for vertebrates; and 2) meroblastic, incomplete cleavage which has evolved five

times in each vertebrate lineage, including hagfish, sharks and other cartilaginous fishes, coelacanths, amniotes and teleosts, (Collazo et al., 1994; Elinson, 2009). This transition (holoblastic to meroblastic) is generally associated with an increase in egg size: yolk volume relative to the ancestral condition of the lineage (Collazo et al., 1994; Elinson, 2009; Hasley et al., 2017).

Yolk is the primary source of nutrition found in an animal's egg, and it provides the energy and building blocks required for growth and development (Jorgensen, 2008; Starck et al., 2021). The yolk sac is formed by tissues that grow outward from the embryo to cover the surface of the large yolk. This extra-embryonic layer was found in

Abbreviations: YCs, yolk cells; VP, vegetal pole; AP, animal pole; PGCs, primordial germ cells; YSL, yolk syncytial layer; *Eleutherodactylus coqui*, *E. coqui*; BrdU, 5-bromo-2-deoxy uridine; DD, 2,4-decadienal; FITC, Fluorescein isothiocyanate.

* Corresponding author.

E-mail address: mshah@frov.jcu.cz (M.A. Shah).

<https://doi.org/10.1016/j.aquaculture.2022.737899>

Received 16 July 2021; Received in revised form 23 December 2021; Accepted 5 January 2022

Available online 8 January 2022

0044-8486/© 2022 Elsevier B.V. All rights reserved.

aquatic animals >500 million years ago (mya) (Ravi and Venkatesh, 2018). In amniotes including, birds, reptiles and mammals, and some teleosts, embryos develop a vascular yolk sac, which works as an extra-embryonic gut, absorbing substances from the yolk, digesting them and transferring nutrients to the embryo via the circulation system (Incardona and Scholz, 2016; Jorgensen, 2008; Sheng and Foley, 2012). The form of the yolk and its utilization varies among animals.

Amphibians (e.g. the African clawed frog *Xenopus laevis*), undergo a holoblastic cleavage pattern generating blastomeres containing an unequal amount of yolk with increasing volume towards the vegetal pole (VP). Germ layers precursors, including ectoderm, mesoderm and endoderm, are arranged in a gradient along the animal-vegetal (top-bottom) axis (Yasuo and Lemaire, 2001). A majority of the fate determinants used during early embryogenesis are localized into a vegetal hemisphere, which supports the importance of the vegetal region for germ layer formation and also for primordial germ cell (PGC) development. The vegetal blastomeres of *X. laevis* produce cellularized yolk (endodermal yolk cells) but no yolk sac. The yolk is stored and digested intracellularly in endodermal cells in the form of yolk platelets (Collazo et al., 1994; Newman et al., 2010).

In contrast, the meroblastic cleavage pattern of teleost (e.g. zebrafish *Danio rerio*) eggs has most of its volume occupied by a continuous and acellular yolk mass, which is covered by a so called yolk cytoplasmic layer. The yolk mass never differentiates to any embryonic layers, although it supplies nutrition and some maternally deposited determinant factors for embryonic patterning including PGC formation (Gilbert, 2010). The material is transported from the yolk to the animal pole (AP) during the cleavage phase using yolk streams. The cleavage divides the AP into a cluster of blastomeres forming the blastoderm, which develops into the germ layers (ectoderm, endoderm and mesoderm) (Maegawa et al., 1999; Mizuno et al., 1996). The teleost meroblastic cleavage forms a yolk syncytial layer (YSL) by the collapse of marginal blastomeres, located between the yolk and the blastoderm during the blastula stage. The YSL has specific functions in embryonic patterning and morphogenetic movements and metabolic and nutrient transport from the yolk to the embryonic body by developing an external cellular yolk sac (Chen and Kimelman, 2000; Desnitskiy, 2015; Feldman et al., 1998; Sant and Timme-Laragy, 2018). Moreover, some teleosts (e.g. Salmoniformes) form a vascularized yolk sac. The YSL and yolk sac in most of teleosts are extra-embryonic (Carvalho and Heisenberg, 2010; Incardona and Scholz, 2016).

During evolution, bony fishes (Osteichthyes) divided into two lineages, ray-finned fishes (Actinopterygii) and lobe-finned fishes (Sarcopterygii). Tetrapods are presumed to have evolved from early bony fishes. Amphibians retained the ancestral state of the developmental characteristics, e.g. the holoblastic cleavage pattern of eggs which formed the cellularized yolk. On the other hand, amniotes (including birds and reptiles) evolved meroblastic cleavage with a colossal amount of acellularized yolk (Buchholz et al., 2007; Collazo et al., 1994; Elinson and Beckham, 2002). During this evolutionary period, mammals (except monotremes) lost their yolk and the fertilized oocytes grew to a diameter of around 100 μm , allowing them to develop in the uterus and undergo holoblastic cleavage (Takeuchi et al., 2009a). Mammals and reptiles, including birds, are all amniotes, i.e. they produce eggs that develop extra-embryonic membranes (amnion, chorion, yolk sac and allantois) (for details see Starck et al., 2021). Despite the absence of yolk in the eggs of placental mammals (e.g. primates), the yolk sac has remained an integral part of embryonic development, since it plays a significant role in haematopoiesis, germ cell development and nutritional supply (Ross and Boroviak, 2020).

At the height of actinopterygian evolution, teleost taxa including 33,000 species developed meroblastic cleavage. These teleosts are the animals that underwent whole-genome duplication (WGD) about 320–350 mya (Glasauer and Neuhauss, 2014; Pasquier et al., 2016). Prior to WGD, the earliest diverged living group of actinopterygians including bichir (*Polypterus*), sturgeon (*Acipenser*), gar (*Lepisosteus*) and

bowfin (*Amia*) has been diverted from the teleost lineage due to retention of some archaic characteristics in their embryogenesis. Several studies have suggested that bichir and sturgeon shared a lot of developmental similarities with sarcopterygians (amphibia) rather than to that of teleosts. For example, 1) localization of the sturgeon's germ plasm at the VP of the oocyte, 2) the holoblastic cleavage pattern which leads to cellularization of the yolk, 3) formation of the blastocoel during blastulation, 4) the presence of morphologically distinct bottle cells during gastrulation, and 5) the presence of the archenteron (primary gut) during neurulation (for detail see Bolker, 1993, 1994; Diedhiou and Bartsch, 2009; Hurley et al., 2007; Inoue et al., 2003; Kikugawa et al., 2004; Pocherniaieva et al., 2018; Takeuchi et al., 2009a, 2009b). On the other hand, holosteans (bowfin and gars), show the interspecific developmental characteristics between holoblastic and meroblastic due to the yolk-rich vegetal region, designated such because the vegetal cells have limited divisions (for detail see Ballard, 1986a, 1986b; Long and Ballard, 2001).

It is generally considered that all amphibians (holoblastic) exhibit the same developmental characteristics. However, the development of *Eleutherodactylus coqui* (*E. coqui*), a frog with a larger egg size: increased yolk volume towards the vegetal pole, provides a clue as to how the holoblastic–meroblastic barrier was breached in the amniote egg's evolution. For instance, *E. coqui* eggs are 20 \times larger than eggs of *X. laevis*. The holoblastic cleavage of the egg produces the cellular yolk mass yolk cells (YCs) at the vegetal pole, which does not contribute to gastrointestinal development; hence, it is extra-embryonic and serves primarily for nourishment, so called nutritional endoderm (Buchholz et al., 2007; Elinson and Beckham, 2002). Interestingly, similar developmental patterns in which vegetal blastomeres develop extra-embryonic YCs were also observed in agnathan lampreys (Petromyzontidae), an extant lineage of jawless fishes, and bichir (Polypteridae), the earliest diverged living group of actinopterygians (Takeuchi et al., 2009a, 2009b).

Sturgeons also belong to the actinopterygian lineage and are called “living fossils” because their morphological characteristics have remained relatively unchanged from the earliest fossil records (Bolker, 1993, 1994). Several previous studies have reported that vegetal blastomeres of sturgeon contribute to embryonic development. For instance, vegetal blastomeres derived YCs develop the “floor of the archenteron” observed by a classical fate-mapping analysis using vital dyes (Ballard and Ginsburg, 1980) and “the digestive system and its derivatives” (Gawlicka et al., 1996; Ginsburg and Dettlaff, 1991) by conventional histological analysis. Conversely, a few recent studies have reported that only germplasm (PGC determinants) is stored in the VP of sturgeon eggs (Linhartová et al., 2015; Pocherniaieva et al., 2018; Saito et al., 2014, 2018; Saito and Psenicka, 2015). To date, observations associated with vegetal blastomeres are scattered in various papers without focusing on their exact role in development. Thus their developmental fate is not yet fully understood. Based on the literature, we speculate that sturgeons present a specific kind of transition towards meroblastic cleavage as their vegetal blastomeres are quite large and produce a massive number of YCs which can be extra-embryonic as in bichir and *E. coqui*. Most importantly their phylogenetic position placed before holosteans (gar and bowfin), shows an obvious transition towards meroblastic cleavage (Ballard and Ginsburg, 1980; Buchholz et al., 2007; Elinson, 2009; Saito et al., 2018; Takeuchi et al., 2009a).

Recently, we have reported an effective technique for controlled blastomere inhibition during sturgeon development. We observed that some embryos with vegetal blastomere inhibition have succeeded in gastrulation (Shah et al., 2021). However, detailed fate mapping of vegetal blastomeres “before and after inhibition of vegetal blastomeres cleavage” remains uninvestigated. Thus, the present study aims to answer the following questions: 1) Do YCs derived from the sturgeon's vegetal blastomeres contribute to embryonic development? 2) Are YCs syncytial, as seen in many teleosts in the YSL? 3) Can sturgeons utilize their yolk in an acellular form rather than YCs? 4) If the VP-inhibited

Blastomeres derived from the vegetal pole provide extra-embryonic nutrition to sturgeon (*Acipenser*) embryos: transition from holoblastic to meroblastic cleavage

M.A. Shah et al.

Aquaculture 551 (2022) 737899

Table 1
Primer sequence for RT-qPCR.

Genes ID	Function	Primer (5–3)	PCR product (bp)	Accession number and references
<i>gata3</i>	The GATA family of transcription factors are of crucial importance during embryonic development, playing complex and widespread roles in cell fate decisions and tissue morphogenesis (reviewed by Tremblay et al., 2018).	CATCGGAACCTTACCCATGCT GTTCTGCCCGTTTCATTTTGT	241	XM_034026628.2 (Tremblay et al., 2018)
<i>sox7</i>	An important transcriptional factor during the intestine development of vertebrates (reviewed by Fu and Shi, 2017).	CATGCAGGACTACCCCAACT CTTGACTGCAGGAGTAGCC	162	XM_034005515.2 (Fu and Shi, 2017)
<i>vegT</i>	The localized transcription factor, which operates sequentially in several developmental pathways during embryogenesis, including dorsoventral and posterior patterning of mesoderm.	ACCGTATCCTTGCTGTCCAC GAAGGATGGCCTTTGTGAAA	211	(Pocherniaieva et al., 2018)
<i>gsk3b</i>	GSK-3 is active in several central intracellular signalling pathways, including cellular proliferation, migration, glucose regulation, and apoptosis (reviewed by Tayebh Noori et al., 2020).	CCCAACGTGTCGTACATCTG GTTCAATTCGCGGATCTGTT	222	XM_034918442.1 (Noori et al., 2020)
<i>Wnt11</i>	Its ligands are expressed around the blastopore and play an important role in regulating cell movements associated with gastrulation and epithelium of the oesophagus and colon, but also in mesenchymal cells of the stomach.	CAACGAGAACGACAAGCAAG ATCTCTCCAGGTCCTCTCA	203	(Pocherniaieva et al., 2018)

embryo can develop, what further consequence can occur (e.g. embryo sterility, autonomous induction of YSL, or YSL-like structures)? The findings of the present study will lay the foundation for a better understanding of the endogenous nutrition in the form of vegetal blastomeres during the embryonic development of sturgeon.

2. Materials and methods

2.1. Ethics

All experimental procedures were performed in accordance with National and Institutional guidelines on animal experimentation and care and were approved by the Animal Research Committee of the Faculty of Fisheries and Protection of Waters, University of South Bohemia in Ceske Budejovice (FFPW USB).

2.2. Preparation of embryos

For observation of embryonic development, sterlet sturgeon (*Acipenser ruthenus*) were bred at the Genetic Fisheries Center, (FFPW USB), Vodnany, Czech Republic. Embryos were obtained by artificial fertilization following the protocol as described previously (Shah et al., 2021). For each experiment, embryos from three different females were dechorionated by using forceps at 0 h post fertilization, and then incubated in dechlorinated tap water at 16 °C using an incubator (Q-cell, 140/40 Basic; Wilkowice, Poland) until they reached the required developmental stages. Embryos were routinely observed, and the water temperature was maintained at 16 °C and changed within 24 h. We used a description of embryonic development for sturgeon by Ginsburg and Dettlaff (1991).

2.3. Labelling of vegetal blastomeres

For the labelling of blastomere of 64–128-cell stage embryos with fluorescein isothiocyanate (FITC)-dextran (Sigma, molecular weight≈500,000) (FD500), the 1% FITC was prepared by dissolving with 0.2 M potassium chloride. Subsequently, the embryos (in triplicate; 20 from each female) were then placed on an agar-coated (1%) dish filled with dechlorinated tap water. Then, FITC-dextran was injected into a blastomere as close to the VP as possible. Each embryo was observed just after injection using a fluorescence stereomicroscope (Leica) to determine whether a single blastomere was labelled; unsatisfactorily labelled and non-labelled embryos were discarded. All procedures were followed according to Saito et al. (2014). Until the required developmental stages were obtained, embryos were cultured as described above (see, sub-heading 2.2). Images were captured using a Leica M165 fluorescence stereomicroscope imaging system.

2.4. Plastic section histology

We used histology to study the developmental fate of cells originating from the vegetal and animal blastomeres and the form of the YCs: yolk in control and VP-inhibited specimens. Embryos including treated (see heading 2.7) and controls at stages 12–14, 16, 21–25, 28, 31 and 36 were fixed with Bouin's fixative for 24 h and then replaced with 80% ethanol (EtOH) for long-term storage. Plastic sections were processed in order to retain the structure of tissues containing a lot of lipids. First, the embryos were infiltrated with Technovit 7100 on a shaker in the following order: 25% Technovit 7100 in EtOH for 2 days, 50% Technovit 7100 in EtOH for 2 days, 75% Technovit 7100 in EtOH for 2 days, 100% Technovit for 5 days two times. Embryos were then polymerized in a mold after adding Technovit 7100 Hardner II at room temperature. The specimens were sectioned using a microtome (Leica RM2235) according to the manufacturer's protocols. The thickness of each section was 2 µm. The sections were stained with hematoxylin and eosin and observed under the microscope. Images were captured using an Olympus microscope (BX51) and the size of nuclei in the A–V hemisphere-derived cells was measured using ImageJ software (NIH).

2.5. Gene expression analysis in YCs

Larvae at stage 36 (just after hatching) were euthanized by using tricaine methanesulfonate (MS-222). Subsequently, larvae from three different females at stage 36 were dissected, and YCs and gut tissue separated. All samples were kept separately in 1 ml microtubes and stored immediately at –80 °C. The total RNA was extracted using a RNeasy Micro Kit (<https://www.qiagen.com>) according to the manufacturer's instructions. The concentration of RNA was determined with the Nanodrop RND 2000 quantification system (Thermo Scientific). A total of 50 ng RNA was used for 100 µl cDNA synthesis by using the SuperScript™ III Reverse Transcriptase kit (Invitrogen). The concentration of reagents in the polymerase chain reaction (PCR), and utilization of equipment were strictly followed as described previously (Pocherniaieva et al., 2018). The nucleotide sequences of selected genes, including the germ layer and housekeeping genes (Protein Wnt11—*wnt11*, Glycogen synthase kinase-3 beta—*gsk3b*, Transcription factor Sox7—*sox7*, T-box protein VegT—*vegT* and Trans-acting T-cell-specific transcription factor GATA-3—*gata3*) were identified in the de novo assembled sterlet transcriptome (unpublished database of the Laboratory of Germ Cells, University of South Bohemia). The primer sequences for *vegT* and *wnt-11* were as published previously (Pocherniaieva et al., 2018), and the remaining were designed by using Primer3 [<http://bioinfo.ut.ee/primer3-0.4.0/>; (for detail, see Table 1; Shah et al., 2021)]. Each real-time quantitative (RT-qPCR) reaction was conducted by using 7 µl mixture, including 0.29 µl of the forward and

Table 2
Validation of sterility of embryos after treatment.

Treatment	No. of embryos injected (DD + GFP- <i>nos3</i>)	No. of embryos with stopped cleavage	No. of surviving embryos	No. of embryos without PGCs
DD with irradiation	168 (<i>n</i> = 3)	128	105	105
DD without irradiation	70 (<i>n</i> = 3)	0	55	0
Control	42 (<i>n</i> = 3)	0	35	0

The number of embryos in treated (vegetal pole inhibited embryos) and control (normal cleaved embryos) groups, respectively. The PGCs were observed and counted under a fluorescent microscope at stages 26 and 36 respectively.

reverse primers (10 μ M), 3.5 μ l of TATAA SYBR Grand Master Mix (TATAA Biocenter), 2 μ l of cDNA, and deionized water. The RT-qPCR was performed in triplicate using a CFX96 Real-Time system (BioRad). The reaction was performed at 95 °C for 3 min, followed by 45 cycles of 95 °C for 15 s, 60 °C for 20 s, and 72 °C for 20 s. At the end of the PCR cycles, a melting curve was recorded from 60 to 95 °C at 0.5 °C intervals. The relative expression level of mRNA for each gene in yolk cells (treated) and in gut tissue (control) was calculated using the $2^{-\Delta\Delta Ct}$ method. The spike (an artificial RNA molecule) was included in the RT-qPCR to exclude the unspecific bias in the quantification (Ivan Bower et al., 2007).

2.6. BrdU incorporation assay and immunolabelling

BrdU - 5-bromo-2-deoxy uridine (B9285-Sigma-Aldrich,) was dissolved in dechlorinated culture water (4 mg/ml) (Nóbrega et al., 2010). Dechorionated embryos in duplicates (10 embryos from each female) were exposed to BrdU in three different phases: (1) from stage 2 to 16, (2) from 14 to 28 and (3) from 25 to 32. After the BrdU pulse, treated and

control embryos were fixed overnight in 4% paraformaldehyde at 4 °C. Following fixation, the second chorion was removed and specimens were dehydrated in a EtOH series, 45 min each. Thereafter, embryos were immersed in xylene with three changes, 45 min each. The embedding, sectioning and deparaffinization were performed according to standard IHC-P protocols (paraffin section immunohistochemistry). BrdU was detected immunohistochemically using the primary—rabbit anti-BrdU (ab152095; Abcam, Cambridge, MA, USA) and secondary—anti-rabbit immunoglobulin G—fluorescein isothiocyanate (FITC; F0382, Sigma) antibodies. The nuclei were stained with 4,6-diamidino-2-phenylindole solution (DAPI, 3 ng/ml). The procedures followed those provided by Abcam (<https://www.abcam.com>). Detection of BrdU labelling and imaging was performed using a fluorescence stereomicroscope (Olympus SZ-12).

2.7. Inhibition of vegetal blastomere and yolk cell division

In order to study the effect of vegetal blastomeres inhibition on the development of embryos, eggs were dechorionated manually and kept in dechlorinated water at 16 °C until the 2-cell stage. Then, embryos from three different females were injected in triplicate into the VP at the 2-cell stage with 0.01% of 2,4-decadienal (DD) and subsequently subjected to irradiance by using visible light (44.86–91.15 W m⁻²) until the 32 cell stage, as described earlier (Shah et al., 2021). For survival and hatching the number of treated (vegetal blastomere cleavage stopped) and control (normally cleaved vegetal blastomeres) groups was measured as percentages. Incubation, observation and imaging of embryos followed procedures as described above (see, heading 2.2 and 2.3).

2.8. Primordial germ cells (PGCs) development in normal (wild-type) and inhibited cleaved embryos

To investigate the development of PGCs in VP-inhibited and normal

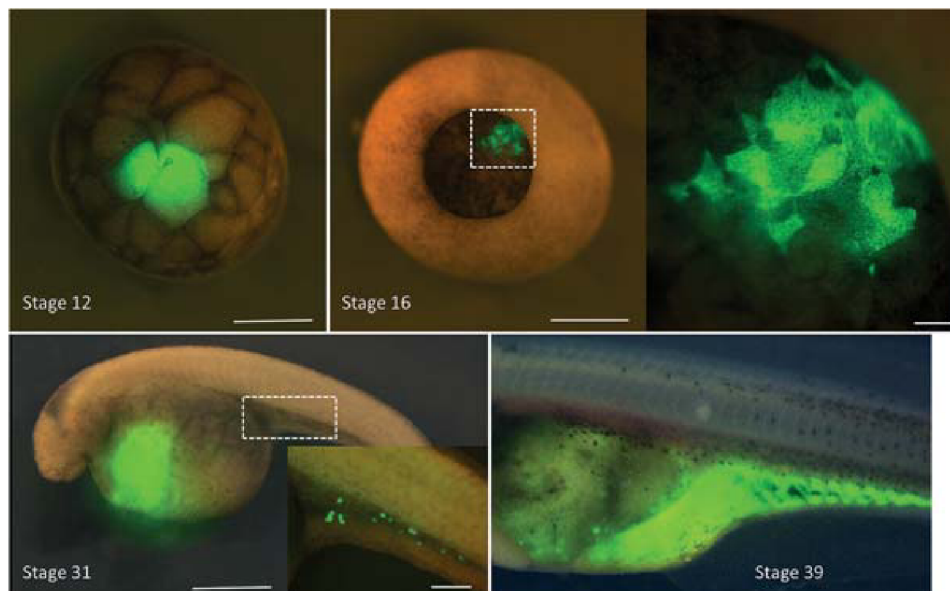


Fig. 1. Fate-mapping of vegetal blastomeres of the sturgeon embryo. Stages 12–39 show blastomeres at the vegetal pole (VP) labelled by injecting FITC-dextran (MW 500,000) at the 64- to 128-cell stage and the descendants were observed under a fluorescent stereomicroscope. Stage 12, vegetal view of the labelled embryo. Stage 16, vegetal view of the labelled embryo. Right side, a magnified image of the square box. Stage 31, lateral view of the labelled embryo. The descendants of the labelled blastomere are located inside the yolk-sac, although the primordial germ cells (PGCs) are detached from the mainly labelled domain and have migrated to a place where the gonad would be formed (rectangular box). Stage 39, the fluorescein isothiocyanate (FITC)-positive cells seemed to be digested and the FITC distributed in the posterior part of the gut, suggesting that the vegetal blastomeres are the extra-embryonic nutrition. Scale bars: 1 mm for stage 12, 16 and 31, and 50 μ m for insert.

Blastomeres derived from the vegetal pole provide extra-embryonic nutrition to sturgeon (*Acipenser*) embryos: transition from holoblastic to meroblastic cleavage

M.A. Shah et al.

Aquaculture 551 (2022) 737899

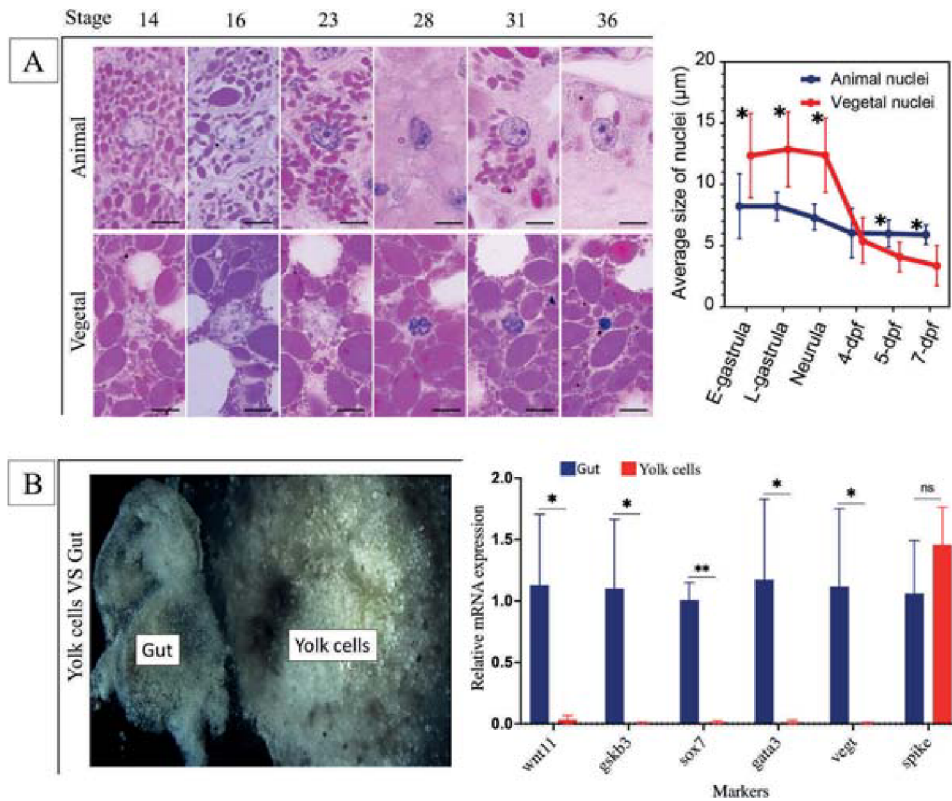


Fig. 2. The fate of yolk cells during the development of the sturgeon embryo. (A) Hematoxylin labelled nucleus of the A–V blastomeres of sturgeon embryos ($n = 3$) during embryonic development. Animal blastomeres show prominent nucleoli, which remain constant throughout the development stages. The size of vegetal nuclei is more extensive than the animal nuclei due to the size of the yolk cell and remains constant as in the animal nuclei until stage 23. After that, there is a sharp decrease in the size of nuclei, which suggests that vegetal cells are suppressed after stage 23. (B) Shows the massive number of yolk cells separated from the gut using simple dissection. The transcriptional activity of yolk cells and gut, shown by the expression of marker genes analyzed by RT-qPCR from triplicates of each group, shows non-expression in yolk cells. Data are presented as mean and S.E. * $P < 0.05$ and ** $P < 0.01$, respectively, indicate statistically significant differences, while ns indicates non-significant difference. dpf, days past fertilization. Scale bars in (A) indicate 20 μm .

cleaved embryos, capped sense *GFP-nos3* 3' UTR mRNA was synthesized in vitro using the mMACHINE kit (Ambion) following instructions as described earlier (Saito et al., 2006). Two batches of embryos in triplicate were injected by *GFP-nos3* 3' UTR mRNA (300 ng/ μl) as co-injection with DD-0.01% solution into the VP at the 2-cell stage. Subsequently one batch of embryos was irradiated by 91.15 W m^{-2} while a second batch remained unirradiated. In parallel, a third batch of embryos was kept as a control (without injection and irradiation) to measure their survival rate (Table 2). The PGCs were traced in *GFP-nos3* injected embryos at stage 26 and 36, respectively using a fluorescence stereomicroscope imaging system (Leica M165) as described by Saito et al. (2006).

2.9. Statistical analysis

The size of nuclei in the animal hemisphere-derived cells and vegetal hemisphere-derived cells was measured using ImageJ software (NIH). The mean of the long and short axial diameters was used as the diameter of each nucleus. All statistical analyses were carried out using R language programming (version 3.5.1) and the GraphPad prism software (version 9). A paired *t*-test was used to determine pairwise comparisons of nuclei mean size between animal and vegetal cells, partial cleaved–yolk (treated) and normal cleaved–yolk cell (control) embryos at each stage of development. For relative mRNA expression between yolk cells and the gut, data in triplicate for each gene from yolk cells (treated) v. gut (control) were analyzed by using multiple *t*-tests (multiple

unpaired *t*-tests of grouped data), and for multiple comparison original FDR (false discovery rate) was set according to the Benjamini and Hochberg procedure (prism 6) (Benjamini and Hochberg, 1995). The significance level was set at $P < 0.05$.

3. Results

3.1. Vegetal blastomeres only contribute to the development of primordial germ cells

A labelled single blastomere located at the VP at the 64- to 128-cell stage continued to divide and produce daughter cells as the embryos developed, although the size of these cells was significantly larger than those of the animal hemisphere (Fig. 1, stage 12 and 16). The FITC-labelled blastomeres developed into a ventral part of the embryo (Fig. 1, stage 31). Meanwhile, we also observed that PGCs were labelled by FITC-dextran and showed migration towards the genital ridge region detaching from the main body of the labelled area (Fig. 1, stage 31-insert) (Saito et al., 2014). Finally, FITC fluorescence was observed widely and strongly in the developing hindgut of hatched larvae (Fig. 1, stage 39). Collectively, the above findings suggested that yolk from the VP gave rise to the PGCs and the rest of the yolk was in the form of YCs.

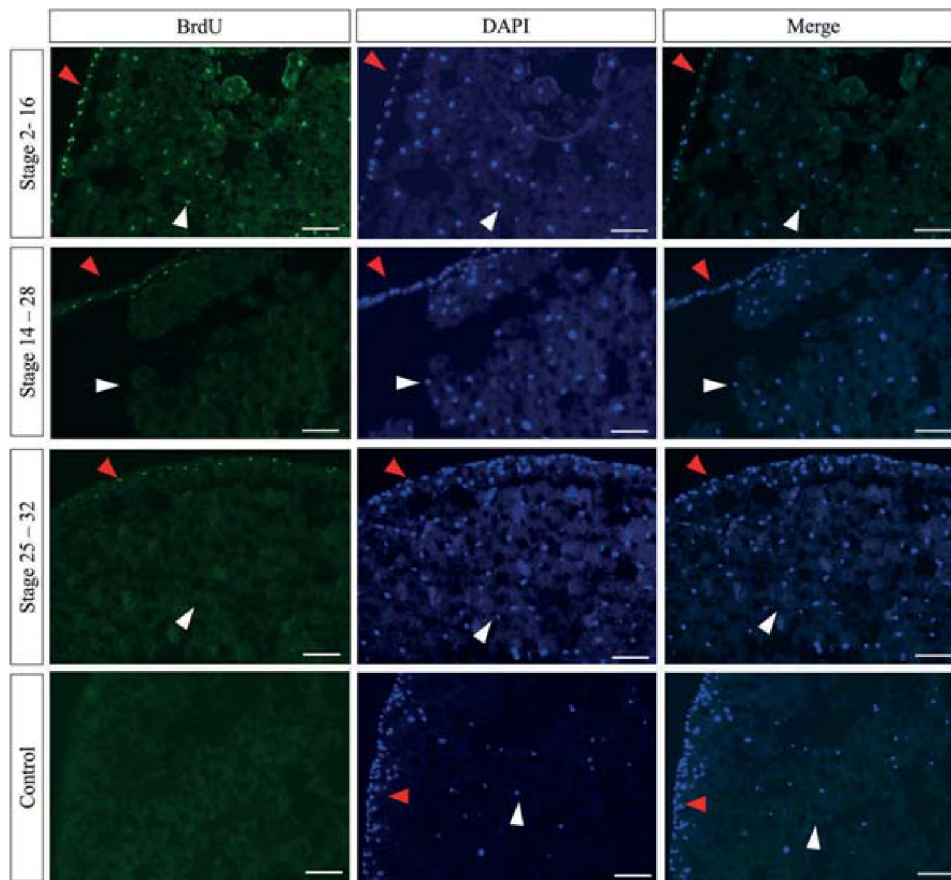


Fig. 3. Yolk cells mitotic assay. The figure depicts BrdU labelling and detection at various stages of development: (1) from stage 12 to 16, (2) from 14 to 28, and (3) from 25 to 32. Yolk cells show positive signals (green dots; from stage 2 to 16). Somatic cells show positive signals compared to yolk cells (green dots in all treated embryos). DAPI shows nucleus labelling (blue dots). Conversely, there is no signal from anti-BrdU antibodies in the negative control (unexposed to BrdU). The somatic and yolk cells are denoted by red and white arrows, respectively. Scale bars indicate 100 μ m. (For interpretation of the references to colour in this figure legend, the reader is referred to the web version of this article.)

3.2. The fate of vegetal yolk blastomeres and cells during embryonic development

For further confirmation, the development of YCs was observed using different approaches. Firstly, plastic section histological analysis showed an apparent morphological difference between AP- and VP cells. In the AP cells, the nuclear membrane was sharply defined and stained well with hematoxylin from the blastula stage to the post-hatching stage (Fig. 2 A-Animal). In the nuclei, prominent nucleoli were observed during the whole process of embryonic development. Conversely, in the VP, we found large sized vegetal cells, YCs. However, observation of the nucleoli and nuclear membrane was quite challenging due to the large size of the cell, and many yolk granules in each cell (Fig. 2 A-Vegetal). In the nuclei of YCs, the nucleoli were poorly observed and their structure was quite unclear. Furthermore, as the embryos developed, the nuclei of YCs became more visible because they became condensed to the extent that they showed a black “dot” shape, and hematoxylin-affinity was increased (Fig. 2 A-Vegetal). Comparatively, the size of the nuclei in the AP cells was significantly ($P < 0.05$) smaller than that of YCs nuclei, except for stage 28. Moreover, the size of AP cell nuclei remained unchanged throughout development, whereas in YCs it was conserved until stage 23, but after that, it declined drastically as the embryos developed (Fig. 2 A). The YCs were found to be “non-syncytium” throughout the development process, suggesting that YCs have no or less proliferation

activity.

We predicted that YCs would not have zygotic mRNA to contribute to embryonic development. Thus, housekeeping and germ layer marker genes would be expressed in gut tissue, but not in YCs (for detail see, Table 1). Thus, for this validation, a phenotypic study was conducted through RT-qPCR (Fig. 2 B). The RT-qPCR analysis of the expression of the germ layer and housekeeping markers including *wnt11*, *gsk3b*, *sox7*, *vegT* and *gata3* (Table 1) revealed that these markers were significantly ($P < 0.05$) less expressed in YCs compared to early gut tissue, which would mean that these cells do not contribute to the embryonic body (Fig. 2 B). We confirmed our suspicions by using a 5-bromo-2-deoxy uridine (BrdU) pulse to characterize YCs proliferation during embryogenesis; BrdU is a nucleoside analog that is specifically incorporated into DNA during the S-phase. Our findings showed that embryos incubated in BrdU were proliferated between stages 2 to 16 (Fig. 3 stages 2–16). However, embryos incubated from 14 to 28 and 25 to 32 showed no proliferation activity in YCs. As a control, all BrdU-incubated embryos (2–16, 14–28, and 25–32) showed positive labelling in all somatic cells, while no signal was observed in untreated embryos (Fig. 3). Thus, all the above findings suggested that after the mid-blastula transition, YCs were transcriptionally inactive and served only for nourishment.

Blastomeres derived from the vegetal pole provide extra-embryonic nutrition to sturgeon (Acipenser) embryos: transition from holoblastic to meroblastic cleavage

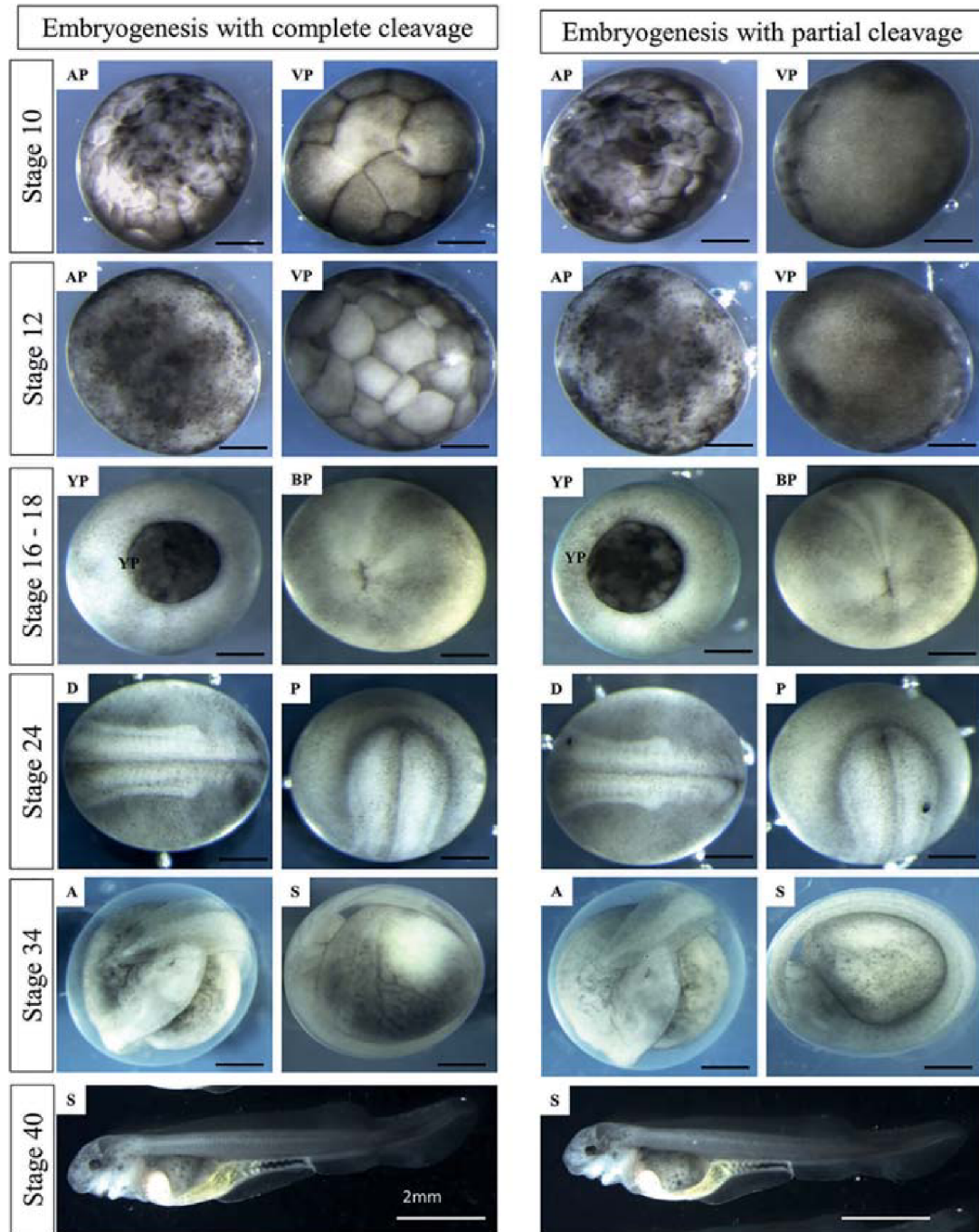


Fig. 4. Inhibition of vegetal blastomere cleavage of sturgeon embryos. The inhibition of vegetal blastomeres (VP) and its impact on the development of embryos are shown. Embryogenesis without cleaving blastomeres was compared with embryogenesis of normal (untreated) embryos over stage 10–40. Until stage 12, embryogenesis of stopped cleavage seemed parallel to the meroblastic cleavage pattern, thereafter embryos followed a typical developmental pattern, i.e. like control embryogenesis. AP = animal pole view, VP = vegetal pole view, S = side view, A = anterior view, P = posterior view, D = dorsal view, YP = yolk plug, BP = blastopore. Scale bars at stage 10–34 indicate 1 mm, at stage 40 indicate 2 mm.

3.3. Inhibition of vegetal blastomeres and its impact on the development of sturgeon embryos

The YCs produced by the vegetal blastomeres appear to play mainly a nutritional role. This finding raises the question of whether the cleavage

of the VP is necessary for development to proceed. To answer this question, we applied the previously developed technique to inhibit cleavage into the VP (Shah et al., 2021). After inhibition of vegetal blastomere cleavage, the treated embryos (221 / 167 / 132 = treated embryos / stopped VP / hatched larvae) remained uncleaved compared

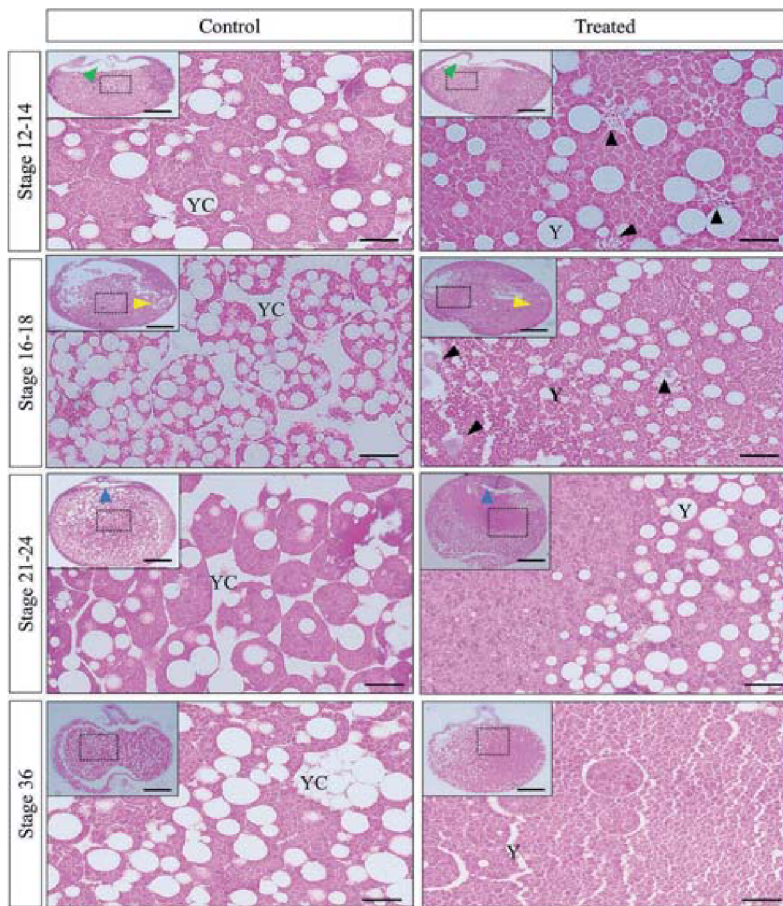


Fig. 5. Microanatomy of yolk cells (YCs) and yolk in treated (VP-inhibited) and untreated (normal cleaved) embryos. Transverse sections of A–V of embryos at stages 12–36 are shown. Treated embryos at stage 12 show normal blastocoel formation with the appearance of untreated but massive amounts of yolk with few yolk cells. At stages 16–18, treated embryos also show blastopore formation as in the controls but a cellular yolk mass with larger sized nuclei, which indicates that nuclei are syncytial and mimic the yolk syncytial layer (YSL) as in teleosts. At stage 21–24, the treated and control specimens show normal neurulation with and without YCs. However, after hatching, treated embryos showed most of the yolk in the form of yolk platelets, which mimic the teleosts (stage 36). YC = yolk cells, Y = yolk only, green arrows = blastocoel, yellow arrows = blastopore, blue arrows = archenteron, black arrows = nuclei in the yolk. Scale bars in (left corner pictures) indicate 1 mm and 10 μ m in zoom-out (yolk/yolk cells) pictures. (For interpretation of the references to colour in this figure legend, the reader is referred to the web version of this article.)

to the control embryos (40 / 0 / 32 = untreated embryos / stopped VP / hatched larvae). Interestingly, we observed that the treated embryos showed a meroblastic-like cleavage pattern (e.g. zebrafish embryogenesis) until stage 12. Thereafter, treated embryos underwent closure of the blastopore and gastrulation was successful (Fig. 4 stage 10–18). After stage 16, the external appearance of treated and control embryos was indistinguishable. The treated embryos continued to develop after hatching, ingest and grow normally (Fig. 4).

The external appearance and histological sections showed that VP-inhibited embryos contained most of the yolk in an acellular form (yolk platelets) instead of YCs (Fig. 5 stage 12–36 and Supplementary Fig. S1). Despite the loss of YCs, blastocoel formation during blastulation, blastopore formation during gastrulation, archenteron formation during neurulation and body cavity structure after hatching were also normal compared to control embryos (Figs. 4 and 5).

3.4. The consequence of vegetal pole cleavage inhibition in sturgeon embryos

After inhibition of VP cleavage, we speculated that 1) embryos would remain sterile due to the inhibition of PGC development in the VP, and 2) could induce YSL or YSL-like structures to separate in an acellular yolk from animal blastomeres. To clarify the first suspicion, whether the VP-inhibited embryos are fertile or sterile, we utilized GFP-*nos3* 3' UTR mRNA coupled with DD treatment as described for partial cleavage inhibition (Fig. 4). The inhibited VP cleavage embryos were completely PGC-less unlike control embryos with non-altered cleavage (Fig. 6 and

Table 2).

For the second suspicion, the YSL-like structure in partial cleaved embryos of sturgeon was compared with the YSL of zebrafish labelled by nuclear dye (Hoechst stain 1:1000). Morphological characteristic of partial cleaved embryos of sturgeon at stage 12 showed several nuclei with a massive amount of yolk, which seemed that the YSL-like structure was as in zebrafish (Fig. 7).

4. Discussion

4.1. Vegetal blastomeres of sturgeon supply endogenous nutrition

Generally, *X. laevis* embryos are considered as a model for holoblastic cleavage patterns in which the three primary germ layers, ectoderm, mesoderm and endoderm, develop from all the blastomeres (A–V). Yolk is stored in a cellularized form and is utilized intracellularly without a yolk sac. The embryos of *E. coqui*, bichir, and lampreys also cleaved holoblastically as in *X. laevis*. Interestingly, owing to increased yolk volume, their germ layer patterning challenges the view that all (animal – vegetal) blastomeres contribute. However, they store their yolk as YCs within a cellular yolk sac and utilize it for nourishment (Buchholz et al., 2007; Takeuchi et al., 2009a). In the present study, for the first time, we showed the developmental fate of vegetal blastomeres of sturgeon during embryonic development. Fate mapping, using the microinjection labelling technique together with fluorescent microscopy, clearly showed that most descendant cells from vegetal blastomeres develop YCs except for PGCs (Fig. 1) (Saito et al., 2014). Moreover, histological

Blastomeres derived from the vegetal pole provide extra-embryonic nutrition to sturgeon (*Acipenser*) embryos: transition from holoblastic to meroblastic cleavage

M.A. Shah et al.

Aquaculture 551 (2022) 737899

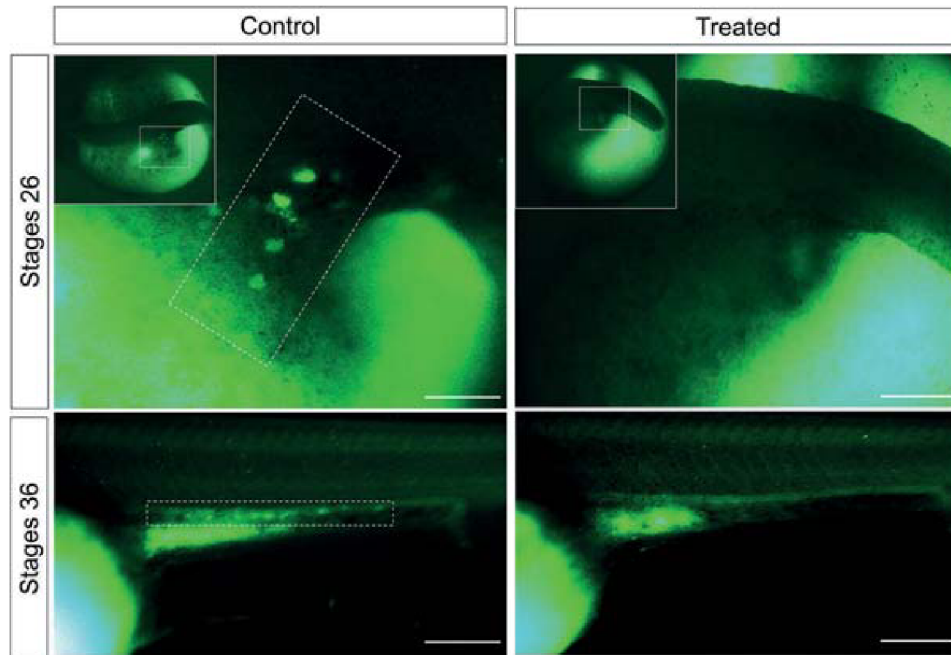


Fig. 6. Partial cleavage (vegetal pole) inhibition leads to the sterility of the embryos. Embryos were injected with 0.01% DD and co-inaction of GFP-*nos3* 3' UTR mRNA (300 mg/ml) into a vegetal pole at the 2-cell stage. Treated embryos (irradiated and stopped vegetal blastomeres). Control embryos (unirradiated and cleaved normally). Stage 26–36 = genital ridge (as already shown in Fig. 1, scale bar = 50 μ m). Dotted lines showed primordial germ cells (PGCs) in control embryos whereas treated embryos had no PGCs.

observations revealed that YCs were substantial in size and did not show apparent nucleoli compared to animal pole cells. The YCs nuclei became condensed as larvae developed (Fig. 2 A).

Besides fate mapping and morphological observation, it was also necessary to study the phenotypic characteristics of YCs. Previously, a study from our laboratory by Pocherniaieva et al. (2018) showed the localization of selected maternally supplied genes in sturgeon oocytes by using RT-qPCR tomography and we distinguished genes with significantly different expression profiles along the animal–vegetal axis. Thus, high prevalence of mRNAs at the VP may play a role in developing embryos (Pocherniaieva et al., 2018). In this study the RT-qPCR amplification of marker genes, including housekeeping and germ layer markers (*wnt11*, *gsk3b*, *sox7*, *vegT* and *gata3*) (for detail about genes function, see Table 2) and mitotic activity of YCs using BrdU chasing, have suggested that YCs were transcriptionally inactive after the mid-blastula transition (Fig. 2 B and Fig. 3). Additionally, inhibition of vegetal blastomeres and YCs has confirmed that these cells do not contribute to the embryonic body, and just serve in providing endogenous nutrition as the embryo develops (Fig. 4).

The sturgeon embryo contains a substantial yolky region (vegetal hemisphere) as seen in salamander *Ensatina eschscholtzii* and *E. coqui* (Buchholz et al., 2007; Collazo and Keller, 2010). The cell division of the vegetal blastomere is significantly slower than that of cells derived from the animal one (Dettlaff et al., 1993). After hatching, these cells were observed to decline and change shape inside the gut tube (see Supplementary Fig. S2). These findings indicate that there is a mechanism already in place at this stage (stage 38) to digest the YCs, and the gut tissue absorbed them as a nutrient. According to Korzhuev and Sharkova (1967), proteolytic enzymes appear in the pre-larval stage of the Russian sturgeon *Acipenser gueldenstaedtii* during the first day after hatching and extracellular digestion is already present at this stage (Dettlaff et al., 1993). Gisbert et al. (1999) have also reported that alkaline phosphatase, acid phosphatase, ATP-ase, non-specific esterase activities and lipase are observed in the digestive tube of Siberian sturgeon *Acipenser*

baerii embryos at the hatching stage (Gisbert et al., 1999). Overall past and current findings also underscore that the sturgeon's gut develops around the entire YCs and utilize them extra-intestinally (yolk inside the gut). However, it remains unknown how the gut develops, and whether the gut development pattern of the sturgeon is either unique or conserved with any vertebrate. We leave this issue as an open question for future studies.

4.2. A way towards the evolution of meroblastic cleavage

During evolution, increased egg size and yolk volume is one factor that can have a substantial effect on early developmental processes, such as cleavage pattern and gastrulation (Elinson, 2009). Generally, all amphibian eggs cleave holoblastically: the egg is divided completely by the first few cleavage furrows. Nonetheless, in some species, particularly those with a large yolky mass, the first few cleavage planes fail to pass entirely through the A–V region (Buchholz et al., 2007; Collazo and Keller, 2010; Hasley et al., 2017). For example, many species of different anuran taxonomic groups with a “pseudo-meroblastic” pattern, including *E. eschscholtzii*, *E. coqui* and *Hyperolius punctulatus*, are particularly appropriate for such comparative studies because they have eggs of varying sizes and yolk volume which are larger than those of *X. laevis* (Buchholz et al., 2007; Chipman et al., 1999; Collazo and Keller, 2010). Moreover, Buchholz et al. (2007) showed that when sizeable vegetal blastomeres at the 60- to 100-cell stage were inhibited in *E. coqui*, the embryo succeeded in gastrulation. Increased egg size led to the origin of the nutritional endoderm, a novel cell type that provides nutrition but does not differentiate into digestive tract tissues. The development of *E. coqui* and *E. eschscholtzii* suggested that amniotes had evolved meroblastic cleavage directly from amphibians and an increased egg yolk was the essential factor leading to the evolution of the extra-embryonic membranes that define the amniotes (Buchholz et al., 2007; Elinson, 2009). The embryos of sturgeon produce a clump of small animal cells but large vegetal blastomeres; they produce a massive

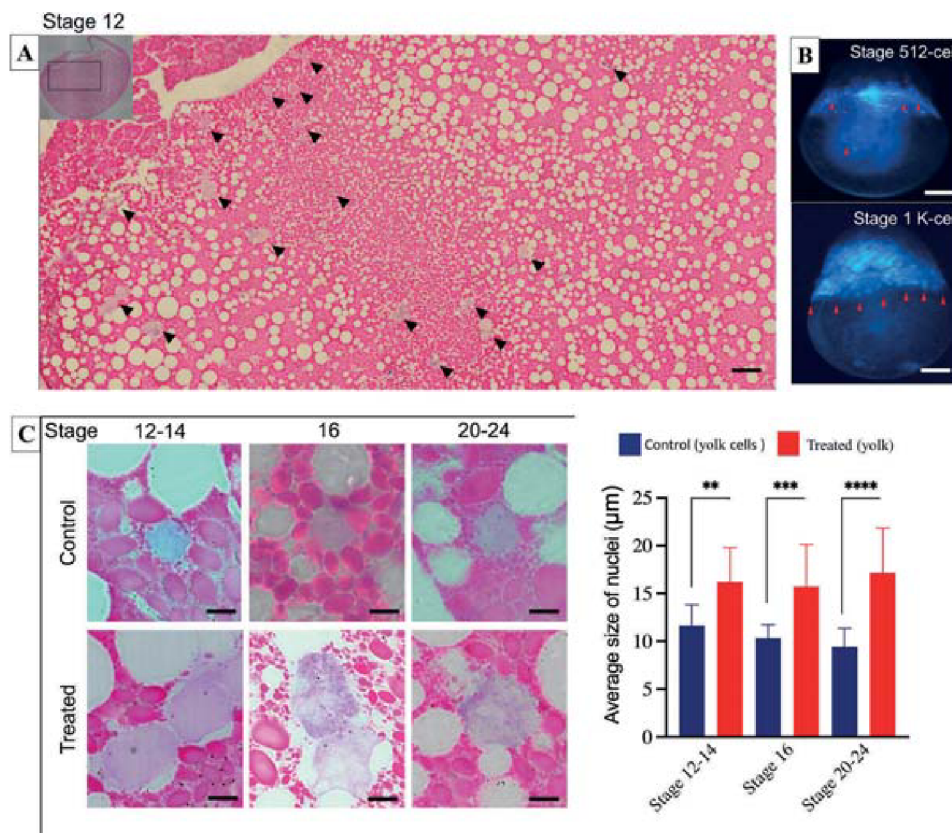


Fig. 7. Partial cleavage (vegetal pole) inhibited embryos showed a yolk syncytial layer (YSL) -like structures. (A) The histology of the inhibited cleavage embryo of sturgeon at stage 12; the picture shows a cellular yolk mass with nuclei near the blastocoel cavity (scale bar = 20 μm). (B) the zebrafish embryo ($n = 12$) with labelled YSL at 512- and 1 k-cell, respectively (scale bar = 50 μm). Black and red arrows show the nuclei in sturgeon and zebrafish, respectively. (C) The average size of hematoxylin labelled nuclei between control (complete cleavage) and treated (partial cleavage) embryos of sturgeon ($n = 10$) in the yolk cells (YCs; normal cleavage embryos) and yolk (partial cleavage embryos) at the blastula (stages 12–14), gastrula (stage 16) and neurula (stages 20–24) stages. The finding reveals that after inhibition of vegetal blastomeres, the size of nuclei in yolk was significantly larger than that of YC nuclei (** $P < 0.01$ and *** $P < 0.001$). Scale bars indicate 20 μm for (A) and (C), and 0.5 mm for (B). (For interpretation of the references to colour in this figure legend, the reader is referred to the web version of this article.)

number of YCs that mimic those of *E. coqui* and *E. eschscholtzii*, bichir, and lampreys. The occurrence of a colossal amount of vegetal yolk mass represents a specific kind of transition from holoblastic to meroblastic cleavage among actinopterygians (Buchholz et al., 2007; Collazo and Keller, 2010; Takeuchi et al., 2009a). Here, to support this supposition, we inhibited vegetal blastomere cleavage in sturgeon embryos (switched from holoblastic to meroblastic) (Fig. 4). Until stage 12, embryos mimicked meroblastic cleavage as in zebrafish (Fig. 4 stage 12, and Fig. 8 stage 10). Thereafter, the treated embryos seemed to parallel the controls in subsequent developmental stages, including blastulation, gastrulation, neurulation and hatching (Figs. 4 and 5). Thus, overall, these findings suggested that vegetal blastomeres did not contribute to embryonic development, except PGCs (Figs. 1–6). The results presented here also pave the way towards illustrating the transition of cleavage (meroblastic–holoblastic) in actinopterygians (Fig. 8) (Ballard, 1986b; Long and Ballard, 2001).

Moreover, based on our findings and previous studies, it is suggested that meroblastic cleavage in actinopterygians evolved by two significant changes during early embryonic development of gar and bowfin: 1) loss of bottle cells during gastrulation, which occurred between the bowfin and chondrosteans and 2) diffusion of the vegetal blastomere into one cell and the evolution of the YSL to separate the blastoderm and yolk mass, which occurred between gar and teleost (Ballard, 1986b; Long and Ballard, 2001). Our result clearly shows that the YCs divide

coincidentally with nuclear division, and there is no YSL or YSL-like structure in the normal cleaved embryo. Moreover, after inhibition of cleavage at the vegetal hemisphere, the average size of nuclei in yolk (partial cleaved embryos) was significantly ($P < 0.05$) larger than the nuclei in YCs (normal cleaved embryos). These findings suggested that most of the YCs remained undivided, but vegetal nuclei continued dividing. Intriguingly, we observed several YC nuclei inside the yolk and most of them were seen near to the blastocoel cavity, mimicking the YSL of zebrafish (Fig. 7). Thus, morphological analysis of the vegetal pole of inhibited embryos of sturgeon suggested that the evolution of meroblastic cleavage might have arisen by the fusion of the vegetal blastomere (after the 2-cell stage) in gar and the YSL had evolved to separate the yolk and blastoderm (Figs. 4 and 8) (Long and Ballard, 2001).

4.3. PGCs development: A potential barrier during the evolution of meroblastic cleavage

The mode of the PGC formation is also altered according to the transition of cleavage from holoblastic to meroblastic (Pocherniaieva et al., 2018; Saito et al., 2014). For instance, in amphibians, the *X. laevis*'s germplasm is localized in the VP and PGCs migrate within the gut-endoderm to reach the gonadal ridge. Compared to *X. laevis*, urodeles have evolved an alternative path to generate PGCs. To elaborate, during the blastula stage, PGCs are presumably induced in the

Blastomeres derived from the vegetal pole provide extra-embryonic nutrition to sturgeon (*Acipenser*) embryos: transition from holoblastic to meroblastic cleavage

M.A. Shah et al.

Aquaculture 551 (2022) 737899

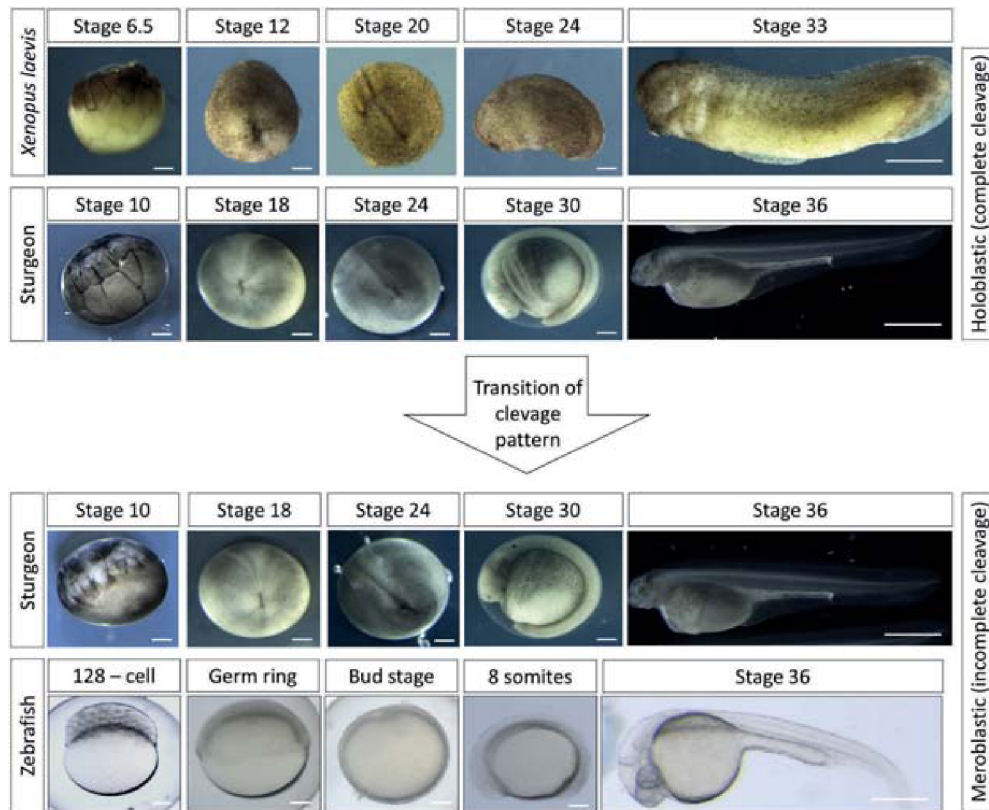


Fig. 8. Sturgeon shows an evolutionary transition from holoblastic to meroblastic cleavage. A comparison of egg cleavage patterns and embryogenesis at various stages between *Xenopus laevis*, sturgeon and zebrafish: *X. laevis* and zebrafish represent the holoblastic and meroblastic egg cleavage pattern, respectively, whereas sturgeon is interspecific between *X. laevis* and zebrafish. Compared to *X. laevis* and zebrafish, sturgeon retained holoblastic cleavage, blastulation, gastrulation and neurulation as in *X. laevis*. However, their vegetal blastomeres do not contribute to the embryonic body as in zebrafish yolk. The fusion of vegetal blastomeres in sturgeon embryos represents a specific kind of transition (meroblastic–holoblastic) in the evolution of cleavage in actinopterygians. The findings presented here are parallel to the demonstration of the evolution of the Lepisosteiformes clad of actinopterygians lineage that occurred ~57 million years ago in ray-finned fishes (Long and Ballard, 2001). Scale bars indicate 1 mm for sturgeon and *X. laevis*, and 0.5 mm for zebrafish.

primordial ectoderm by cellular interactions between cells in the vegetal and animal hemispheres, and migrate dorsally along with the meso-endodermal interspace and the dorsal mesentery, where they split to the right and left sides and form the gonadal ridge (Bachvarova et al., 2009; Sutasurja and Nieuwkoop, 1974). Comparatively, despite profound changes in the yolk-rich vegetal region of sturgeon embryos the formation of PGCs via germplasm, localized to the vegetal region, has been conserved in anurans (*X. laevis*), and their migratory pattern is conserved within teleosts (Saito et al., 2014). Additionally, in our previous study we have reported that during normal sturgeon development, many of the “mis-migrated” PGCs are observed (Saito et al., 2014). Thus, potential reasons for this expansion of germplasm are participation in the formation of the nutritional endoderm. This ensures that some primordial germ cells, among the few vegetal cells, move to the genital ridge, which is observed in *E. coqui* (Elinson et al., 2011) (Fig. 1). Based on PGCs localization and migration, sturgeons (chondrosteans) are interspecific between amphibians and teleosts, however, their comparison with gar and bowfin (holosteans) is still an open question for future studies.

5. Conclusion

Based on results discussed above we concluded that: 1) sturgeon embryos undergo the same development as the ancestors of vertebrates and this continues to be retained in their stem lineages. The potential

reason for holoblastic cleavage and production of YCs is due to localization of the germplasm in the vegetal cortex. 2) The division of vegetal blastomeres of sturgeon embryos produce a massive number of YCs which become transcriptionally inactive after mid-blastula transition and serve only as nutrition as larvae develop. 3) When the division of vegetal blastomeres and YCs was inhibited, the embryos developed normally and could utilize the yolk in an acellular form instead of using YCs, mimicking teleosts (Supplementary Fig. S1). 4) It has been found that inhibited vegetal blastomere embryos remain sterile which suggests that (a) YCs in the sturgeon embryo only facilitate the migration of PGCs towards the genital ridge during embryonic development, (b) gar have evolved meroblastic cleavage by fusion of the vegetal blastomere and have an alternative path to generate PGCs (such as translocation of germplasm in the embryo from the vegetal hemisphere to the animal hemisphere) during the evolution of meroblastic cleavage (Saito et al., 2014). However, this can further be verified by investigating the localization and migration of PGCs in gar and their comparison with other taxa such as *X. laevis*, sturgeon and zebrafish.

Supplementary data to this article can be found online at <https://doi.org/10.1016/j.aquaculture.2022.737899>.

Funding

The research was supported by the Ministry of Education, Youth and Sports of the Czech Republic project Biodiversity (CZ.02.1.01/0.0/0.0/0/

16.025/0007370), Czech Science Foundation (20-23836S) and Grant Agency of the University of South Bohemia (019/2021/Z).

Declaration of Competing Interest

The authors declare no competing interests.

Acknowledgements

We thank Ing. Zuzana Bláhová for generous help during preparation of GFP-nos1 3'UTR. We also thank Dr. Jan Stundl for critical revision and suggestions.

References

- Bachvarova, R.F., Crother, B.L., Johnson, A.D., 2009. Evolution of germ cell development in tetrapods: comparison of urodeles and amniotes. *Evol. Dev.* 11, 603–609. <https://doi.org/10.1111/j.1525-142X.2009.00366.x>.
- Ballard, W.W., 1986a. Morphogenetic movements and a provisional fate map of development in the holostean fish *Amia calva*. *J. Exp. Zool.* 238, 355–372. <https://doi.org/10.1002/jez.1402380309>.
- Ballard, W.W., 1986b. Stages and rates of normal development in the holostean fish, *Amia calva*. *J. Exp. Zool.* 238, 337–354. <https://doi.org/10.1002/jez.1402380308>.
- Ballard, W.W., Ginsburg, A.S., 1980. Morphogenetic movements in acipenserid embryos. *J. Exp. Zool.* 213, 69–103. <https://doi.org/10.1002/jez.1402130110>.
- Benjamini, Y., Hochberg, Y., 1995. Controlling the false discovery rate: a practical and powerful approach to multiple testing. *J. R. Stat. Soc.* 57, 289–300. <https://doi.org/10.1111/j.2517-6161.1995.tb02031.x>.
- Bolker, J.A., 1993. Gastrulation and mesoderm morphogenesis in the white sturgeon. *J. Exp. Zool.* 266, 116–131. <https://doi.org/10.1002/jez.1402660206>.
- Bolker, J.A., 1994. Comparison of gastrulation in frogs and fish. *Integr. Comp. Biol.* 34, 313–322. <https://doi.org/10.1093/icb/34.3.313>.
- Buchholz, D.R., Singamsetty, S., Karadge, U., Williamson, S., Langer, C.E., Elinson, R.P., 2007. Nutritional endoderm in a direct developing frog: a potential parallel to the evolution of the amniote egg. *Dev. Dyn.* 236, 1259–1272. <https://doi.org/10.1002/dvdy.21153>.
- Carvalho, L., Heisenberg, C.P., 2010. The yolk syncytial layer in early zebrafish development. *Trends Cell Biol.* 20, 586–592. <https://doi.org/10.1016/j.tcb.2010.06.009>.
- Chen, S., Kimelman, D., 2000. The role of the yolk syncytial layer in germ layer patterning in zebrafish. *Development*. 127, 4681–4689. <https://doi.org/10.1242/dev.127.21.4681>.
- Chipman, A.D., Haas, A., Khaner, O., 1999. Variations in anuran embryogenesis: yolk-rich embryos of *Hyperolius punctulatus* (Hyperoliidae). *Evol. Dev.* 1, 49–61. <https://doi.org/10.1111/j.1525-142X.1999.t01.3-3.x>.
- Collazo, A., Keller, R., 2010. Early development of *Ensatina eschscholtzii*: an amphibian with a large, yolk egg. *EvoDevo*. 1, 6. <https://doi.org/10.1186/2041-9139-1-6>.
- Collazo, A., Bolker, J.A., Keller, R., 1994. A phylogenetic perspective on teleost gastrulation. *Am. Nat.* 144, 133–152. <https://doi.org/10.1086/285665>.
- Desnitskiy, A.G., 2015. On the features of embryonic cleavage in diverse fish species. *Russ. J. Dev. Biol.* 46, 385–392. <https://doi.org/10.1134/S106236041506003X>.
- Dettlaff, Tatiana A., Ginsburg, Anna S., Schmalhausen, Olga I., 1993. Sturgeon Fishes, Developmental Biology and Aquaculture. Springer, Berlin, Heidelberg. <https://doi.org/10.1007/978-3-642-77057-9>.
- Diedhiou, S., Bartsch, P., 2009. Staging of the early development of polypterid (Cladistia). Development of non-teleost fishes. In: Kunz, Yvette W., Luer, Carl A., Kapoor, B.G. (Eds.), *Development of Non-Teleost Fishes*. Science Publishers, Enfield, Jersey, Plymouth, pp. 104–169. <https://doi.org/10.1201/b10184-3>.
- Elinson, R.P., 2009. Nutritional endoderm: a way to breach the holoblastic-meroblastic barrier in tetrapods. *J. Exp. Zool.* 312B, 526–532. <https://doi.org/10.1002/jez.b.21218>.
- Elinson, R.P., Beckham, Y., 2002. Development in frogs with large eggs and the origin of amniotes. *Zoology*. 105, 105–117. <https://doi.org/10.1078/0944-2006-00060>.
- Elinson, R.P., Sabo, M.C., Fisher, C., Yamaguchi, T., Orii, H., Nath, K., 2011. Germ plasm in *Eleutherodactylus coqui*, a direct developing frog with large eggs. *EvoDevo* 2, 20 (2011). <https://doi.org/10.1186/2041-9139-2-20>.
- Feldman, B., Gates, M.A., Egan, E.S., Dougan, S.T., Rennebeck, G., Sirotkin, H.I., Talbot, W.S., 1998. Zebrafish organizer development and germ-layer formation require nodal-related signals. *Nature*. 395, 181–185. <https://doi.org/10.1038/26013>.
- Fu, L., Shi, Y.B., 2017. The Sox transcriptional factors: functions during intestinal development in vertebrates. *Semin. Cell Dev. Biol.* 63, 58–67. <https://doi.org/10.1016/j.semdb.2016.08.022>.
- Gawlicka, A., McLaughlin, L., Hung, S.S.O., De La Noüe, J., 1996. Limitations of carrageenan microbound diets for feeding white sturgeon, *Acipenser transmontanus*, larvae. *Aquaculture*. 141, 245–265. [https://doi.org/10.1016/0044-8486\(95\)01220-6](https://doi.org/10.1016/0044-8486(95)01220-6).
- Gilbert, S.F., 2010. *Developmental Biology*, Ninth ed. Sinauer Associates, Oxford University Press.
- Ginsburg, A.S., Dettlaff, T.A., 1991. The Russian sturgeon *Acipenser Güldenstädti*. Part I. Gametes and early development up to time of hatching. In: Dettlaff, T.A., Vassetzky, S.G. (Eds.), *Animal Species for Developmental Studies*. Springer, Boston, MA, pp. 15–65. https://doi.org/10.1007/978-1-4615-3654-3_2.
- Gisbert, E., Sarasquete, M.C., Williot, P., Castello-Orvay, F., Castello-Orvay, F., 1999. Histochemistry of the development of the digestive system of Siberian sturgeon during early ontogeny. *J. Fish Biol.* 55, 596–616. <https://doi.org/10.1111/j.1095-8649.1999.tb00702.x>.
- Glasauer, S.M.K., Neuhauss, S.C.F., 2014. Whole-genome duplication in teleost fishes and its evolutionary consequences. *Mol. Gen. Genomics*. 289, 1045–1060. <https://doi.org/10.1007/s00438-014-0889-2>.
- Hasley, A., Chavez, S., Danilchik, M., Wühr, M., Pelegri, F., 2017. Vertebrate embryonic cleavage pattern determination. In: Pelegri, F., Danilchik, M., Sutherland, A. (Eds.), *Vertebrate Development*. Advances in Experimental Medicine and Biology, vol. 953. Springer, Cham, pp. 117–171. https://doi.org/10.1007/978-3-319-46095-6_4.
- Hurley, I.A., Mueller, R.L., Dunn, K.A., Schmidt, E.J., Friedman, M., Ho, R.K., Coates, M. I., 2007. A new time-scale for ray-finned fish evolution. *Proc. R. Soc. B* 274, 489–498. <https://doi.org/10.1098/rspb.2006.3749>.
- Incardona, J.P., Scholz, N.L., 2016. The influence of heart developmental anatomy on cardiotoxicity-based adverse outcome pathways in fish. *Aquat. Toxicol.* 177, 515–525. <https://doi.org/10.1016/j.aquatox.2016.06.016>.
- Inoue, J.G., Miya, M., Tsukamoto, K., Nishida, M., 2003. Basal actinopterygian relationships: A mitogenomic perspective on the phylogeny of the “ancient fish.”. *Mol. Phylogenet. Evol.* 26, 110–120. [https://doi.org/10.1016/S1055-7903\(02\)00331-7](https://doi.org/10.1016/S1055-7903(02)00331-7).
- Ivan Bower, N., Joachim Moser, R., Robert Hill, J., Arabella Lehnert, S., 2007. Universal reference method for real-time PCR gene expression analysis of preimplantation embryos. *Biotechniques*. 42, 199–206. <https://doi.org/10.2144/000112314>.
- Jorgensen, P., 2008. *Yolk. Curr. Biol.* 18, 103–104. <https://doi.org/10.1016/j.cub.2007.10.037>.
- Kikugawa, K., Katoh, K., Kuraku, S., Sakurai, H., Ishida, O., Iwabe, N., Miyata, T., 2004. Basal jawed vertebrate phylogeny inferred from multiple nuclear DNA-coded genes. *BMC Biol.* 2, 3 (2004). <https://doi.org/10.1186/1741-7007-2-3>.
- Korzhuev, P.A., Sharkova, L.B., 1967. On peculiarities of digestion of the Russian sturgeon in the Caspian Sea. In: Karzinkin, G.S. (Ed.), *Metabolism and Biochemistry of Fishes*. Nauka, Moscow, pp. 205–209 (in Russian).
- Linhartová, Z., Saito, T., Kaspar, V., Rodina, M., Prásková, E., Hagihara, S., Pšenicka, M., 2015. Sterilization of sterlet *Acipenser ruthenus* by using knockdown agent, antisense morpholino oligonucleotide, against dead end gene. *Theriogenology*. 84, 1246–1255. <https://doi.org/10.1016/j.theriogenology.2015.07.003>.
- Long, W.L., Ballard, W.W., 2001. Normal embryonic stages of the longnose gar, *Lepisosteus osseus*. *BMC Dev. Biol.* 1, 6 (2001). <https://doi.org/10.1186/1471-213X-1-6>.
- Maegawa, S., Yasuda, K., Inoue, K., 1999. Maternal mRNA localization of zebrafish DAZ-like gene. *Mech. Dev.* 81, 223–226. [https://doi.org/10.1016/S0925-4773\(98\)00242-1](https://doi.org/10.1016/S0925-4773(98)00242-1).
- Mizuno, T., Yamahara, E., Wakahara, M., Kuroiwa, A., Takeda, H., 1996. Mesoderm induction in zebrafish. *Nature*. 383, 131–132. <https://doi.org/10.1038/383131a0>.
- Newman, K., Venkatarama, T., Zhou, Y., Luo, X., King, M.L., Lai, F., 2010. Repression of zygotic gene expression in the *Xenopus* germline. *Development*. 137, 651–660. <https://doi.org/10.1242/dev.038554>.
- Nóbrega, R.H., Greebe, C.D., van de Kant, H., Bogerd, J., de França, L.R., Schulz, R.W., 2010. Spermatogonial stem cell niche and spermatogonial stem cell transplantation in zebrafish. *PLoS One* 5 (9), e12808. <https://doi.org/10.1371/journal.pone.0012808>.
- Noori, T., Dehpour, A.R., Sureda, A., Fakhri, S., Sobarzo-Sanchez, E., Farzaei, M.H., Shirooie, S., 2020. The role of glycogen synthase kinase 3 beta in multiple sclerosis. *Biomed. Pharmacother.* 132, 110874. <https://doi.org/10.1016/j.biopha.2020.110874>.
- Pasquier, J., Cabau, C., Nguyen, T., Jouanno, E., Severac, D., Braasch, I., Bobe, J., 2016. Gene evolution and gene expression after whole genome duplication in fish: the PhyloFish database. *BMC Genomics* 17, 368 (2016). <https://doi.org/10.1186/s12864-016-2709-z>.
- Pocherniaieva, K., Psenicka, M., Sidova, M., Havelka, M., Saito, T., Sindelka, R., Kaspar, V., 2018. Comparison of oocyte mRNA localization patterns in sterlet *Acipenser ruthenus* and African clawed frog *Xenopus laevis*. *J. Exp. Zool.* 330, 181–187. <https://doi.org/10.1002/jez.b.22802>.
- Ravi, V., Venkatesh, B., 2018. The divergent genomes of teleosts. *Annu. Rev. Anim. Biosci.* 6, 47–68. <https://doi.org/10.1146/annurev-animal-030117-014821>.
- Ross, C., Boroviak, T.E., 2020. Origin and function of the yolk sac in primate embryogenesis. *Nat. Commun.* 11, 3760 (2020). <https://doi.org/10.1038/s41467-020-17575-w>.
- Saito, T., Psenicka, M., 2015. Novel technique for visualizing primordial germ cells in sturgeons (*Acipenser ruthenus*, *A. gueldenstädtii*, *A. baerii*, and *Huso huso*). *Biol. Reprod.* 93, 1–7. <https://doi.org/10.1095/biolreprod.115.128314>.
- Saito, T., Fujimoto, T., Maegawa, S., Inoue, K., Tanaka, M., Arai, K., Yamahara, E., 2006. Visualization of primordial germ cells in vivo using GFP-nos1 3'UTR mRNA. *Int. J. Dev. Biol.* 50, 691–700. <https://doi.org/10.1387/ijdb.062143ts>.
- Saito, T., Psenicka, M., Goto, R., Adachi, S., Inoue, K., Arai, K., Yamahara, E., 2014. The origin and migration of primordial germ cells in sturgeons. *PLoS One* 9 (2), e86861. <https://doi.org/10.1371/journal.pone.0086861>.
- Saito, T., Hilal, G., Iegorova, V., Rodina, M., Psenicka, M., 2018. Elimination of primordial germ cells in sturgeon embryos by ultraviolet irradiation. *Biol. Reprod.* 99, 556–564. <https://doi.org/10.1093/biolre/i0y076>.
- Sant, K.E., Timme-Laragy, A.R., 2018. Zebrafish as a model for toxicological perturbation of yolk and nutrition in the early embryo. *Curr. Environ. Health Rep.* 5, 125–133. <https://doi.org/10.1007/s40572-018-0183-2>.

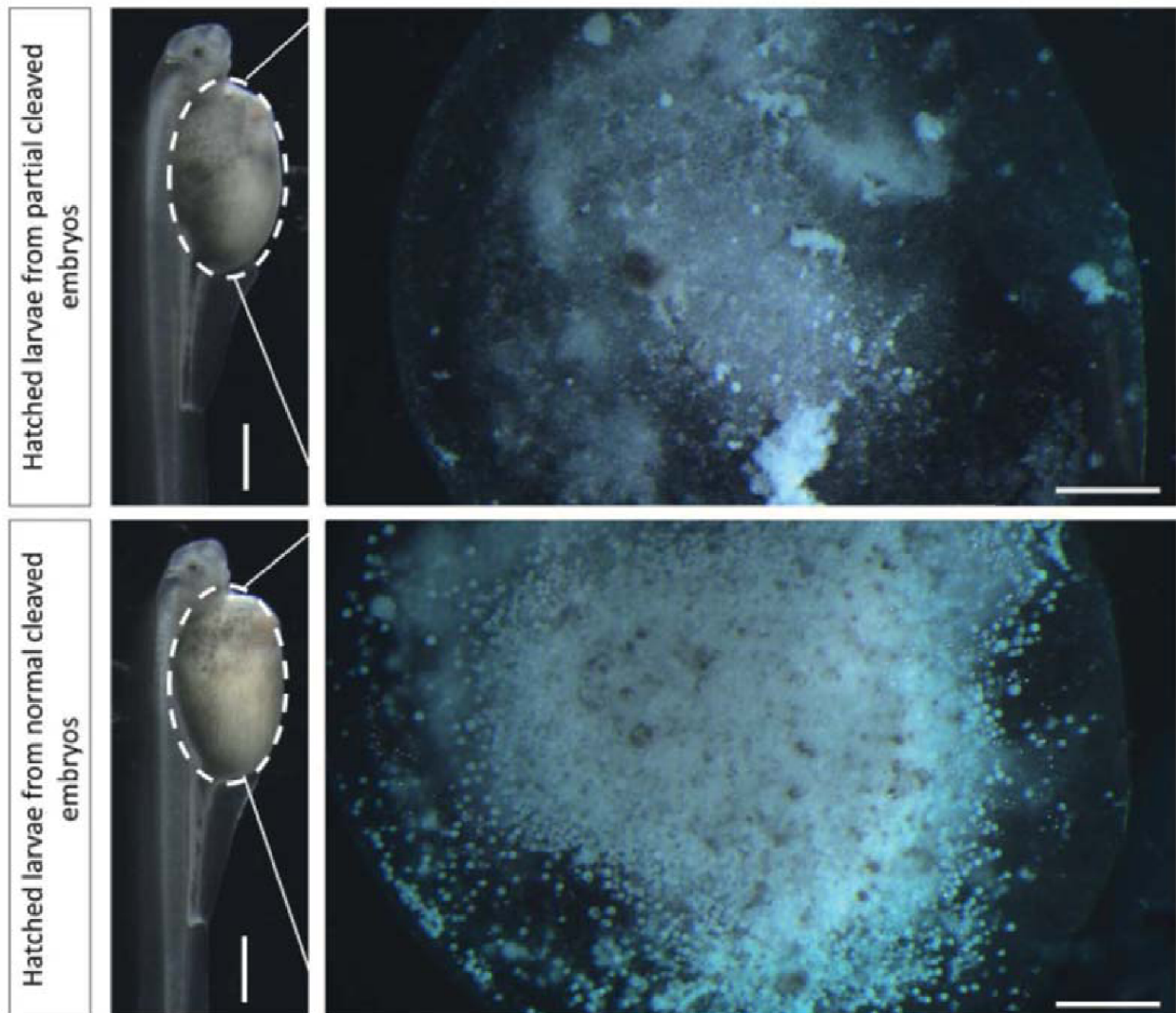
Blastomeres derived from the vegetal pole provide extra-embryonic nutrition to sturgeon (Acipenser) embryos: transition from holoblastic to meroblastic cleavage

M.A. Shah et al.

Aquaculture 551 (2022) 737899

- Shah, M.A., Saito, T., Šindelka, R., Iegorova, V., Rodina, M., Baloch, A.R., Pšenicka, M., 2021. Novel technique for definite blastomere inhibition and distribution of maternal RNA in sterlet *Acipenser ruthenus* embryo. *Fish. Sci.* 87, 71–83. <https://doi.org/10.1007/s12562-020-01481-7>.
- Sheng, G., Foley, A.C., 2012. Diversification and conservation of the extraembryonic tissues in mediating nutrient uptake during amniote development. *Ann. N. Y. Acad. Sci.* 1271, 97–103. <https://doi.org/10.1111/j.1749-6632.2012.06726.x>.
- Starck, J.M., Stewart, J.R., Blackburn, D.G., 2021. Phylogeny and evolutionary history of the amniote egg. *J. Morphol.* 282, 1080–1122. <https://doi.org/10.1002/jmor.21380>.
- Sutasurja, L.A., Nieuwkoop, P.D., 1974. The induction of the primordial germ cells in the urodeles. *W. Roux' Archiv f. Entwicklungsmechanik.* 175, 199–220. <https://doi.org/10.1007/BF00582092>.
- Takeuchi, M., Takahashi, M., Okabe, M., Aizawa, S., 2009a. Germ layer patterning in bichir and lamprey; an insight into its evolution in vertebrates. *Dev. Biol.* 332, 90–102. <https://doi.org/10.1016/J.YDBIO.2009.05.543>.
- Takeuchi, M., Okabe, M., Aizawa, S., 2009b. The Genus *Polypterus* (Bichirs): A Fish Group Diverged at the Stem of Ray-Finned Fishes (Actinopterygii). *Cold Spring Harb Protoc.* p. 2009. <https://doi.org/10.1101/pdb.emo117>.
- Tremblay, M., Sanchez-Ferras, O., Bouchard, M., 2018. Gata transcription factors in development and disease. *Development.* 145, dev164384. <https://doi.org/10.1242/dev.164384>.
- Yasuo, H., Lemaire, P., 2001. Generation of the germ layers along the animal-vegetal axis in *Xenopus laevis*. *Int. J. Dev. Biol.* 45, 229–235. <https://doi.org/10.1387/ijdb.11291851>.

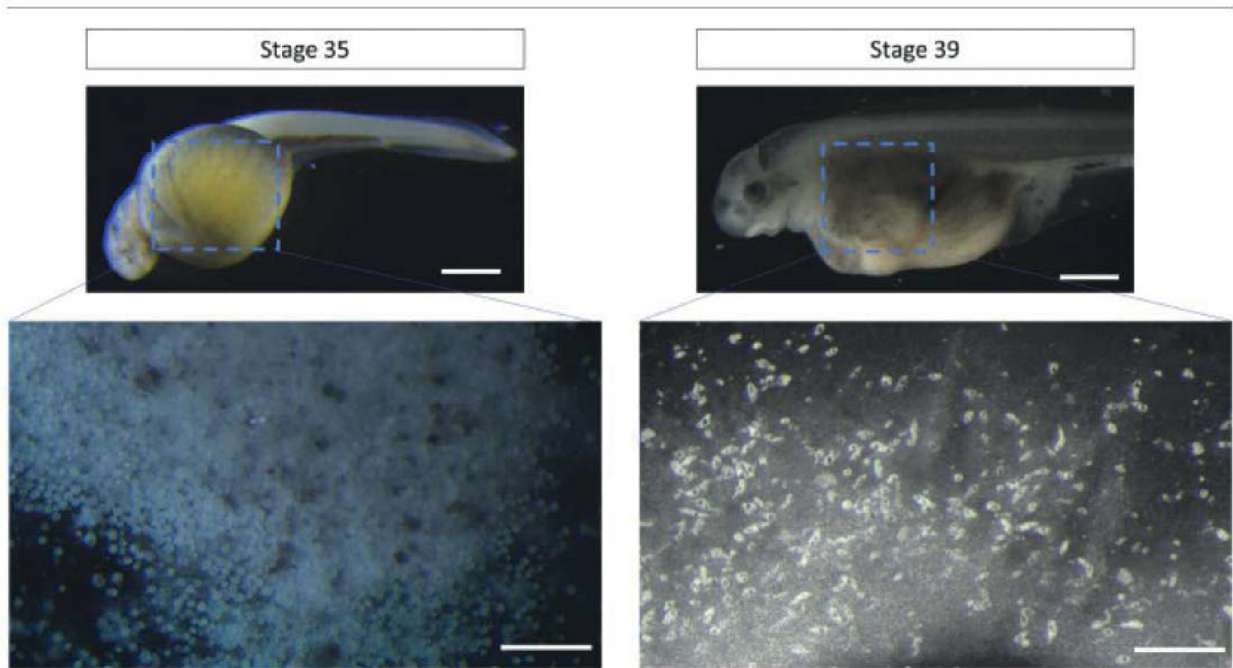
The following are the supplementary data related to this article.



[Download : Download high-res image \(2MB\)](#)

[Download : Download full-size image](#)

Supplementary Fig. S1. Form of yolk in treated and normal (wild) type embryos. The condition of yolk cells (YCs) after treatment (inhibition of vegetal blastomeres). The dissection of control embryos at stage 36, showed a massive number of YCs with normal shape and size, and with nuclei (not shown). In contrast, dissection of treated (vegetal pole inhibited) embryos at the same stage showed that most of the gut contained yolk platelets with few YCs, which suggests that these YCs provide extra-embryonic nutrition. Scale bar indicates 1 mm.



[Download](#) : [Download high-res image \(1MB\)](#)

[Download](#) : [Download full-size image](#)

Supplementary Fig. S2. **Form of yolk cells (YCs) in normal (wild) type embryos at different lecithotrophic stages.** The dissection of the gut just before hatching (stage 35) showed that most of the YCs found were round in shape and regular in size. However, after hatching (stage 39), we observed decomposition of YCs containing yolk platelets, suggesting that the sturgeon embryo starts digestion of the YCs after hatching and utilizes them for nutritional purposes. Scale bar indicates 1 mm.

CHAPTER 4

THE GUT DEVELOPMENT OF STURGEON IS UNIQUE AMONG VERTEBRATES: A COMPARATIVE STUDY

Mujahid Ali Shah, Viktoriia Iegorova, Radek Šindelka, David Gela, Marek Rodina, Roman Franěk, Jan Stundl, Taiju Saito, Martin Pšenička. The gut development of sturgeon is unique among vertebrates: A comparative study. Manuscript.

According to agreement between the authors, it is allowed to include the manuscript in this Ph.D. thesis

My share on this work was about 60%.

The gut development of sturgeon is unique among vertebrates: A comparative study

Mujahid Ali Shah¹, Viktoriia Iegorova², Radek Šindelka², David Gela¹, Marek Rodina¹, Roman Franěk¹, Jan Stundl^{1,3}, Taiju Saito^{1,4*}, Martin Pšenička^{1*}

¹ University of South Bohemia in Ceske Budejovice, Faculty of Fisheries and Protection of Waters, South Bohemian Research Center of Aquaculture and Biodiversity of Hydrocenoses, Zatisi 728/II, 389 25 Vodnany, Czech Republic

² Laboratory of Gene Expression, Institute of Biotechnology of the Czech Academy of Sciences, Vestec, Czech Republic

³ Division of Biology and Biological Engineering, California Institute of Technology, Pasadena, CA, United States

⁴ South Ehime Fisheries Research Centre, Ehime University, Ainan, Ehime, 798-4206, Japan

Contact

Taiju Saito* taiju76@gmail.com

Martin Pšenička* psenicka@frov.jcu.cz

Abstract

During evolution, every animal has retained specific developmental features. So far, the developmental pattern of sturgeon's (*Acipenser*) gut and its evolutionary conservation is poorly understood. Hence, the present study aims to investigate the sturgeon's gut development and compare it to that of other vertebrate taxa, including model and non-model vertebrates. First, we employed histological analysis of gut-endoderm development. Second, we confirmed morphologically observed endodermal cells using HCR-IN-SITU hybridization – endodermal RNA (sox17) staining during neurulation. Third, we utilized in-vivo labelling of endodermal cells using microinjection of Carboxy-DCFDA {5-(and-6)-Carboxy-2',7'-Dichlorofluorescein Diacetate} during early neurulation and traced them until hatching. Finally, for comparison with other vertebrates including holoblastic (African clawed frog, bichir, and mice) and meroblastic (chicken, gar, and zebrafish) representatives, we used only histological observation. To develop the gut, sturgeon's endodermal cells formed the archenteron (primitive gut) like frog and bichir. However, during neurulation, the archenteric cavity has inflated and expanded laterally and roofed semicircle of extraembryonic yolk cells. During pharyngula, the cavity encompasses whole amount of yolk cell mass "yolk inside the gut." Based on cross-species comparison in this study, sturgeon retained a distinctive mode of gut developmental pattern during its evolution.

Keywords: Sturgeon, endoderm, holoblastic cleavage, meroblastic cleavage, vertebrate evolution

1. Introduction

Generally, in all vertebrates, three primary germ layers, including 1) endoderm, 2) mesoderm and 3) ectoderm produce the organ/tissue. The ectoderm gives rise to the nervous system, neural crest derivatives and skin. The heart, kidney, gonads and gut muscles and blood-forming tissues develop from the mesoderm. The respiratory and gastrointestinal tract and all of their associated organs develop from the endoderm (Gilbert, 2010; Kiecker et al., 2016). Using advanced fate mapping techniques, recent studies on vertebrate model organisms; including African clawed frog – *Xenopus laevis* zebrafish, chicken and mice; have extensively described which cells in the embryo give rise to the endoderm and how those cells form a primitive gut tube (Wallace and Pack, 2003; Zorn and Wells, 2009; Gilbert, 2010). To understand the

gut-endoderm morphogenesis between vertebrates and its true evolutionary divergences, it is crucial to study cross-species comparisons of the origin and fate of gut-endoderm development across vertebrates, including model and non-model (Figure 1).

The embryo of *X. laevis* is regarded as a model to study the ancient mode of development pattern (e.g., holoblastic). In this pattern, germ layers precursors are arranged in a gradient along with the animal-vegetal (top-bottom) axis. The ectoderm, mesoderm, and endoderm are developed from the animal, equatorial, and vegetal hemispheres, respectively (Gilbert, 2010). During blastulation, blastocoel separates ectoderm from endoderm and permits cell migration, and during gastrulation, morphologically distinct “bottle cells” initiate cell involution via dorsal lip of blastopore, which leads to the formation of the archenteron (primitive gut). The cells of the archenteron floor end up on the same side of the gut tube as those from the dorsal roof. The entire gut is developed and underlaid with mesenchymal cells, and utilized their yolk intracellularly in the form yolk platelets (Keller, 1981; Shih and Keller, 1994; Zorn and Wells, 2009; Kurth et al., 2012).

In contrast, the modern group of Actinopterygii, e.g., zebrafish embryos divide partially due to massive amount of yolk mass; only the animal hemisphere forms the blastoderm (blastomeres) that sits on top of the yolk cell. It is composed of a middle layer of deep cells (DCs) and a multinucleate yolk syncytial layer (YSL) between the middle layer and yolk cell (Strehlow et al., 1994; Chen and Kimelman, 2000). The YSL separate the yolk from blastomeres and plays a crucial role in the transportation of nutrient/metabolic from yolk to the embryonic body. Moreover, YSL is also important for embryonic patterning and morphogenetic movements (Carvalho and Heisenberg, 2010). The germ ring is formed as gastrulation progresses by the thickening of DCs at the leading edge of the vegetally expanding blastoderm. The germ ring’s DCs involution forms two layers: epiblast and hypoblast. The epiblast gives rise to ectodermal cell lines, while hypoblast contributes to the formation of the embryonic endoderm (Ober et al., 2003). The entire gut develops and lies on the yolk sac, the yolk is substantially used up, and feeding commences, allowing for nutritional intake to be processed in the gut (Kimmel et al., 1995).

Similarly, owing to colossal yolk mass, archosaurs retain a meroblastic cleavage pattern and have a flattened blastodisc on yolk mass and display a pattern of gastrulation very different from that of amphibian embryos (Zorn and Wells, 2009). At the same time, placental mammals retain same gastrulation pattern as archosaurs, even though they have significantly less yolk (Takeuchi et al., 2009b), because, mammals and reptiles, including birds, are all amniotes (i.e., they produce eggs that develop extraembryonic membranes). Gastrulation begins in an epithelial layer called the epiblast in chickens and mice. Cells in the epiblast transition from epithelial to mesenchymal and migrate through the primitive streak (analogous to dorsal blastopore lip in *X. laevis*) and incorporate in the mesoderm (middle) or endoderm (outer) layer (Zorn and Wells, 2009). The cells of the presumptive definitive endoderm invade and displace an outer layer of extraembryonic tissue cells, which form supporting structures such as the yolk sac (hypoblast in chicken and the visceral endoderm in mouse). Lineage tracing studies during the late gastrula stage have shed light on endoderm and how a two-dimensional sheet of cells forms the primitive gut tube (E7.5 in mouse, HH4 in chicken) (Rosenquist, 1971; Lawson et al., 1986; Lawson and Schoenwolf, 2003; Tremblay and Zaret, 2005; Kimura et al., 2007; Tam et al., 2007).

In comparison to the modern model vertebrates (mentioned above), sturgeon – an ancient primitive vertebrate – belongs to the ray-finned fish (actinopterygian). Several comparative studies have suggested that early embryonic developmental pattern of sturgeon, bichir, and *X. laevis* is very similar (Bolker, 1993; 1994; Collazo et al., 1994; Takeuchi et al., 2009a,b; Saito et al., 2014; Pocherniaieva et al., 2018; Naraine et al., 2022). For example, two decades ago, it was reported that vegetal blastomeres/yolk cells; YCs of sturgeon embryos contribute to embryonic development (Ballard and Ginsburg, 1980; Ginsburg and Dettlaff, 1991; Gawlicka et al., 1996). In contrast, recently, we have reported that the YCs of sturgeon

embryo do not contribute to the germ layer formation (Shah et al., 2022). Thus, these YCs are extraembryonic as in yolk of teleost (zebrafish) and YCs of bichir – earliest diverged living group of actinopterygian fishes, agnathan lampreys (Petromyzontidae) – an extant lineage of jawless fishes and *Eleutherodactylus coqui* (frog with direct development) – an anuran (Buchholz et al., 2007; Takeuchi et al., 2009b). Moreover, in the case of gut development in bichir and *E. coqui*, researchers have also reported that YCs from ventral part of archenteron do not contribute to gut development. The entire gut is established as a tubular structure underlaid with mesenchymal cells, and YCs mass exists on the anterior-ventral side of the embryo. The YCs are not underlaid with the mesenchymal cells as in *X. laevis*, but it is directly surrounded by surface ectoderm as in the yolk sac in teleosts (zebrafish) and is therefore extra-embryonic (Wallace and Pack, 2003; Buchholz et al., 2007; Takeuchi et al., 2009b). Furthermore, morphoanatomical studies have revealed that the lamprey embryo's archenteron is continuous with the blastopore. The entire primitive gut including the pharynx initially developed from the archenteron. Due to the abundance of yolk, the archenteron shows the delayed epithelialization and forms the secondary gut cavity within the yolk (Shiple, 1885; Kupffer, 1890; Damas, 1943; Piavis, 1971; Richardson et al., 2010; Li et al., 2019).

Similarly, for more than two decades, it has been reported that when chondrosteans larvae hatch, the alimentary canal is undifferentiated, filled with yolk, and does not communicate with the external environment. During neurulation, a darkly pigmented epithelioid sheet covers a large mound of YCs on the archenteric floor of sturgeon embryos. However, the differentiations that transform the archenteron cavity and its linings into the definitive gut have not yet been described (Ballard and Needham, 1964; Ballard and Ginsburg, 1980; Buddington and Doroshov, 1986; Shah et al., 2022). Therefore, in the present study, we have investigated the sturgeon's gut development and its comparison with other vertebrate taxa including holoblastic (bichir, *X. laevis*, and mice) and meroblastic (gar, zebrafish, and chicken) representative for better understanding evolutionary conservation (Figure 1).

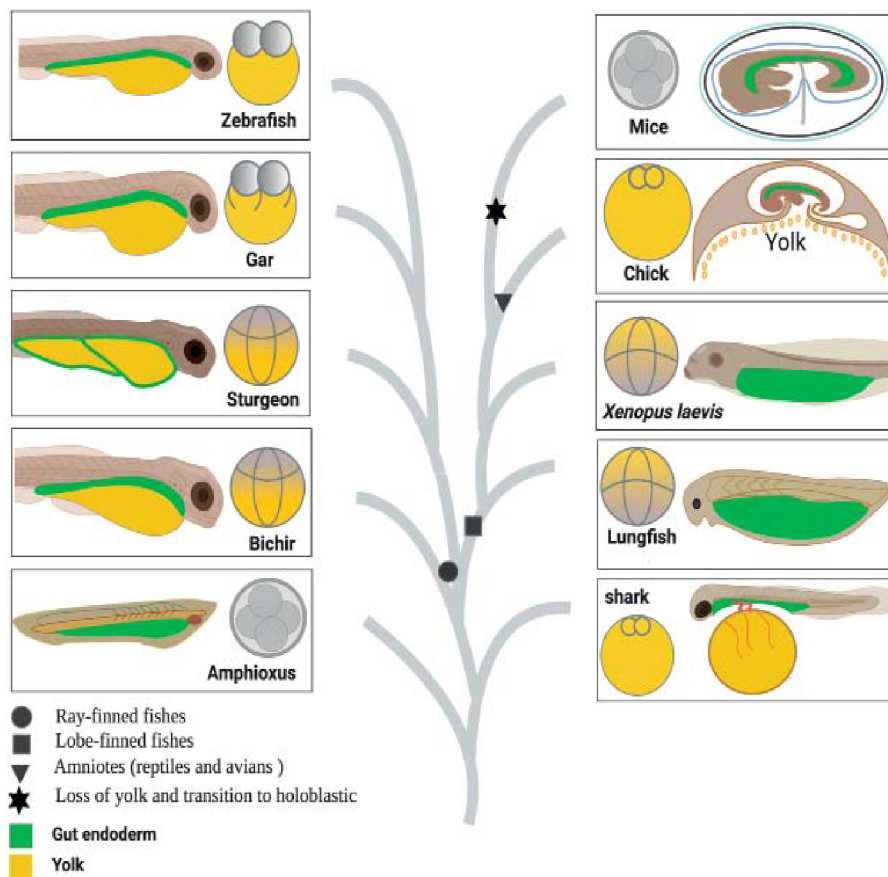


Figure 1. Comparison of egg cleavage patterns and gut anatomy among vertebrates based on their phylogeny relationship. Figure 1 represents the evolution of egg cleavage pattern and gut development among vertebrates. The illustration has been created based on literature review and current findings (Rosenquist, 1971; Lawson et al., 1986; Lawson and Schoenwolf, 2003; Ober et al., 2003; Tremblay and Zaret, 2005; Kimura et al., 2007; Tam et al., 2007; Takeuchi et al., 2009b; Zorn and Wells, 2009; Kemp, 2011).

2. Results and discussion

2.1. Gut development of sturgeon

Phylogenetically, sturgeon (Acipenseriformes) is an outgroup to *X. laevis* (Amphibia; Anura) and zebrafish (Teleost; Cypriniformes), nevertheless, their egg cleavage pattern is holoblastic {see, Figure 1 (Bolker 1993, 1994; Takeuchi et al., 2009a)}. Therefore, over the last few decades, whether embryonic developmental pattern of sturgeon is conserved with zebrafish-meroblastic or *Xenopus*-holoblastic, is an interesting topic in the field of developmental biology. In this regard, several comparative studies have attempted to specify the compare the developmental pattern of sturgeon to other vertebrates. For examples, maternal RNA localization in oocytes and embryos (Pocherniaieva et al., 2018; Naraine et al., 2022), cleavage pattern of embryos (Bartsch et al., 1997; Cooper and Virta 2007), germ cell specification (Saito et al., 2014), gastrulate deviations (Bolker 1993, 1994; Cooper and Virta, 2007), and organs/tissue formation (Minarik et al., 2017). Nevertheless, all previous studies compared the sturgeon either with amphibians (*X. laevis*) or bony fishes (non-teleost and teleost). Previously, we also reported that blastomeres/cells derived from vegetal pole are endogenous nutrition, except PGCs (Shah et al., 2022). To the best of our knowledge, using precise fate mapping techniques, the development of gut in sturgeon and its evolutionary conservation has not yet been investigated.

Here, we shed light on the development of sturgeon primitive gut in a comparative evolutionary context of vertebrates. Morphological observations of hatched larvae using plastic section histology show the obvious structure of gut epithelial tissue that surround all YCs (Figure 2A). Further, following our previous study (Shah et al., 2022), immunohistochemistry detection of FITC-dextran (vegetal blastomeres labelled at stage 12) after hatching (stage 38) showed that almost all FITC-labelled YCs were found to be broken “inside-the-gut” and FITC was enriched on the inner surface of the gut (Figure 2). In some embryos, a part of the gut was slightly labelled with the FITC, which is secreted from broken YCs. The broken state of the cells might be owing to the enzymatic digestion of YCs and utilized these YCs for endogenous nutrition {for reference (Korzhev and Sharkova, 1967; Ginsburg and Dettlaff, 1991; Gisbert et al., 1999)} (Figure 2B).

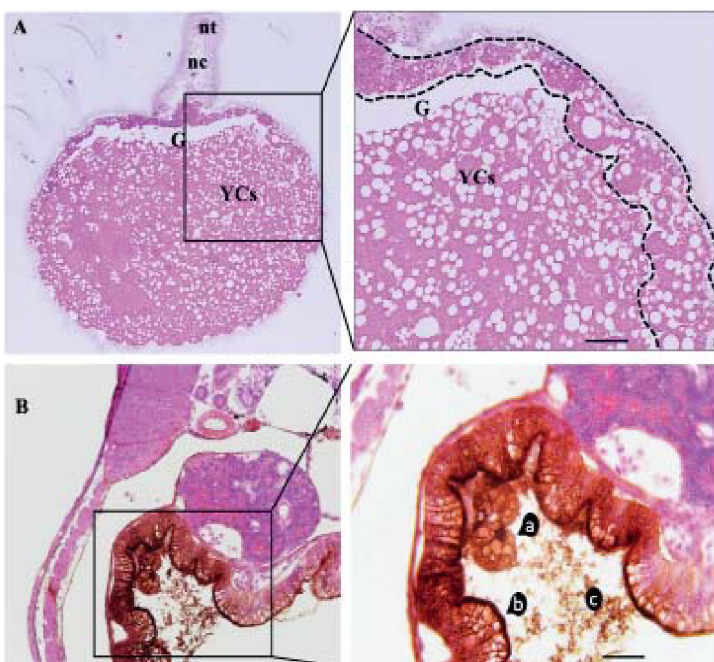


Figure 2. Histological observation of gut and immunohistochemistry of FITC-labelled vegetal blastomeres (yolk cells) inside gut.

A) transverse section of hatched larvae (stage 36) shows the obvious structure of gut epithelial tissue, which encompasses the whole yolk (yolk-inside-gut). B) The immunolabeling of FITC-dextran-labelled part of gut {(the vegetal blastomeres produces the extraembryonic yolk cells (YCs), for detail see (Shah et al., 2022))}. Immunolabeling of FITC dextran at stage 38 shows YCs were FITC-enriched and broken inside the gut. Insert rectangular box and dotted lines – gut epithelial, nt – neural tube, nc – notochord, G – gut, YCs. a – yolk cells, b – enriched-FITC in the inner lining of gut, c – broken state of YCs. Scale bars indicate 20 μ m.

As previously reported by Ballard and Ginsburg (1980), the YCs are wrapped by archenteron's cavity, with protruding floor like an inverted cup, anteriorly, posteriorly, and on both sides. To reveal whether morphological observed cells were endodermal {(Ballard and Ginsburg, 1980), our data Figure 2 and 5), we analyzed expression of endodermal gene Sox17, which has confirmed that these cells have endodermal origin from the archenteron on dorsal side. Subsequently, the archenteron's cavity encompassed the semicircle area of the YCs instead form a tubular gut on the top of YCs (Figure 3). In addition, we further confirmed that stained cells (SOX17-HCR-FISH) were endodermal using the microinjection of Carboxy-DCFDA – cell labelling dye. The dye was injected through the neural plate, next to the midline at early neurula stage (Figure 4). The positive injected embryos demonstrated that the cell from archenteron continues to divide and move lateroventral to encompassed YCs, as anticipated by Ballard and Ginsburg, 1980 around three decades ago and as in our data from histological observation (Ballard and Ginsburg, 1980) (Figure 4 and 5).

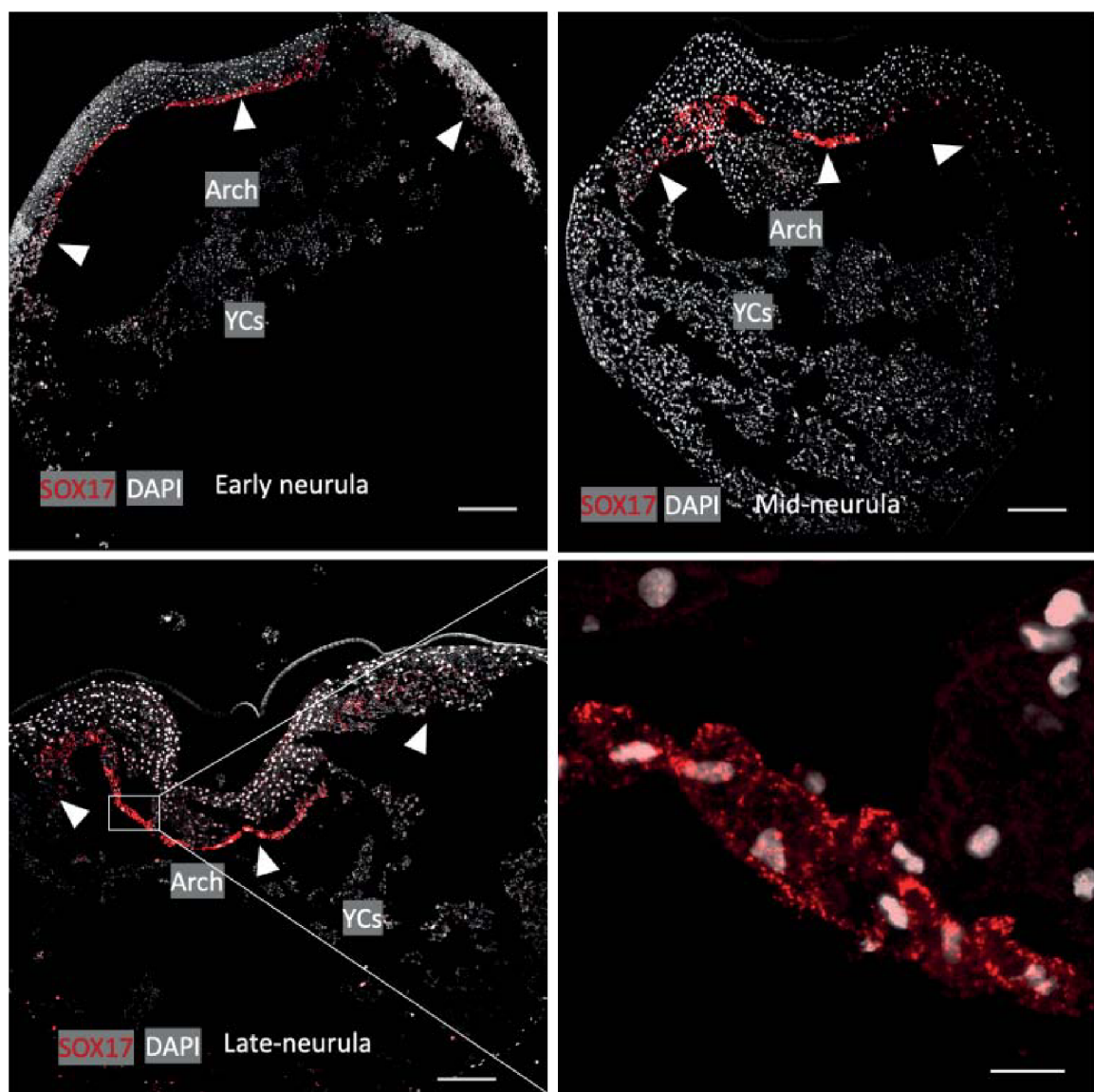


Figure 3. Expression of Sox17 in the primitive gut of sturgeon.

Staining of endoderm using marker gene – Sox17. Early neurula (stage 20) shows the archenteron that encompasses the semicircle area of yolk cells. During mid stage and late neurula (stage 22–24), a tubular gut on dorsal position of yolk was not observed. The zoom out picture is a magnified view of positive labelling of endoderm. Grayscale shows DAPI labelling, red colour, and arrows show the positive signals from endodermal cells. yolk; YCs – yolk cells. Arch – archenteron. Scale bars indicate 100 μ m.

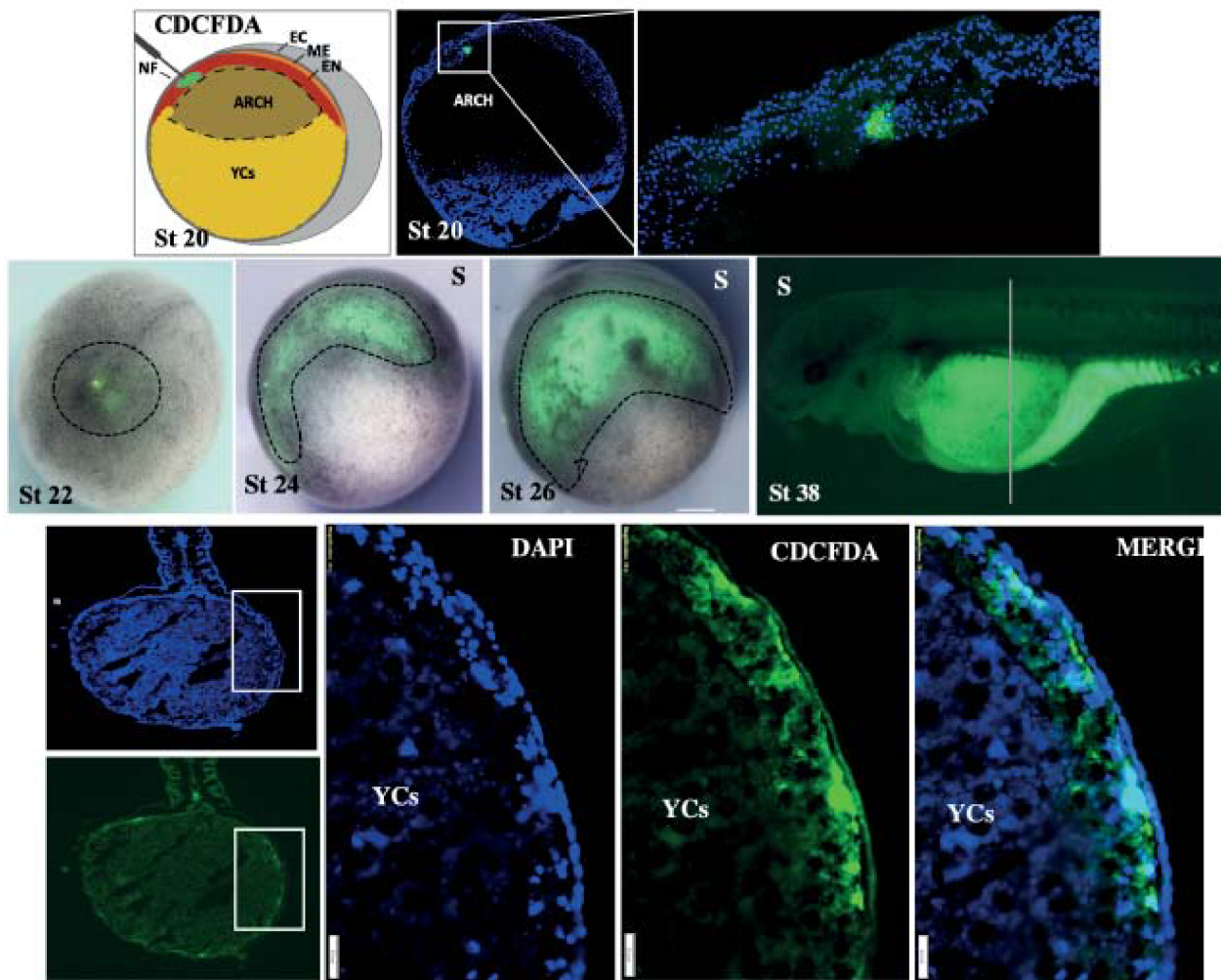


Figure 4. Labelling of endodermal cells using microinjection carboxy-dcfda.

CDCFDA Fate mapping (stage 20). The dye was precisely injected into the endoderm cells of archenteron (see figure 3) through the opening of the neural tube during early neurula (stage 20). After 30 minutes, embryos were fixed and median sectioned to ensure positive labelling of endodermal cells (green colour shows the dye within the endodermal cells (see figure 3 stage 20), zoom-out of rectangular box at stage 20). The embryos show positive labelling at 22–26 stage, indicating by dotted lines. The specimens at stage 38 and section of dorsoventral of same stage (38*) show the positive labelling of endoderm cells in green colour. Sectioned specimens were counter stain with DAPI, show the blue colour. Marge image distinguishes the endoderm and ectoderm. D – dorsal view, S – side view, EC – ectoderm, ME – mesoderm, EN – endoderm, NF – Neural fold. Scale bars indicating the 1 mm in (stage 38), 200 μ m in (transverses section view of stage 38), and 50 μ m in (magnified view from rectangular box of transverses sections).

2.2. Comparison of sturgeon with *X. laevis*, bichir and mice – holoblastic representatives

The embryos of bichir, sturgeon and *X. laevis* shared a lot of developmental similarities; for details see (Bolker, 1993; 1994; Collazo et al., 1994; Takeuchi et al., 2009a,b; Pocherniaieva et al., 2018; Saito et al., 2014; Naraine et al., 2022). However, in case of gut development, a comparative study has not been conducted so far. Thus, here we compare the developmental pattern of a sturgeon gut with selected holoblastic representative animals (Figure 5). To

elaborate, *X. laevis* embryos contains all endoderm determinants in vegetal pole, and their yolk stored and utilized in the form of endodermal cells (intracellularly) (Chalmers and Slack, 2000), Figure 1 and 5}. Chalmers and Slack (2000) have briefly described the fate mapping of gut development by labelling the middle endodermal cells between the floor of the archenteron and the very ventral endoderm. The labelled cells were incorporated into the definitive gut (Chalmers and Slack, 2000). Consistently, the histological identification of *X. laevis* embryos at the neurula stage clearly showed that the endoderm lines the archenteron cavity. The dorsal endoderm is made up of a single layer of cells, whereas the ventral endoderm is made up of several layers of large endodermal cells (with intracellular yolk) (Figure 5, *Xenopus*). From the mid-neurula to the pharyngula stage, the archenteron gradually closes, and the gut cavity is a continuation of the archenteron. The definitive gut cavity is formed, containing the cells of the original archenteron as well as the more ventral endoderm (Figure 5, *Xenopus*).

In comparison, embryo of lamprey, bichir, sturgeon, and *E. coqui*, contains more yolk volume than *X. laevis*. During neurula, in the embryos of these species, the ventral part of archenteron is composed of a massive amount of YCs instead of endodermal cells (Figure 5). These YCs do not contribute to the gut and only provide the nutrition as larvae develop (Buchholz et al., 2007; Takeuchi et al., 2009b; Shah et al., 2022), Figure 5). Moreover, according to Takeuchi et al. (2009), bichir embryos with such extracellular vegetal YCs appear to be an evolutionary prepattern of the gut being established as a tubular structure, and the yolk cell mass exists on the anterior-ventral side of the embryo (Takeuchi et al., 2009b; Wallace and Pack, 2003). Consistently, histological analysis of bichir samples at the neurula stage showed that a horizontal archenteron bulge was formed on both sides: internally and rostrally. During late neurulation, the endodermal cells that give rise to their anlage are now distinguishable. The newly developed gut is underlaid with mesenchyme, which occurs on the roof of a massive amount of YCs (Figure 5, Bichir).

Interestingly, the presence of YCs causes the horizontal type of archenteron in lamprey to give rise to the entire primitive gut, including the pharynx. However, due to the presence of YCs, lamprey forms the second gut cavity within the yolk sac. However, detailed fate mapping, such as using molecular approaches, is required to confirm it (Shiple, 1885; Kupffer, 1890; Damas, 1943; Piavis, 1971; Richardson et al., 2010; Li et al., 2019).

Besides a volume of yolk associated with the development of gut-endoderm, the mice embryo has less/no yolk and retained holoblastic cleavage pattern. In mice form, stage 8.0 to stage 9.25 is considered neurulation (Jacobson and Tam, 1982). For example, during gastrulation in mice, gut endoderm developed on the embryo's surface, where definitive endoderm (derived from the epiblast) cells intercalated into the overlying visceral endoderm (derived from the primitive endoderm) and formed the extraembryonic tissues (Nowotschin et al., 2019a). Along the anterior-posterior axis, the developing gut tube epithelium forms definitive endoderm (middle, E8.5). The anterior, middle and posterior endoderm form the foregut, midgut and hindgut, respectively {(Frankenberg, 2012) (Nowotschin et al., 2019b) Figure 5, Mice}.

Compared to the above vertebrates, sturgeon develops their gut around the yolk – YCs (as described above) – and utilizes it inside the gut (Figure 1–5 and Figure S1). To the best of our knowledge, this kind of developmental pattern has only been observed in sturgeon so far. Concludingly, the lining of the presumptive sturgeon's gut and the vitelline syncytium of other fishes have similar mechanisms for utilizing yolk reserves. It seems reasonable for developing larvae of sturgeon to contain the yolk materials (YCs) inside the developing gut by encircling it with endodermal cells and to use the yolk for nutritional purposes at the lecithotrophic state (before first feeding) by using a newly developed digestion system {for reference (Korzhev and Sharkova, 1967; Ballard and Ginsburg, 1980; Ginsburg and Dettlaff, 1991; Gisbert et al., 1999)}.

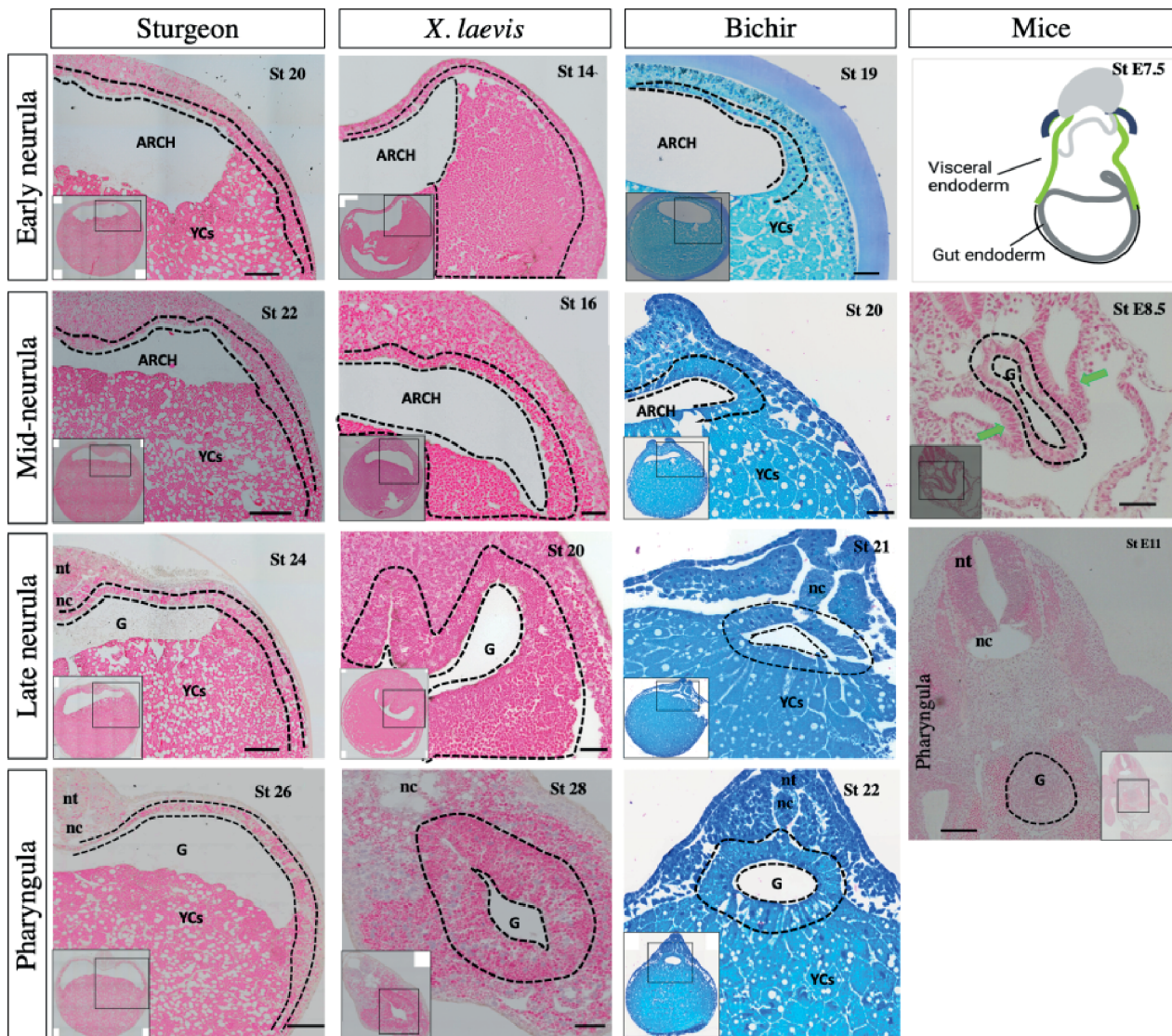


Figure 5. Morphological observation of gut development among sturgeon, *X. laevis*, bichir and mice. **Sturgeon:** Transverse sections of embryo from early to late neurulation (stage 20 to 24) and pharyngula (stage 26) shows the early development pattern of the gut. During neurulation, the endodermal cells of archenteron (future gut cavity) encompass the semicircle area of yolk mass/cells. During pharyngula, endodermal cells continue to divide and continue encompass the whole mound of yolk cells. ***X. laevis*:** Transverse sections of embryo from early to late neurulation (stage 13 to 20) and pharyngula (stage 28) shows the development of the gut. During the neurulation, archenteron shows the same structure as sturgeon, however, the cells from ventral side of archenteron are endoderm (yolk endoderm cells). During pharyngula, gut shows the prominent tubular structure of gut-endoderm, whereas yolk is intracellular (inside the endodermal cells). For detail see (Andrew D. Chalmers and Slack, 2000). **Bichir:** Transverse sections of embryo from early to late neurulation (stage 19–22) and pharyngula (stage 26) show the developmental pattern of the gut. During neurulation, the archenteron seen on the roof of yolk cells. The cells of archenteron do not move ventral to encompass the yolk cells. During pharyngula, endoderm cells show the prominent tubular structure of gut, whereas the yolk is stored in a YCs “cellularized form” inside cellular yolk sac. For details, see (Takeuchi et al., 2009b). **Mice:** Drawing of very early neurula (stage 7.5) and transverse sections of mid-neurula (stage 8.5) and pharyngula (stage 11.5) shows the development of the gut. During the neurula stage, visceral endodermal (green colour) developed the extraembryonic layers, indicated by green arrows. The gray colour is definitive endoderm, which forms the gut tube. For details see (Frankenberg, 2012; Nowotschin et al., 2019a,b). Arch – archenteron, nt – neural tube, nt – notochord, G – gut, YCs – yolk cells, Dotted lines – endodermal cells. Scale bars indicate the 100 μ m.

2.3. Comparison of sturgeon with gar, zebrafish, and chicken – meroblastic representatives

Phylogenetically, sturgeon, gar and zebrafish belong to ray-finned fishes (Figure 1). Beside sharing of lot of much developmental similarities with *Xenopus* and bichir, still sturgeons are interspecific between amphibians and teleosts in case of PGCs development and migration (Saito et al., 2014). In the case of gut development, here we present the comparison of sturgeon with gar (phylogenetically placed after sturgeon), zebrafish, and chicken (see, Figure 1). Unexpectedly, the gut development of gar and its evolutionary conservation was also unknown. Thus, to study the development of the gar gut, the designed fate-mapping approach allowed us to specifically mark the endodermal cells. The morphological observation at pharyngula and larval stage using plastic section histology clearly showed that the development of gut-endoderm occurs on the dorsal position of yolk mass, which is therefore a tubular structure, as observed in bichir and zebrafish (Figure 5 and 6) (Wallace and Pack, 2003; Ng et al., 2005; Takeuchi et al., 2009b; Comabella et al., 2013). Second, fluorescence microscopy of the CDCFDA-labelled specimens during neurulation, and tracing them until they became gut tissue, has revealed that histologically observed cells were endodermal and formed the tubular gut as zebrafish (Figure S2).

Compared to sturgeon, gar and zebrafish contain uncleaved vegetal pole of egg (see, Figure 1). In these species, only animal pole of egg contributes to develop the gut that sits on the top of the yolk, i.e., “yolk-outside-gut”. The entire yolk is surrounded by the YSL and vitelline envelope in zebrafish and gar, respectively (D’Amico and Cooper, 2001; Comabella et al., 2013) (Figure 6). In gar and zebrafish, it seems reasonable that “yolk is outside the gut” otherwise, the endodermal tissue will be slackened and wrinkled after absorption of the yolk, or it needs to be reconstructed drastically to fit the appropriate size as the yolk become smaller, as seen in sturgeon (Figure 7). In fact, in many teleosts, the yolk is surrounded by YSL, which is thought to play an important role in the yolk absorption, and the YSL disappear as larvae develops, and the gut keeps its size compact during the whole process of the embryonic development (Long and Ballard, 2001; Wallace and Pack, 2003; Carvalho and Heisenberg, 2010; Comabella et al., 2013).

In addition to teleost and non-teleost, the chicken (e.g., amniotes) also have uncleaved yolk as zebrafish. The entire gut is developed and lied on the top of the yolk sac as seen in zebrafish (Figure 1). However, chicken embryos develop extra-embryonic membranes to utilize the huge amount of yolk; for example, the splanchnopleuric mesenchyme, which is composed of mesoderm external to the coelom, plus the endoderm (Gilbert, 2010). The Splanchnopleure, instead of forming a close gut, grows over the yolk, and becomes a yolk sac (Figure 6, chicken). This yolk region is in contact with the midgut and primitive gut present above the yolk (Figure 6, chicken).

Comparatively, in sturgeon, endodermal cells from archenteron encompass YCs for endogenous nutrition, which seems like the Splanchnopleure-like structure of chicken. However, sturgeons do not develop the extra embryonic layers and retains the unique mode of gut development pattern to utilize the yolk (Figure 5–7 and Figure S1). Thus, it is also indicated that during the evolution, the increased yolk led to the development of the extraembryonic layer to utilize the yolk in amniotes.

Besides the encompassment of YCs inside the newly developed gut of sturgeon, the torsion of the gastrointestinal tract was observed immediately after hatching. The body size containing the abdominal cavity grows large, loosened/surplus with the absorption of egg yolk (loose), which appears to be in the abdominal cavity (Figure 7). The pattern of the “yolk-inside-gut” is accompanied by a significant growth of endodermal cells in order to encircle a vast area composed of YCs, about 3 mm of embryo diameter (sturgeon species). The abdominal cavity lies anterodorsally to the body, which constitutes a considerable mass, loose/excess with a massive amount of YCs. It is likely that the yolk volume might be involved in the evolution of the unique developmental pattern of the gut in sturgeon (Figure 1 and 7).

Fishes are typically classified into three major groups: superclass Agnatha (jawless fishes), class Chondrichthyes (cartilaginous fishes), and superclass Osteichthyes (bony fishes). The latter two groups include all jawed vertebrates. Based on results presented here, we concluded that the endogenous nutrition in vertebrates is digested either intra-cellularly in endodermal cells (as in *Xenopus*) or extra-cellularly (as nutritional YCs in bichir) and (as yolk in zebrafish and archosaurs). In any case, the digestive tract starts its function with digestion of exogenous nutrition after lecithotrophic state (after first feeding). In the case of sturgeons, they digest their endogenous nutrition (vegetal cells containing yolk platelets; YCs) inside of their newly developed digestive system and they start excretion from their gut already before feeding (Figure 7, stage 42). To the best of our knowledge, sturgeon endogenous nutrition is neither extra-cellular as in bichir, teleosts, and archosaurs, nor intracellular as in frog.

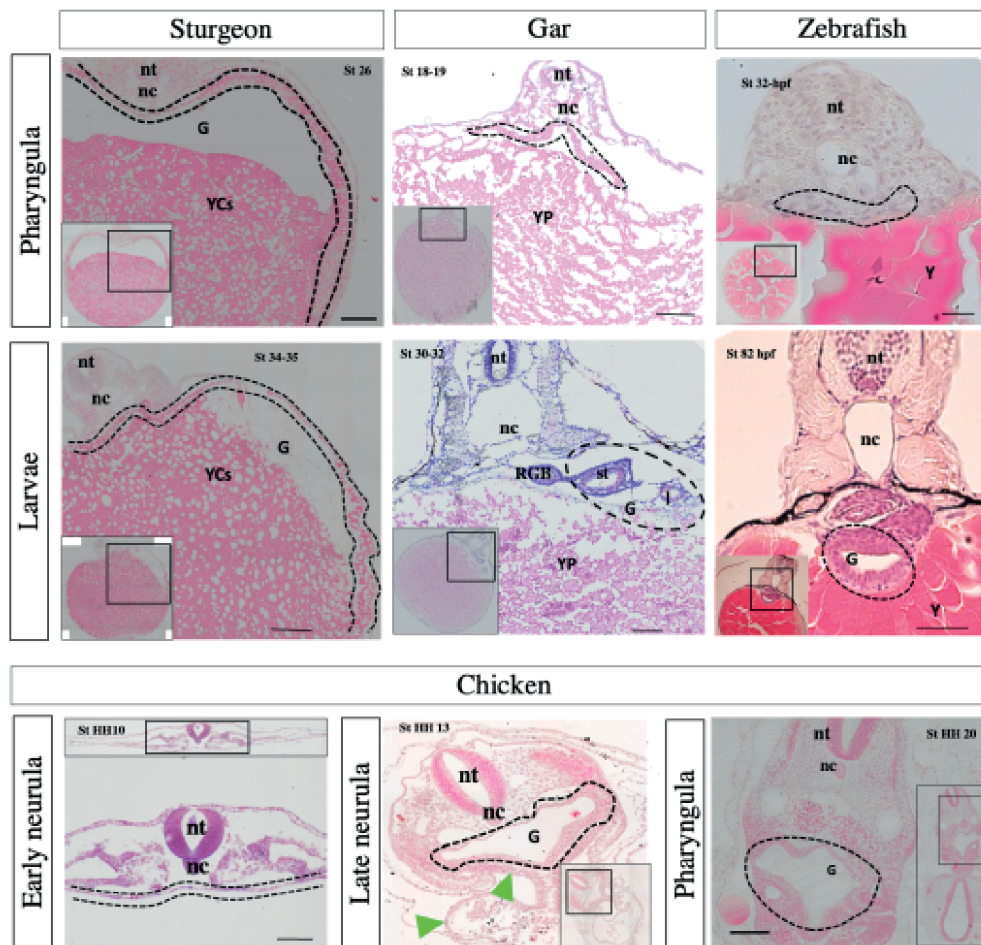


Figure 6. Morphological observation of gut development among sturgeon, gar, zebrafish and chicken. **Sturgeon:** Transverse sections of embryo from pharyngula and larvae shows the development of gut (as described above). **Gar:** Transverse sections of embryo from pharyngula (stage 18–19) and larvae (stage 30 to 32) shows the development of gut. Stages 18–19 show the endodermal cells on the dorsal position of yolk, which is quite similar to the pharyngula of zebrafish (stage 32-hpf). Similarly, the larval stage of gar (Stages 30–32) clearly shows that the gut is a tubular structure on top of huge yolk mass, as seen in zebrafish (stage 72-hpf). There is only a difference in yolk structure; yolk platelets in gar and platelet-less yolk in zebrafish. For details see (Wallace and Pack, 2003; Ng et al., 2005; Comabella et al., 2013). **Chicken:** Transverse sections of embryos from neurula (stage HH10–HH13) to pharyngula (stage HH20) shows the development of the gut. During neurula, a flattened endoderm layer is localized above the yolk mass and below the mesoderm/nerve cord. Embryos also show the obvious structure of tubular gut and extraembryonic layer (Gilbert, 2010; Frankenberg, 2012). Dotted lines – endodermal cells, green arrows – extraembryonic splanchnopleure, Arch – archenteron (future gut), nt – neural tube, st – stomach, I – intestine, RGB – respiratory gas bladder, nc – notochord, G – gut, YCs – yolk cells, YP – yolk platelets, Y – yolk. Scale bars indicate the 20 μm .

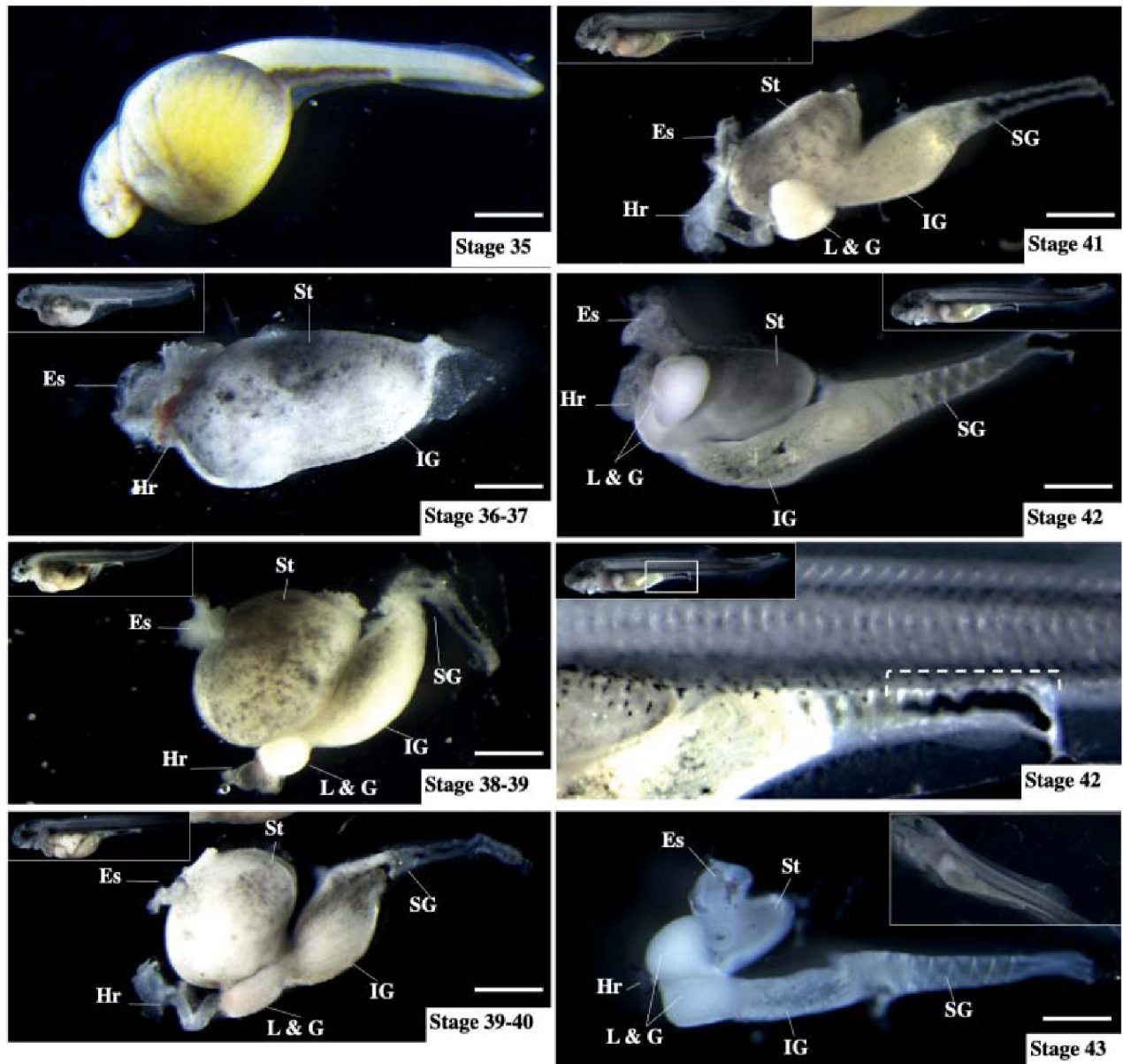


Figure 7. Ontogeny of sturgeon gut during lecithotrophic stages.

The morphological changes in the gut development after hatching/during lecithotrophic stages. The gut was separated from the trunk using dissection during the Stage 36–43. During all stages, the yolk cells were found inside the gut. However, after stage 36, the yolk cells were found in a broken state inside the gut and till stage 43, the larvae completed the endogenous nutrition. Stage 42 (rectangular box) shows the rectum with poop, which indicates that the yolk cells are digested intrainstestinally. Es – oesophagus, Hr – heart, L & G – liver and gall bladder, IG – intermediate gut, SG – segmented gut, St – stomach. Scale bars indicate the 1 mm.

3. Materials and methods

3.1. Ethics

The present study was performed in accordance with the Board of Animal Research at Faculty of Fisheries and Protection of Waters, University of South Bohemia, Czech Republic.

3.2. Samples

The specimens of African claws frog – *X. laevis*, mouse, chicken, sterlet, bichir, gar and zebrafish were prepared as follows: Zebrafish and sterlet sturgeon were bred at Genetic Fisheries Centre, Faculty of Fisheries and Protection of Waters in Vodnany, Czech Republic, and stages were selected according to (Kimmel et al., 1995; Dettlaff et al., 1993). Gar specimens were prepared at the Department of Integrative Biology, College of Natural Science, Michigan State University, USA (Jaroszewska and Dabrowski, 2009), and stages were selected according to (Long and Ballard, 2001). Bichir specimens were prepared at Department of Zoology, Charles University, Czech Republic, and stages were selected according to (Diedhiou and Bartsch, 2009). *X. laevis* specimens were prepared from the Laboratory of Gene Expression, Vestec, Czech Republic (Sindelka et al., 2010) and stage were selected according to <https://www.xenbase.org/entry/>. Mouse and chicken specimens were at department of animal science, Warsaw University of Life Science, Poland. The developmental stages were followed by (Hamburger and Hamilton, 1951; Kaufman, 1992). Due to limited number of gar samples, we compared only pharyngula and larval stages of gar, zebrafish, and sturgeon.

3.3. Histology

To study the morphological development of gut formation of sturgeon and other taxa, the plastic sections histology was processed. Specimens in triplicates from all animals were fixed in Bouin's fixative (usually for large specimens) or 4% PFA for 24 hours and then stored in 70% EtOH and dehydrated in a series of alcohol (75%, 90% and 100% for 1 hour), embedded in JB-4 plastic, sectioned at 5 μ m, stained with H&E, mounted with DPX, and observed under the light microscope. The pictures were taken using Olympus microscope. The histology sections of bichir were obtained from Department of Zoology, Charles University, Prague, Czech Republic (Stundl et al., 2020).

3.4. Immunohistochemistry of FITC labelled embryos of sterlet sturgeon

In our previous study, we injected 10% FITC Dextran–5000.00 MW (FD5) in vegetal pole at developing stage 10 and speculated that vegetal blastomeres contain extraembryonic YCs which will be encompassed by the gut (Shah et al., 2022). Thus, the FD5 labelled embryos in triplicates at stage 38 and were then fixed and embedded as described earlier (Shah et al., 2022). Specimens were sectioned about 8 μ m and 0.01% poly-L-lysine (glass microscope slides) were used to collect the tissue sections. The anti-FITC antibody (Invitrogen, #71-1900) chromogen method was employed to detect the FD5 dictation and visualization. Thereafter, specimens were counterstained with H & E staining, pictures were taken using Olympus microscope.

3.5. *in-situ* labelling and confocal microscopy

Multiplexed, quantitative, high-resolution RNA fluorescence *in-situ* hybridization (HCR-FISH) was used as instructed by Molecular Instrument (MI), *imaging and molecules of life*[™]. The probes, Sox17 (GeneID:117394216) and β -actin probe (Gene ID: 117431529) were obtained from MI. We used the *in-situ* staining on paraffin embedded section for the first time on sturgeon embryos. The protocol was followed as instructed by MI for zebrafish FFPE-samples. Embryos at required developmental stages were fixed in 4% PFA overnight at 4 °C, dehydrated in an ethanol series followed by xylene, embedded in paraffin, sectioned at 5 μ m. Sections were baked at 60 °C for one hour, deparaffinized in xylene, and 100% ethanol. Specimens were then rehydrated with ethanol series, followed by antigen retrieval. After treatment with protease-K 1 l.ml⁻¹ for 10 min at 38 °C in a humidified chamber, hybridization with target probes and amplification was performed. The DAPI (fluoroshield 4',6-diamidino-2-phenylindole) was used for counter staining. Detection of positive signals and pictures were taken using confocal microscope (Olympus FV 3000).

3.6. Labelling and tracing of sturgeon endodermal cells

For the labelling of endodermal cells of sterlet sturgeon embryos, 50 mM of CDCFDA [5-(and-6)-carboxy-2',7'-dichlorofluorescein diacetate, cat. no.: 22026, AAT Bioquest, Inc.] stock was prepared by dissolving in DMSO (dimethylsulfoxide) and stored at -20 °C. A working concentration (50 μ M) was prepared by diluting stock into 10% sucrose solution. Decapsulated sterlet sturgeon embryos were placed in agar coated Petri dish with 2mm hole to position the embryos. The dye was precisely injected into the endodermal cells of archenteron through the opened cranial neural tube. The dye passed freely into the adjacent endodermal lining, forming cell membrane-impermeant products that cannot stain the ectoderm situated across the basal lamina. Embryos were analyzed 30 min post injection and 22–24 developmental stages under fluorescent microscope to ensure the positive injection (Figure 4). Embryos were allowed to develop under dark condition until the gut tube was fully developed. The labelled specimens at stage 38 were anaesthetized in Tricaine methanesulfonate (MS222), fixed into 4% PFA under dark conditions and embedded in Tissue-Tek O.C.T and stored at -80 °C. For cryosection, embedded blocks were kept in cryostat chamber (-20 °C) for 20 minutes to equilibrate the temperature. The thickness of the cut was 8 μ m at transverse sections. The slices were collected on Superfrost slides and stained with Fluoroshield[™] with DAPI (Sigma) and covered with cover slip. For gar endoderm analyses, labelled specimens were obtained from Department of Zoology, Charles University, Prague, Czech Republic, the protocol is described by (Minarik et al., 2017). Images were taken using fluorescence microscope (Olympus SZ-12).

Acknowledgements

The research was supported by the Ministry of Education, Youth and Sports of the Czech Republic project Biodiversity (CZ.02.1.01/0.0/0.0/16_025/0007370), Czech Science Foundation (20-23836S) and Grant Agency of the University of South Bohemia (019/2021/Z). We gratefully acknowledge the Department of Zoology at Charles University in Prague, Czech Republic, for providing labelled specimens of gar and histology of bichir embryos.

References

- Ballard, W.W., Ginsburg, A.S., 1980. Morphogenetic movements in acipenserid embryos. *Journal of Experimental Zoology* 213, 69–103.
- Ballard, W.W., Needham, R.G., 1964. Normal embryonic stages of *Polyodon spathula* (Walbaum). *Journal of Morphology* 114, 465–477.
- Bartsch, P., Gemballa, S., Piotrowski, T., 1997. The embryonic and larval development of *Polypterus senegalus* cuvier, 1829: Its staging with reference to external and skeletal features, behaviour and locomotory habits. *Acta Zoologica* 78, 309–328.
- Bolker, J.A., 1993. Gastrulation and mesoderm morphogenesis in the white sturgeon. *Journal of Experimental Zoology* 266, 116–131.
- Bolker, J.A., 1994. Comparison of gastrulation in frogs and fish. *Integrative and Comparative Biology* 34, 313–322.
- Buchholz, D.R., Singamsetty, S., Karadge, U., Williamson, S., Langer, C.E., Elinson, R.P., 2007. Nutritional endoderm in a direct developing frog: A potential parallel to the evolution of the amniote egg. *Developmental Dynamics* 236, 1259–1272.
- Buddington, R.K., Doroshov, S.I., 1986. Structural and functional relations of the white sturgeon alimentary canal (*Acipenser transmontanus*). *Journal of Morphology* 190, 201–213.
- Carvalho, L., Heisenberg, C.P., 2010. The yolk syncytial layer in early zebrafish development. *Trends in Cell Biology* 20, 586–592.
- Chalmers Andrew, D., Slack, J.M.W., 2000. The *Xenopus* tadpole gut: fate maps and morphogenetic movements. *Development* 392, 381–392.
- Chen, S., Kimelman, D., 2000. The role of the yolk syncytial layer in germ layer patterning in zebrafish. *Development* 127, 4681–9.
- Collazo, A., Bolker, J.A., Keller, R., 1994. A phylogenetic perspective on teleost gastrulation. *The American Naturalist* 144, 133–152.
- Comabella, Y., Hernández Franyutti, A., Hurtado, A., Canabal, J., García-Galano, T., 2013. Ontogenetic development of the digestive tract in Cuban gar (*Atractosteus tristoechus*) larvae. *Reviews in Fish Biology and Fisheries* 23, 245–260.
- Cooper, M.S., Virta, V.C., 2007. Evolution of gastrulation in the ray-finned (actinopterygian) fishes. *Journal of Experimental Zoology Part B: Molecular and Developmental Evolution* 308B, 591–608.
- D’Amico, L.A., Cooper, M.S., 2001. Morphogenetic domains in the yolk syncytial layer of axiating zebrafish embryos. *Developmental Dynamics* 222, 611–624.
- Damas, H., 1943. Recherches sur le développement de “*Lampetra fluviatilis*” I: ., contribution à l’étude de la céphalogenèse des vertébrés. Liège: H. Vaillant-Carmanne (impr. de H. Vaillant-Carmanne). *Archives of Biology* 55, 284. (in French)

- Dettlaff, T.A., Ginsburg, A.S., Schmalhausen, O.I., 1993. Sturgeon fishes: Developmental Biology and Aquaculture. Springer, New York, pp. 92–100.
- Diedhiou, S., Bartsch, P., 2009. Staging of the early development of *Polypterus* (Cladistia: Actinopterygii). Development of Non-teleost Fishes, pp. 104–169.
- Frankenberg, E., 2012. Vertebrate intestinal endoderm development. Developmental Dynamics 240, 501–520.
- Gawlicka, A., McLaughlin, L., Hung, S.S.O., De La Noüe, J., 1996. Limitations of carrageenan microbound diets for feeding white sturgeon, *Acipenser transmontanus*, larvae. Aquaculture 141, 245–265.
- Gilbert, S.F., 2010. Developmental Biology, Developmental Biology, Ninth ed. Sinauer Associates, Oxford University Press.
- Ginsburg, A.S., Dettlaff, T.A., 1991. The Russian sturgeon *Acipenser Güldenstädti*. Part I. Gametes and Early Development up to Time of Hatching. In: Dettlaff, T.A., Vassetzky, S.G. (Eds), Animal Species for Developmental Studies Springer, Boston, pp. 15–65.
- Gisbert, E., Sarasquete, M.C., Williot, P., Castello-Orvay, F., Castelló-Orvay, F., 1999. Histochemistry of the development of the digestive system of Siberian sturgeon during early ontogeny. Journal of Fish Biology 55, 596–616.
- Hamburger, V., Hamilton, H.L., 1951. A series of normal stages in the development of the chick embryo. Journal of Morphology 88, 49–92.
- Jacobson, A.G., Tam, P.P.L., 1982. Cephalic neurulation in the mouse embryo analyzed by SEM and morphometry. The Anatomical Record 203, 375–396.
- Jaroszewska, M., Dabrowski, K., 2009. Early ontogeny of semionotiformes and *Amiiformes* (*Neopterygii*). In: Kunz, Y.W., Luer, C.A., Kapoor, B.G. (Eds), Development of Non-teleost Fishes, Science Publishers, pp. 230–274. <https://doi.org/10.1201/b10184-5>.
- Kaufman, M.H., 1992. The atlas of mouse development. New York, London: Elsevier Academic Press.
- Keller, R.E., 1981. An experimental analysis of the role of bottle cells and the deep marginal zone in gastrulation of *Xenopus laevis*. Journal of Experimental Zoology 216, 181–101.
- Kemp, A., 2011. Comparison of embryological development in the threatened Australian lungfish *Neoceratodus forsteri* from two sites in a Queensland river system. Endangered Species Research 15, 87–101.
- Kiecker, C., Bates, T., Bell, E., 2016. Molecular specification of germ layers in vertebrate embryos. Cellular and Molecular Life Sciences 73, 923–947.
- Kimmel, C.B., Ballard, W.W., Kimmel, S.R., Ullmann, B., Schilling, T.F., 1995. Stages of embryonic development of the zebrafish. Developmental Dynamics 203, 255–310.
- Kimura, W., Yasugi, S., Fukuda, K., 2007. Regional specification of the endoderm in the early chick embryo. Development Growth and Differentiation 49, 365–372.
- Korzhev, P.A., Sharkova, L.B. 1967. On peculiarities of digestion of the Russian sturgeon in the Caspian Sea. In: Karzinkin, G.S. (Ed.), Metabolism and Biochemistry of Fishes Nauka, Moscow, pp. 205–209. (in Russian)
- Kupffer, C. von, 1890. Die Entwicklung von *Petromyzon planeri*. Archiv für Mikroskopische Anatomie 35, 469–558. (in German)
- Kurth, T., Weiche, S., Vorkel, D., Kretschmar, S., Menge, A., 2012. Histology of plastic embedded amphibian embryos and larvae. Genesis: The Journal of Genetics and Development 250, 235–250.

- Lawson, A., Schoenwolf, G.C., 2003. Epiblast and primitive-streak origins of the endoderm in the gastrulating chick embryo. *Development* 130, 3491–3501.
- Lawson, K.A., Meneses, J.J., Pedersen, R.A., 1986. Cell fate and cell lineage in the endoderm of the presomite mouse embryo, studied with an intracellular tracer. *Developmental Biology* 115, 325–339.
- Li, J., Han, Y., Ma, Q., Liu, H., Pang, Y., Li, Q., 2019. Early development of Lamprey *Lampetra japonica* (Martens, 1868). *Aquaculture Research* 50, 1501–1514.
- Long, W.L., Ballard, W.W., 2001. Normal embryonic stages of the longnose gar, *Lepisosteus osseus*. *BMC Developmental Biology* 1: <http://www.biomedcentral.com/1471-213X/1/6>.
- Minarik, M., Stundl, J., Fabian, P., Jandzik, D., Metscher, B.D., Psenicka, M., Gela, D., Osorio-Pérez, A., Arias-Rodríguez, L., Horáček, I., Cerny, R., 2017. Pre-oral gut contributes to facial structures in non-teleost fishes. *Nature* 547, 209–212.
- Naraine, R., Iegorova, V., Abaffy, P., Franek, R., Soukup, V., Sindelka, R., 2022. Evolutionary conservation of maternal RNA localization in fishes and amphibians revealed by TOMO-Seq. *Developmental Biology* 489, 146–160.
- Ng, A.N.Y., De, Jong-Curtain, T.A., Mawdsley, D.J., White, S.J., Shin, J., Appel, B., Dong, P.D.S., Stainier, D.Y.R., Heath, J.K., 2005. Formation of the digestive system in zebrafish: III. Intestinal epithelium morphogenesis. *Developmental Biology* 286, 114–135.
- Nowotschin, S., Hadjantonakis, A.K., Campbell, K., 2019a. The endoderm: A divergent cell lineage with many commonalities. *Development (Cambridge)* 146, 1–12.
- Nowotschin, S., Setty, M., Kuo, Y.Y., Liu, V., Garg, V., Sharma, R., Simon, C.S., Saiz, N., Gardner, R., Boutet, S.C., Church, D.M., Hoodless, P.A., Hadjantonakis, A.K., Pe'er, D., 2019b. The emergent landscape of the mouse gut endoderm at single-cell resolution. *Nature* 569, 361–367.
- Ober, E.A., Field, H.A., Stainier, D.Y.R., 2003. From endoderm formation to liver and pancreas development in zebrafish. *Mechanisms of Development* 120, 5–18.
- Piavis, G.W., 1971. London, Academic Press. Embryology In: Hardisty, M.W., Potter, I.C. *The Biology of Lampreys*, 361–400.
- Pocherniaieva, K., Psenicka, M., Sidova, M., Havelka, M., Saito, T., Sindelka, R., Kaspar, V., 2018. Comparison of oocyte mRNA localization patterns in sterlet *Acipenser ruthenus* and African clawed frog *Xenopus laevis*. *Journal of Experimental Zoology Part B, Molecular and Developmental Evolution* 330, 181–187.
- Richardson, M.K., Admiraal, J., Wright, G.M., 2010. Developmental anatomy of lampreys. *Biological Reviews* 85, 1–33.
- Rosenquist, G.C., 1971. The location of the pregut endoderm in the chick embryo at the primitive streak stage as determined by radioautographic mapping. *Developmental Biology* 26, 323–335.
- Saito, T., Pšenička, M., Goto, R., Adachi, S., Inoue, K., Arai, K., Yamaha, E., Pšenička, M., 2014. The origin and migration of primordial germ cells in sturgeons. *PLoS ONE* 9, e86861.
- Shah, M.A., Fatira, E., Iegorova, V., Xie, X., Gela, D., Rodina, M., Franěk, R., Pšenička, M., Saito, T., 2022. Blastomeres derived from the vegetal pole provide extra-embryonic nutrition to sturgeon (*Acipenser*) embryos: Transition from holoblastic to meroblastic cleavage. *Aquaculture* 551, 737899.
- Shah, M.A., Saito, T., Šindelka, R., Iegorova, V., Rodina, M., Baloch, A.R., Franěk, R., Tichopád, T., Pšenička, M., 2021. Novel technique for definite blastomere inhibition and distribution of maternal RNA in sterlet *Acipenser ruthenus* embryo. *Fisheries Science* 87, 71–83.
- Shih, J., Keller, R., 1994. Gastrulation in *Xenopus laevis*: involution—a current view. *Seminars in Developmental Biology* 5, 85–90.

- Shiple, A.E., 1885. On the formation of the mesoblast , and the persistence of the blastopore in the lamprey. *Proceedings of the Royal Society of London* 39, 244–248.
- Sindelka, R., Sidova, M., Svec, D., Kubista, M., 2010. Spatial expression profiles in the *Xenopus laevis* oocytes measured with qPCR tomography. *Methods* 51, 87–91.
- Strehlow, D., Heinrich, G., Gilbert, W., 1994. The fates of the blastomeres of the 16-cell zebrafish embryo. *Development* 120, 1791–1798.
- Stundl, J., Pospisilova, A., Matějková, T., Psenicka, M., Bronner, M.E., Cerny, R., 2020. Migratory patterns and evolutionary plasticity of cranial neural crest cells in ray-finned fishes. *Developmental Biology* 467, 14–29.
- Takeuchi, M., Okabe, M., Aizawa, S., 2009a. The genus polypterus (*Bichirs*): a fish group diverged at the stem of ray-finned fishes (*Actinopterygii*). *CSH Protocols* 1, 1–12. doi:10.1101/pdb.emo117.
- Takeuchi, M., Takahashi, M., Okabe, M., Aizawa, S., 2009b. Germ layer patterning in bichir and lamprey; an insight into its evolution in vertebrates. *Developmental Biology* 332, 90–102.
- Tam, P.P.L., Khoo, P.L., Lewis, S.L., Bildsoe, H., Wong, N., Tsang, T.E., Gad, J.M., Robb, L., 2007. Sequential allocation and global pattern of movement of the definitive endoderm in the mouse embryo during gastrulation. *Development* 134, 251–260.
- Tremblay, K.D., Zaret, K.S., 2005. Distinct populations of endoderm cells converge to generate the embryonic liver bud and ventral foregut tissues. *Developmental Biology* 280, 87–99.
- Tyler, M.S., 2001. Zebrafish development. *Developmental biology: A guide for experimental study* 15, 1–22.
- Wallace, K.N., Pack, M., 2003. Unique and conserved aspects of gut development in zebrafish. *Developmental Biology* 255, 12–29.
- Zorn, A.M., Wells, J.M., 2009. Vertebrate endoderm development and organ formation. *Annual Review of Cell and Developmental Biology* 25, 221–251.

Supplementary figures

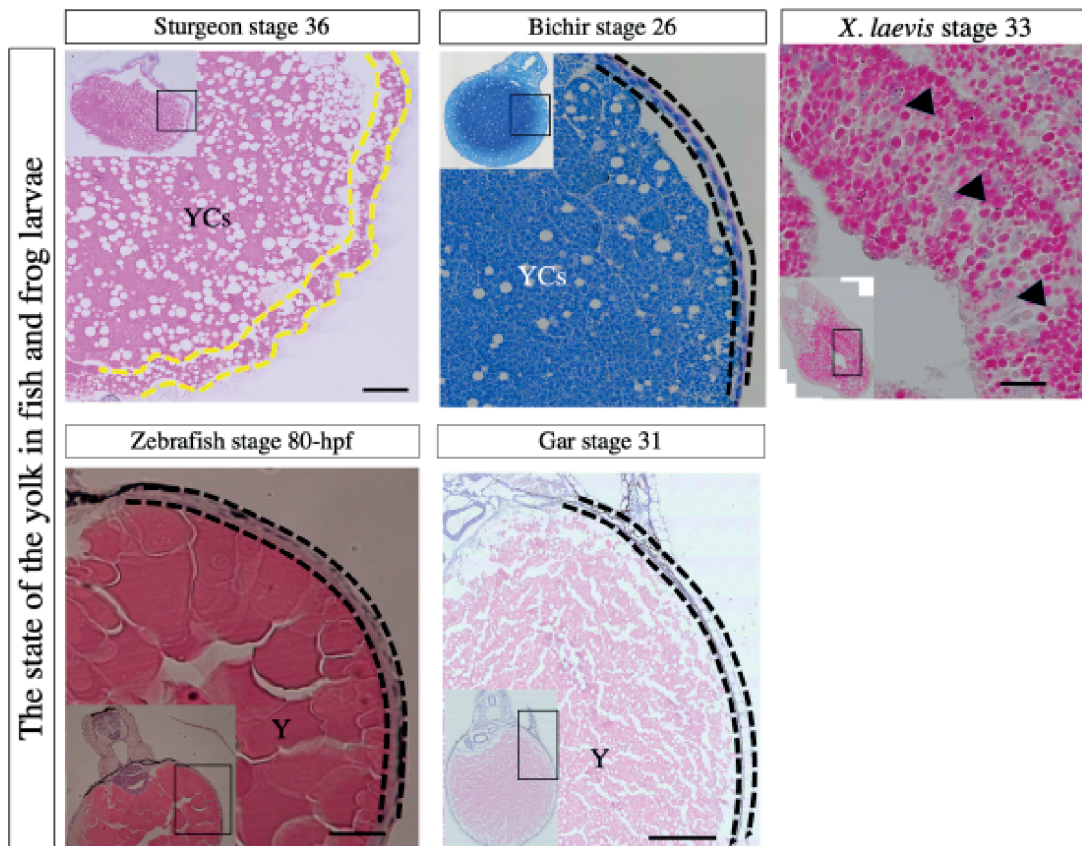


Figure S1. Magnified view of yolk surrounded by gut epithelial tissue in the larvae of sturgeon (indicated by yellow dotted lines). In comparison, in other fishes including bichir, gar, and zebrafish, the yolk is surrounded by ectoderm (indicated by black dotted line). On the other hand, in xenopus, the yolk is intracellular (indicated by black arrows). Scale bars are 20 μ m.

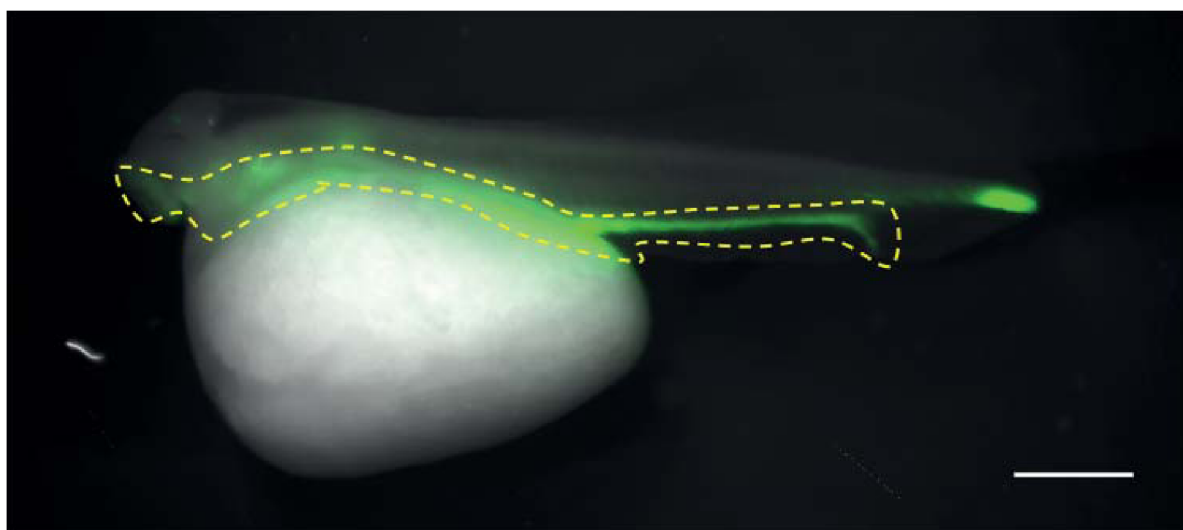


Figure S2. In vivo labelling of gut-endoderm of gar.

Embryos of gar fish injected at neurula stage (as described for sturgeon) and allowed to develop till hatching. The pictures were taken using fluorescence stereomicroscope Olympus SZ-12. Dotted line indicates the positive labelling of endoderm cells, whereas some ectodermal cells were also labelled during the injection that shows staining on tail region. For details see (Minarik et al., 2017).

CHAPTER 5

GENERAL DISCUSSION

ENGLISH SUMMARY

CZECH SUMMARY

ACKNOWLEDGEMENTS

LIST OF PUBLICATIONS

TRAINING AND SUPERVISION PLAN DURING STUDY

CURRICULUM VITAE

General discussion

Sturgeons, the basal non-teleost fish, are considered living fossils because they evolved around 200 million years ago. They retain the holoblastic cleavage pattern. During the past decades, comparative studies of early embryogenesis in sturgeon and African clawed frog – *Xenopus laevis* illustrated very similar developmental mechanisms, such as germplasm localization, cleavage pattern, formation of the blastocoel, bottle cells, blastopore, gastrocoel and archenteron {for detail see Chapter 1, and (Ballard and Ginsburg, 1980; Pocherniaieva et al., 2018; Bolker, 1994, 1993; Naraine et al., 2022)}. In addition, our current research has revealed that sturgeon embryo development represents a distinct cleavage pattern transition from holoblastic to meroblastic cleavage and a unique mode of gut development among jawed vertebrates (Chapter 2–4).

Previously, using advanced methods for spatial individual gene expression and transcriptomic analyses: qPCR tomography and Tomo-Seq, respectively, it has been reported that the vegetal pole (VP) of *X. laevis* egg contains many known and newly identified determinants of endoderm specification and PGC formation. In contrast, the endoderm determinants in sturgeon were found in the equatorial region, and the VP is linked only with the formation of PGCs (Sindelka et al., 2010; Pocherniaieva et al., 2018; Naraine et al., 2022). Moreover, Saito and Pšenička et al. confirmed that exclusively germplasm (preformed PGC determinants) is stored in the VP of sturgeon eggs. Further, sterilization of sturgeon was performed using antisense morpholino oligonucleotide against the *dnd1* (dead end) gene (crucial for PGC development) into the VP of sturgeon embryos, and in parallel, Saito et al. invented a novel method of sturgeon sterilization using UV irradiation applied on the VP of the embryo just after fertilization (Saito et al., 2014, 2018; Linhartová et al., 2015; Saito and Psenicka, 2015). Based on the above studies, we speculate that the VP of the sturgeon egg contains only determinants for PGCs, and the rest serves as endogenous nutrition. Therefore, our current research investigated the detailed fate mapping of yolk-rich vegetal blastomeres/YCs to reveal the evolutionary transition (from holoblastic to meroblastic) of cleavage pattern in ray-finned fishes. In this regard, we proposed to inhibit the cleavage of the vegetal hemisphere in order to determine whether the sturgeon embryo: 1) can survive, which would mean that no vital cell line is formed in the vegetal hemisphere; 2) can partial cleavage pattern inhibition affect the asymmetry preservation of maternal localization? 3) Can sturgeon utilize its endogenous nutrition (yolk platelets) extracellularly, which will mimic teleost nutrition usage (absence of YCs). 4) If the VP-inhibited embryos develop, they should be sterile and have autonomous YSL induction or YSL-like structures to separate the yolk from the animal blastoderm. 5) If the vegetal blastomeres of sturgeon do not contribute to gut development as seen in *X. laevis*, it will be interesting to determine how sturgeon develop their gut and whether it is conserved across taxa or unique to sturgeon.

In Chapter two of thesis, we examined our first goal, which was to develop a novel technique for inhibiting specific blastomeres and its effect on the localization of biomolecules such as maternal mRNA. In this regard, various techniques have been developed for several animal species. For example, Valles et al. (2002) have utilized a mechanical approach, i.e., a strong magnetic field, to alter the geometry of the first two cleavage furrows in *X. laevis* embryos; however, this technique was inappropriate for stopping the complete cleavage furrows (Valles et al., 2002). In *X. laevis* embryos, the injection of cytochalasin-B's optimal concentration (10 $\mu\text{g}\cdot\text{ml}^{-1}$) was used to regress the early blastomere cleavage. The cytochalasin-B could not stop the definite blastomere cleavage, and importantly it is a very toxic compound (de Laat et al., 1973). In contrast, we used different concentrations (1 μg > 100 μg > and 10 μg) of cytochalasin-B in the present study. We have found that 1 $\mu\text{g}\cdot\text{ml}^{-1}$ can stop the cleavage furrows; however, it was much more toxic to embryos, and inhibition of blastomere was not specified (Chapter 2). Furthermore, several molecular approaches such as *c-mos* RNA, PAK1 and MAPK proteins

injection have been utilized (Sagata et al., 1989; Masui, 2000; Buchholz et al., 2007). Despite their effectiveness, the microinjection of these chemicals is a complicated and time-consuming process for non-model species (Yew et al., 1991; Haccard et al., 1993; Rooney et al., 1996; Buchholz et al., 2007).

Based on the literature review, we found that *trans,trans-2,4-Decadienal* (DD) caused delayed development and malformation in the embryo and gametes of several aquatic animals, including, sea urchins (Romano, 2003; Hansen et al., 2004; Romano et al., 2010, 2011), copepods (Ivanova et al., 2003; Romano, 2003), ascidians (Tosti et al., 2003), Lugworm, ragworms, and common starfish (Caldwell et al., 2004, 2002). Consistently, we also discovered that DD, even at very low concentrations, harms the development of *Acipenser ruthenus* embryos. Nevertheless, all previous studies have focused on the general effects of DD using the incubation method. We have employed DD treatment in localized parts of embryos for the first time. Our results showed that the alone lethal concentration of DD (0.01%) applied by microinjection could not inhibit localized / blastomere cleavage patterns (Chapter 2).

We conducted a further thorough literature review and discovered that DD causes GSH depletion, which directly reduces endogenous nitric oxide (NO) levels. Reduced NO levels result in early *mkp1* upregulation, ERK inactivation, and changes in the downstream transcription of the metabolic enzyme dehydrogenase *dhg* and the critical developmental genes *ets* and *mx* causing *Ciona intestinalis* metamorphosis to be delayed. (Castellano et al., 2015). In general, hypersensitivity to UV-B light can cause this same stress (Li et al., 2017). On the one hand, DD has also been used for human carcinoma cells treatment (Miralto et al., 1999). Curcumin (*Curcuma longa*) has been shown to improve the anti-cancer effect under visible light irradiation; nevertheless, curcumin and visible light alone could not stop cancer cell proliferation (Rutz et al., 2019). Thus, we combined light irradiation with DD injection treatments. We found that DD (0.01%) injection and visible light irradiation (44.86–91.15 W m⁻² + 395–700nm) are optimal for inhibiting the localized/partial cleavage pattern. However, DD injection and light irradiation alone was not enough to stop the definite blastomere inhibition. Compared to previous methods (discussed above), the presented technique for inhibiting or arresting specific blastomere cleavage in sturgeon embryos is more convenient, cost-effective, and efficient (Chapter 2). This technique could be utilized for fate mapping (e.g., signal blastomere contribution to development) in sturgeons (see, Chapter 3) and other non-model fishes like bichir, bowfin, and paddle fish.

According to a recent study by Pocherniaieva et al., maternal mRNAs and proteins distributed along the oocyte's A-V axis are essential for embryo development. (Pocherniaieva et al., 2018). We hypothesized that after inhibiting vegetal blastomeres, embryos would have developed a yolk stream and/or the treatment would influence the localization of maternal messenger ribonucleic acids (mRNAs). As a result of our review of the literature, we chose the following genes: *axin1* (Axis inhibition protein 1) – critical for the correct patterning of the early embryo (Kofron et al., 2001), *hyal4* (Hyaluronidase 4) – expressed, during embryogenesis (Porter and Jänicke, 1999), and *cdk1b* (Cyclin-dependent kinase 1-B) – regulate the cell cycles (Tanaka et al., 2017), *casp3* (caspase-3) – crucial to the process of apoptosis (Porter and Jänicke, 1999), *dnd1* (Dead end protein 1) – germ cell-specific molecular marker in fish (Baloch et al., 2019a), *vasa* (DEAD-box helicase) – associated with migration of PGCs (Saito et al., 2006) for spatial RNA localization analysis in sterlet sturgeon embryos (Chapter 1, heading 1.4). It was found by using quantitative polymerase chain reaction (qPCR) tomography that treatment did not affect the localization of selected mRNAs. This suggests that RNA localization is complete by the end of oogenesis and that early embryonic cleavage is not required for A–V asymmetry preservation. On the other hand, we speculated that DD treatment might influence the localization of other molecules, such as proteins. However, because the proteomic analysis was not a part of this study, we left this as an open question for future research.

Moreover, animal blastomeres of sturgeon embryos are relatively smaller than vegetal blastomeres and contain determinants of germ layer patterning, whereas vegetal blastomeres contain germ cell determinates (Saito et al., 2014; Pocherniaieva et al., 2018). Therefore, during the treatment optimization, animal blastomere inhibited embryos failed in the gastrula stage, while vegetal blastomere inhibited embryos succeeded the gastrulation. Thus, in Chapter three of the thesis, we continued investigating detailed fate mapping of vegetal blastomeres with and without inhibition of cleavage pattern (Chapter 3).

Concludingly, in Chapter two, we present the inhibition of cleavage pattern in defined blastomeres of sturgeon embryos using a combination of DD injection and visible light irradiation. Furthermore, qPCR tomography revealed that blastomere inhibition does not affect the localization of maternal RNA gradient. Still, to understand the development of a sturgeon's embryo, ample knowledge about the contribution of early blastomeres to adult tissues is needed. Several protocols have been established for model species such as *X. laevis* and *Danio rerio*. However, in sturgeon developmental biology, our research group is always at the forefront of research and innovation concerning promising techniques (Saito et al., 2014; Saito and Psenicka, 2015; Minarik et al., 2017; Pocherniaieva et al., 2018; Baloch et al., 2019b).

In Chapter three of thesis, we have reported detailed fate mapping of vegetal blastomeres/YCs of sturgeon embryos to (a) determine whether YCs contribute the embryonic development or are simply extra-embryonic, (b) determine whether sturgeon can use its endogenous nutrition (yolk platelets) extracellularly, (c) determine whether autonomous induction of YSL or YSL-like structures occurs after inhibition of vegetal blastomeres, (d) determine how PGCs developed during the evolution of meroblastic cleavage in ray-finned fish. The main problem with studying vegetal blastomeres was a technical limitation for observation due to the large size and abundance of lipid and yolk granules. Thus, we took advantage of the microinjection labeling technique and fluorescent microscopy to observe the role of vegetal blastomeres in embryonic development, and we have found that vegetal blastomeres only provided PGCs (Chapter 3). Moreover, based on the literature review (see Chapter 1, heading 1.4), we selected some germ layer markers and housekeeping (*sox7*, *vegT*, *wnt11*, *gsk3b* and *gata3*) genes in order to study the phenotypic characteristic of YCs. We found that expression of genes was significantly lower compared to gut tissue. YCs derived from vegetal blastomeres appear to be extra-embryonic. However, it was also necessary to know that when YCs stop their proliferating activity. Morphological analyses and YCs mitotic assay using plastic section histology and BrdU plus, respectively, revealed that after the mid-blastula transition, YCs became transcriptionally inactive and served only as a source of nutrition for the developing embryo.

During the evolution, the increased egg size and yolk is one factor that can have a substantial effect on early developmental processes, such as cleavage pattern and gastrulation (Elinson and Beckham, 2002; Buchholz et al., 2007; Elinson, 2009; Hasley et al., 2017;). For example, *Ensatina eschscholtzii* and *Eleutherodactylus* (amphibian) eggs cleave holoblastically; however, due increase in yolk volume, the first few cleavage planes do not reach to the vegetal end (Buchholz et al., 2007; Collazo and Keller, 2010; Hasley et al., 2017). We discovered that sturgeon vegetal blastomeres cleaved slower than animal blastomeres and produced a large number of YCs that resembled *E. eschscholtzii* and *E. coqui*. The presence of a large number of YCs indicates a particular type of transition from holoblastic to meroblastic cleavage (Buchholz et al., 2007; Takeuchi et al., 2009; Collazo and Keller, 2010) (Chapter 3). According to Buchholz et al., the embryos of *E. coqui* with inhibited large vegetal blastomeres (up to 60- to the 100-cell stage) developed normally. Thus, increased egg size resulted in YCs (nutritional endoderm), a type of cell that provides nutrition but does not develop into the tissues of the digestive tract (Buchholz et al., 2007). Similarly, Takeuchi et al. have also shown that vegetal blastomeres of bichir and lamprey also serve as extra-embryonic nutrition (Takeuchi et al., 2009). According to our hypothesis, YCs

in sturgeon embryos were extra-embryonic, as seen in *E. coqui*, bichir, and lamprey (Chapter 3). Furthermore, inhibiting vegetal blastomere cleavage (shifting from holoblastic to meroblastic) in sturgeon embryos mimicked meroblastic cleavage until stage 12 after inhibition. Despite the massive numbers of YCs that have been lost, embryos developed as usual. We also discovered that after inhibiting vegetal blastomeres, sturgeon embryos utilize their yolk in an acellular rather than YCs-dependent manner. Moreover, we did not observe any difference between normal and partial cleaved embryos regarding their developmental speed (data not shown). Thus, vegetal blastomeres constitute the extra-embryonic portion, except PGCs (Chapter 3).

According to our findings, when compared to animal pole cells, vegetal cells; YCs are significantly larger and without apparent nucleoli. We also discovered that the size of YCs nuclei declined during development. Moreover, the number of YCs inside the developing gut declined and changed the shape as the larvae developed (Chapter 3, supplementary file). According to a previous study, the endogenous nutrition phase of the alimentary canal is already present at this stage (Korzhev, and Sharkova, 1967; Ginsburg and Dettlaff, 1991; Gisbert et al., 1999). Thus, this finding indicated that sturgeon develop their gut around yolk cells in order to use them intra-intestinally (Ballard and Needham, 1964; Ballard and Ginsburg, 1980; Buddington and Doroshov, 1986; Shah et al., 2022). Thus, in Chapter four, we investigated sturgeon gut development and compared it to other taxa in order to better understand evolutionary divergence (Chapter 4).

Furthermore, the early embryonic development of gar and bowfin suggests that the meroblastic cleavage in ray-finned fish evolved via two significant changes. 1) Bowfin embryos lost bottle cells during gastrulation. 2) Gar embryos fused their vegetal blastomeres into a single cell and evolved YSL to separate the blastoderm from the yolk (Ballard, 1986; Long and Ballard, 2001). In our study, we observed that in normal cleaved sturgeon embryos, each YC had a single nucleus at the center of the cell; they were not a syncytium. Our results showed no YSL or YSL-like structure in the sturgeon embryo; only YCs divide coincidentally with nuclear division. However, when cleavage at the vegetal blastomere was inhibited, most of the YCs remained undivided, and yolk-cell nuclei were seen just beneath the blastocoel cavity, mimicking the YSL-like structure teleost. The size of nuclei derived from the vegetal pole of partial cleaved embryos was significantly larger than that of normal cleaved embryos. The inhibition of vegetal blastomeres might lead the microtubule failure, and the nuclear expansion is caused by microtubule accumulation around the nucleus (Hara and Merten, 2015). However, this can be confirmed in future research. Furthermore, partial cleaved sturgeon embryos revealed an acellular form yolk that resembled the yolk structure of gar. Our findings presented in Chapter three have paved the way toward the transition of cleavage (meroblastic–holoblastic) pattern in ray-finned fishes (Ballard, 1986; Long and Ballard, 2001).

The transition from holoblastic to meroblastic cleavage altered PGC formation (Saito et al., 2014) (Chapter 1, Figure 4). Sturgeon germplasm is localized in the VP of the egg (Pocherniaieva et al., 2018). On the other hand, despite these profound changes in the yolk-rich vegetal region, the formation of PGCs via germplasm, localized to the vegetal region, has been conserved with anurans. However, unlike urodeles, sturgeons have not evolved an alternative pathway for producing primordial germ cells (Ikenishi et al., 1974; Pocherniaieva et al., 2018). Moreover, according to Saito et al., many of the “mis-migrated” PGCs were observed during the normal sturgeon development (Saito et al., 2014). Instead, they have increased the relative amount of germplasm coverage in the vegetal region. Potential reasons for this germplasm expansion include participation in the formation of the YCs and ensuring that some primordial germ cells, among the massive number of YCs, reach the genital ridge, as observed in *E. coqui* embryos (Elinson et al., 2011). In the case of PGCs development, sturgeon are interspecific *X. laevis* and teleost (Saito et al., 2014). On the other hand, studies have suggested that the meroblastic cleavage in gar evolved through the fusion of vegetal blastomeres. On the other hand, we

discovered that sturgeon embryos remain sterile after inhibition of the inhibited vegetal blastomere, implying that gar has a different path to generate PGCs. However, localization and migration of PGCs in gar and its comparison with taxa have been left as open questions for future research.

In Chapter three, we propose a possibility that the sturgeon's embryos undergo the same development as the ancestors of vertebrates and continue to be retained in their stem lineages. The potential reasons to retain the holoblastic cleavage pattern is the localization of germplasm in the vegetal cortex. Since yolk cells (nutritional endoderm) facilitate, primordial germ cells get to the genital ridge during embryonic development (Chapter 3).

In Chapter four of thesis, we extended our previous study (Chapter three) to describe our concluding objective i.e., how sturgeon develop the gut to utilize its endogenous nutrition; YCs. In addition, we also presented a comparison of the sturgeon's gut with other taxa in order to understand its evolutionary divergence. As hypothesized previously that sturgeon digest their YCs within the gut (intra-intestinally) (Chapter 3). Our finding revealed that the endodermal cells in sturgeon embryos form the archenteron like bichir and *X. laevis*. In contrast to *X. laevis*, the ventral part of the archenteron in a sturgeon embryo is made up of YCs rather than endodermal cells. During neurula, the endodermal cells did not form the bulge like bichir but continued to proliferate ventrodorsally and encompass the YCs "yolk-inside-gut" (Chapter 4).

The embryo of lamprey, bichir, *X. laevis*, and *E. coqui* use the same cleavage (holoblastic) pattern as sturgeon. However, due to the size of eggs/yolk volume, the endoderm determinates of lamprey, bichir, sturgeon and *E. coqui* are not preserved to *X. laevis* (Beckham et al., 2003; Buchholz et al., 2007; Takeuchi et al., 2009; Pocherniaieva et al., 2018). For example, *X. laevis* embryos contain more yolk platelets towards VP (inside endodermal cells), and these yolky endodermal cells tend to develop gut-endoderm and its derived organs (Shih and Keller, 1994; Chalmers and Slack, 2000; Zorn and Wells, 2009). Comparatively, due to yolky-rich vegetal region in the embryos of lamprey, bichir, sturgeon and *E. coqui*, the endodermal determinates do not localize at VP (Beckham et al., 2003; Takeuchi et al., 2009b; Pocherniaieva et al., 2018). However, in these species, YCs only serve as nutrition, do not contribute to the gut tissue (Buchholz et al., 2007; Takeuchi et al., 2009; Shah et al., 2022) (Chapter 3). Moreover, during gastrulation, embryos of *X. laevis* develop the archenteron, and the archenteron cavity eventually forms the definitive gut tube. In contrast, the embryos of bichir and *E. coqui* developed archenteron during gastrulation, and the archenteron continued to form the gut tube, which is underlaid with mesenchyme occurs on the roof of YCs. Thus, the massive amount of yolk utilized extraintestinally "outside-the-gut" which surround by ectoderm (Takeuchi et al. 2009b) (Chapter 4).

In addition to amphibian and non-teleost fish (holoblastic representative), mice embryo also cleaves holoblastically, however yolk is absent. The epithelium of the developing gut tube forms along the anterior-posterior axis till stage E8.5. The foregut tube was formed by the anterior endoderm, the hindgut tube by the posterior endoderm, and the midgut by the middle region. Till stage E9.5 completes the gut tube formation (Frankenberg, 2012). The embryo of mice develops the extra-embryonic membranes (amnion, chorion, yolk sac and allantois) essential for nutritional supply (Ross and Boroviak, 2020).

Besides holoblastic representative (mentioned above), we also compare the sturgeon's gut with meroblastic representative (gar, zebrafish and chicken) animals. To elaborate, gar (phylogenetically placed after sturgeon) and zebrafish showed a clear difference in yolk composition; gar yolk contains a high concentration of yolk platelets, whereas zebrafish contains platelet-less yolk. The presence of yolk platelets may be due to the fusion of 2-cell vegetal blastomeres during the evolution of meroblastic cleavage, which is consistent with our previous finding, namely, that after inhibiting YCs division in sturgeon embryos, the yolk structure was similar to gar (Chapter 3). The gut development of gar is conserved to zebrafish, i.e., whole yolk mass occurs "outside the gut,"

and the gut lies on the dorsal position of the yolk sac (Long and Ballard, 2001). However, the localization of endoderm determinants in gar eggs and its comparison with other taxa has yet to be described.

In addition, amniotes (e.g., chick) showed very similar gut development to zebrafish, i.e., entire gut lay on the dorsal position of the yolk sac. However, chicken embryos develop the splanchnopleuric (extra-embryonic membrane) mesenchyme composed of mesoderm external to the coelom plus the endoderm. Instead of forming a close gut, the Splanchnopleure will grow over the yolk and become a yolk sac (Gilbert, 2010). This yolk region is in contact with the midgut, and a primitive gut is present above the yolk. Finally, the yolk sac is communicated with the midgut through an opening – yolk stalk or umbilical stalk.

In contrast to the holoblastic and meroblastic representatives of vertebrates (mentioned above), sturgeon developed their gut around the yolk (as described above) and used it inside-gut. Based on cross-species comparison in this study, this developmental pattern has only been observed in sturgeon so far. It appears logical for developing sturgeon larvae to keep the yolk materials (YCs) inside the developing gut by encircling it with endodermal cells and to use the yolk for nutritional purposes during the lecithotrophic state (before first feeding) by using the newly developed digestion system {for reference see (Korzhuev and Sharkova, 1967; Ginsburg and Dettlaff, 1991; Gisbert et al., 1999)}. Similarly, the lining of the presumptive sturgeon's gut and the vitelline syncytium of other fishes have similar mechanisms for utilizing yolk reserves. Furthermore, in sturgeon, endodermal cells continue to encompass YCs, resembling the chicken's Splanchnopleure structure. They do not, however, develop the extra-embryonic layers. It is also revealed that the increased yolk was responsible for the extra-embryonic development. The size/ amount of YCs may have played a role in the evolution of the sturgeon's unique gut developmental pattern. It can be concluded that this type of gut formation evolved in sturgeon to aid in the digestion of "yolk-inside-gut."

In this thesis, the following conclusion and suggestions have been drawn.

1. For the first time, we reported a novel technique for inhibiting specific blastomeres in sturgeon embryos, which can be applied to other non-teleost species such as bichir, paddle fish, and bowfin.
2. Our findings show that RNA localization is complete by the end of oogenesis and that early embryonic cleavage is not required for A-V asymmetry preservation. Maternal proteins can be studied further.
3. The vegetal blastomeres of sturgeon embryos produce primordial germ cells and cellular yolk mass (yolk cells; YCs). After mid-blastula transition YCs become and inactive and only serve to provide nourishment.
4. The sterility of sturgeon after inhibition of the vegetal blastomere revealed that the vegetal pole only stored the PGC precursors. Because the vegetal pole of gar and bowfin does not cleave normally, localization of germplasm in gar and bowfin, as well as PGC migration, can be studied in the future.
5. Inhibiting vegetal blastomeres revealed that sturgeons could utilize their yolk in an acellular form rather than YCs. However, it will be interesting to inhibit vegetal blastomeres of bowfin and bichir and compare them with sturgeon.
6. We have reported the gut development of the sturgeon for the first time. Furthermore, cross-species comparison revealed that sturgeon retained a unique mode of gut developmental pattern during the evolution of fishes.

References

- Ballard, W.W., 1986. Stages and rates of normal development in the holostean fish, *Amia calva*. *Journal of Experimental Zoology* 238, 337–354.
- Ballard, W.W., Needham, R.G., 1964. Normal embryonic stages of *Polyodon spathula* (Walbaum). *Journal of Morphology* 114, 465–477.
- Ballard, W.W., Ginsburg, A.S., 1980. Morphogenetic movements in acipenserid embryos. *Journal of Experimental Zoology* 213, 69–103.
- Baloch, A.R., Franěk, R., Saito, T., Pšenička, M., 2019a. Dead-end (dnd) protein in fish – a review. *Fish Physiology and Biochemistry* 47, 777–784.
- Baloch, A.R., Fu, M., Rodina, M., Metscher, B., Tichopád, T., Shah, M.A., Franěk, R., Pšenička, M., 2019b. Delivery of iron oxide nanoparticles into primordial germ cells in sturgeon. *Biomolecules* 333, 1–10.
- Beckham, Y.M., Nath, K., Elinson, R.P., 2003. Localization of RNAs in oocytes of *Eleutherodactylus coqui*, a direct developing frog, differs from *Xenopus laevis*. *Evolution and Development* 5, 562–571.
- Bolker, J.A., 1993. Gastrulation and mesoderm morphogenesis in the white sturgeon. *Journal of Experimental Zoology* 266, 116–131.
- Bolker, J.A., 1994. Comparison of gastrulation in frogs and fish. *Integrative and Comparative Biology* 34, 313–322.
- Buchholz, D.R., Singamsetty, S., Karadge, U., Williamson, S., Langer, C.E., Elinson, R.P., 2007. Nutritional endoderm in a direct developing frog : A Potential parallel to the evolution of the amniote egg. *Developmental Dynamics* 236, 1259–1272.
- Buddington, R.K., Doroshov, S.I., 1986. Structural and functional relations of the white sturgeon alimentary canal (*Acipenser transmontanus*). *Journal of Morphology* 190, 201–213.
- Caldwell, G.S., Olive, P.J.W.W., Bentley, M.G., 2002. Inhibition of embryonic development and fertilization in broadcast spawning marine invertebrates by water soluble diatom extracts and the diatom toxin 2-trans,4-trans decadienal. *Aquatic Toxicology* 60, 123–137.
- Caldwell, G.S., Bentley, M.G., Olive, P.J.W., 2004. First evidence of sperm motility inhibition by the diatom aldehyde 2 E , 4 E -decadienal. *Marine Ecology Progress Series*, 273, 97–108.
- Castellano, I., Ercolesi, E., Romano, G., Ianora, A., Palumbo, A., Palumbo, A., 2015. The diatom-derived aldehyde decadienal affects life cycle transition in the ascidian *Ciona intestinalis* through nitric oxide / ERK signalling. *Open Biology* 5: 140182. doi: 10.1098/rsob.140182.
- Chalmers Andrew, D., Slack, J.M.W., 2000. The *Xenopus* tadpole gut: fate maps and morphogenetic movements. *Development* 392, 381–392.
- Collazo, A., Keller, R., 2010. Early development of *Ensatina eschscholtzii*: an amphibian with a large, yolky egg. *EvoDevo* 1, 6. <http://www.evodevojournal.com/content/1/1/6>
- de Laat, S.W., Luchtel, D., Bluemink, J.G., 1973. The action of cytochalasin B during egg cleavage in *Xenopus laevis*: Dependence on cell membrane permeability. *Developmental Biology* 31, 163–177.
- Elinson, R.P., 2009. Nutritional endoderm: A way to breach the holoblastic-meroblastic barrier in tetrapods. *Journal of Experimental Zoology Part B: Molecular and Developmental Evolution* 312B, 526–532.
- Elinson, R.P., Sabo, M.C., Fisher, C., Yamaguchi, T., Orii, H., Nath, K., 2011. Germ plasm in *Eleutherodactylus coqui*, a direct developing frog with large eggs. *EvoDevo* 2, 20. <http://www.evodevojournal.com/content/2/1/20>

- Frankenberg, E., 2012. Vertebrate intestinal endoderm development. *Developmental Dynamics* 240, 501–520.
- Gilbert, S.F., 2010. *Developmental Biology*, Developmental Biology, Ninth ed. Sinauer Associates, Oxford University Press.
- Ginsburg, A.S., Dettlaff, T.A., 1991. The Russian sturgeon *Acipenser güldenstädti*. Part I. Gametes and Early Development up to Time of Hatching. In: Dettlaff, T.A., Vassetzky, S.G. (Eds), *Animal Species for Developmental Studies* Springer, Boston, pp. 15–65.
- Gisbert, E., Sarasquete, M.C., Williot, P., Castello-Orvay, F., Castelló-Orvay, F., 1999. Histochemistry of the development of the digestive system of Siberian sturgeon during early ontogeny. *Journal of Fish Biology* 55, 596–616.
- Haccard, O., Sarcevic, B., Lewellyn, A., Hartley, R., Roy, L., Izumi, T., Erikson, E., Maller, J.L., 1993. Induction of metaphase arrest in cleaving *Xenopus* embryos by MAP kinase. *Science* 262, 1262–1265.
- Hansen, E., Even, Y., Genevière, A.M., 2004. The $\alpha,\beta,\gamma,\delta$ -unsaturated aldehyde 2-trans-4-trans-decadienal disturbs DNA replication and mitotic events in early sea urchin embryos. *Toxicological Sciences* 81, 190–197.
- Hara, Y., Merten, C.A., 2015. Dynein-based accumulation of membranes regulates nuclear expansion in *Xenopus laevis* egg extracts. *Developmental Cell* 33, 562–575.
- Hasley, A., Chavez, S., Danilchik, M., Wühr, M., Pelegri, F., 2017. Vertebrate embryonic cleavage pattern determination. *Advances in Experimental Medicine and Biology* 953, 117–171.
- Ianora, A., Zoologica, S., Dohrn, A., 2003. The effects of diatoms on copepod reproduction : A review. *Phycologia* 42, 351–363.
- Ikenishi, K., Kotani, M., Tanabe, K., 1974. Ultrastructural changes associated with UV irradiation in the “germinal plasm” of *Xenopus laevis*. *Developmental Biology* 36, 155–168.
- Kofron, M., Klein, P., Zhang, F., Houston, D.W., Schaible, K., Wylie, C., Heasman, J., 2001. The role of maternal axin in patterning the *Xenopus* embryo. *Developmental Biology* 237, 183–201.
- Korzhuev, P.A., Sharkova, L.B. 1967. On peculiarities of digestion of the Russian sturgeon in the Caspian Sea. In: Karzinkin, G.S. (Ed.), *Metabolism and Biochemistry of Fishes* Nauka, Moscow, pp. 205–209. (in Russian)
- Li, F.C., Wang, J., Wu, M.M., Fan, C.M., Li, X., He, J.M., 2017. Mitogen-activated protein kinase phosphatases affect UV-B-induced stomatal closure via controlling NO in guard cells. *Plant Physiology* 173, 760–770.
- Linhartová, Z., Saito, T., Kašpar, V., Rodina, M., Prášková, E., Hagihara, S., Pšenička, M., 2015. Sterilization of sterlet *Acipenser ruthenus* by using knockdown agent, antisense morpholino oligonucleotide, against dead end gene. *Theriogenology* 84, 1246–1255.
- Long, W.L., Ballard, W.W., 2001. Normal embryonic stages of the longnose gar, *Lepisosteus osseus*. *BMC Developmental Biology* 1: <http://www.biomedcentral.com/1471-213X/1/6>.
- Masui, Y., 2000. The elusive cytostatic factor in the animal egg. *Nature Reviews Molecular Cell Biology* 1, 228–231.
- Minarik, M., Stundl, J., Fabian, P., Jandzik, D., Metscher, B.D., Psenicka, M., Gela, D., Osorio-Pérez, A., Arias-Rodríguez, L., Horáček, I., Cerny, R., 2017. Pre-oral gut contributes to facial structures in non-teleost fishes. *Nature* 547, 209–212.
- Miralto, A., Barone, G., Romano, G., Poulet, S.A., Ianora, A., Russo, G.L., Buttino, I., Mazzarella, G., Laablr, M., Cabrini, M., Glacobbe, M.G., 1999. The insidious effect of diatoms on copepod reproduction. *Nature* 402, 173–176.

- Naraine, R., Iegorova, V., Abaffy, P., Franek, R., Soukup, V., Sindelka, R., 2022. Evolutionary conservation of maternal RNA localization in fishes and amphibians revealed by TOMO-Seq. *Developmental Biology* 489, 146–160.
- Pocherniaieva, K., Psenicka, M., Sidova, M., Havelka, M., Saito, T., Sindelka, R., Kaspar, V., 2018. Comparison of oocyte mRNA localization patterns in sterlet *Acipenser ruthenus* and African clawed frog *Xenopus laevis*. *Journal of Experimental Zoology Part B, Molecular and Developmental Evolution* 330, 181–187.
- Porter, A.G., Jänicke, R.U., 1999. Emerging roles of caspase-3 in apoptosis. *Cell Death and Differentiation* 6, 99–104.
- Romano, G., 2003. A marine diatom-derived aldehyde induces apoptosis in copepod and sea urchin embryos. *Journal of Experimental Biology* 206, 3487–3494.
- Romano, G., Costantini, M., Buttino, I., Ianora, A., Palumbo, A., 2011. Nitric oxide mediates the stress response induced by diatom aldehydes in the sea urchin *Paracentrotus lividus*. *PLoS ONE* 6, 2–10.
- Romano, G., Miralto, A., Ianora, A., 2010. Teratogenic effects of diatom metabolites on sea urchin *Paracentrotus lividus* embryos. *Marine Drugs* 8, 950–967.
- Rooney, R.D., Tuazon, P.T., Meek, W.E., Carroll, E.J., Hagen, J.J., Gump, E.L., Monnig, C.A., Lugo, T., Traugh, J.A., 1996. Mitogen-activated protein kinase. *Journal of Biological Chemistry* 271, 21498–21504.
- Ross, C., Boroviak, T.E., 2020. Origin and function of the yolk sac in primate embryogenesis. *Nature Communications* 11, 1–14.
- Rutz, J., Maxeiner, S., Juengel, E., Bernd, A., Kippenberger, S., Zöller, N., Chun, F.K.H., Blaheta, R.A., 2019. Growth and proliferation of renal cell carcinoma cells is blocked by low curcumin concentrations combined with visible light irradiation. *International Journal of Molecular Sciences* 20, 1–17.
- Sagata, N., Watanabe, N., Vande Woude, G.F., Ikawa, Y., 1989. The c-mos proto-oncogene product is a cytotostatic factor responsible for meiotic arrest in vertebrate eggs. *Nature* 342, 512–518.
- Saito, T., Psenicka, M., 2015. Novel technique for visualizing primordial germ cells in sturgeons (*Acipenser ruthenus*, *A. gueldenstaedtii*, *A. baerii*, and *Huso huso*). *Biology of Reproduction* 93, 1–7.
- Saito, T., Fujimoto, T., Maegawa, S., Inoue, K., Tanaka, M., Arai, K., Yamaha, E., 2006. Visualization of primordial germ cells *in vivo* using GFP-nos1 3'UTR mRNA. *International Journal of Developmental Biology* 50, 691–700.
- Saito, T., Pšenička, M., Goto, R., Adachi, S., Inoue, K., Arai, K., Yamaha, E., Pšenička, M., 2014. The origin and migration of primordial germ cells in sturgeons. *PLoS ONE* 9, e86861.
- Saito, T., Guralp, H., Iegorova, V., Rodina, M., Psenicka, M., 2018. Elimination of primordial germ cells in sturgeon embryos by ultraviolet irradiation†. *Biology of Reproduction* 99, 556–564.
- Shah, M.A., Fatira, E., Iegorova, V., Xie, X., Gela, D., Rodina, M., Franěk, R., Pšenička, M., Saito, T., 2022. Blastomeres derived from the vegetal pole provide extra-embryonic nutrition to sturgeon (*Acipenser*) embryos: Transition from holoblastic to meroblastic cleavage. *Aquaculture* 551, 737899.
- Shih, J., Keller, R., 1994. Gastrulation in *Xenopus laevis*: involution—a current view. *Seminars in Developmental Biology* 5, 85–90.
- Sindelka, R., Sidova, M., Svec, D., Kubista, M., 2010. Spatial expression profiles in the *Xenopus laevis* oocytes measured with qPCR tomography. *Methods* 51, 87–91.

- Takeuchi, M., Takahashi, M., Okabe, M., Aizawa, S., 2009. Germ layer patterning in bichir and lamprey; an insight into its evolution in vertebrates. *Developmental Biology* 332, 90–102.
- Tanaka, T., Ochi, H., Takahashi, S., Ueno, N., Taira, M., 2017. Genes coding for cyclin-dependent kinase inhibitors are fragile in *Xenopus*. *Developmental Biology* 426, 291–300.
- Tosti, E., Romano, G., Buttino, I., Cuomo, A., Ianora, A., Miralto, A., 2003. Bioactive aldehydes from diatoms block the fertilization current in ascidian oocytes. *Molecular Reproduction and Development* 66, 72–80.
- Valles, J.M., Jordan, W.B., Mowry, K.L., Lin, K., Denegre, J.M., 2002. Cleavage planes in frog eggs are altered by strong magnetic fields. *Proceedings of the National Academy of Sciences* 99, 14729–14732.
- Yew, N., Oskarsson, M., Daar, I., Blair, D.G., Vande Woude, G.F., 1991. *mos* gene transforming efficiencies correlate with oocyte maturation and cytotostatic factor activities. *Molecular and Cellular Biology* 11, 604–610.
- Zorn, A.M., Wells, J.M., 2009. Vertebrate endoderm development and organ formation. *Annual Review of Cell and Developmental Biology* 25, 221–251.

English summary

A vertebrate embryo's cleavage pattern is either holoblastic (complete) or meroblastic (partial). Holoblastic cleavage is thought to be ancestral to vertebrates and is most likely to occur in amphibians, mammals, and chondrosteans. Meroblastic cleavage has evolved five times in vertebrate lineages, including hagfish, elasmobranchs, coelacanth, teleosts, and amniotes. In holoblastic cleavage (as in *Xenopus laevis* embryos), all blastomeres contribute to one of the germ layers. On the contrary, in meroblastic cleavage pattern (as in teleosts and amniotes – including birds and reptiles), only the animal pole contributes the formation of the germ layers. The transition from holoblastic to meroblastic is usually occurred by an increase in egg size in comparison to the lineage's ancestral state. For example, the embryos of several frog and non-teleost fish species, cleaved holoblastically, but due to increased egg size and yolk volume, vegetal pole is considered to be incompatible with cell division and has altered cleavage pattern and formation of germ layers.

Sturgeons are called living fossils and belong to the actinopterygian lineage, evolved about 200 million years ago (mya). Their eggs are 2 x larger than that of *X. laevis*. Despite the variation in sizes, their embryos retain nearly characteristics the same as that of *X. laevis*. Nevertheless, vegetal blastomeres of sturgeons are bigger and divide slower than that of *X. laevis*. It was speculated that vegetal blastomeres of sturgeon are extraembryonic as in yolk of teleost (zebrafish) and Yolk cells of (YCs) of bichir – earliest diverged living group of actinopterygian fishes, agnathan lampreys (Petromyzontidae) – an extant lineage of jawless fishes and an anuran – *Eleutherodactylus coqui*. Furthermore, the gut development pattern of sturgeon (Acipenser) and its evolutionary conservation was poorly understood so far. Thus, in this study, we have investigated the fate-mapping of sturgeon's vegetal blastomeres and gut development and compare it to that of other taxa.

First, to develop the robust technique for specific blastomeres inhibition of sturgeon embryos, we have used diatoms-derived polyunsaturated aldehydes, 2, 4-Decadienal (DD; a model aldehyde for experimental studies). The sturgeon's embryos were injected with optimal DD percentage (0.01 v/v) and subsequently irradiating them by visible light (91.15–44.86 W m²). Notably, DD plus light, and not DD injection or light irradiation alone can inhibit cleavage. Furthermore, qPCR-tomography revealed that localized pattern of maternal mRNA remained constant through animal-vegetal axis in partially cleaved embryos when compared to normal.

Second, we continued with fate-mapping of sturgeon vegetal blastomeres. We found that these blastomeres gave rise to primordial germ cells (PGCs), and the rest of the descendants were vegetal yolk cells. Plastic section histology showed that the nuclei of vegetal yolk cells sharply declined as embryos developed. When the cleavage of the vegetal pole was inhibited, embryogenesis continued, without producing the vegetal yolk cells. The acellular yolk mass was similar to the modern teleost (e.g., zebrafish). In addition, RT-qPCR and BrdU pulse revealed that yolk cells become transcriptionally inactive after mid-blastula transition. Here, our results suggested that the meroblastic cleavage in actinopterygian lineage had evolved by the fusion of vegetal blastomeres, which is parallel to the closely related group, e.g., gar (Lepisosteidae), that evolved at approximately 57 mya.

Lastly, we continued the observation of sturgeon gut development and its comparison with other taxa including holoblastic (*X. laevis*, bichir, and mice) and meroblastic (chicks, gars, and zebrafish) representatives. For this purpose, we used histology, in-situ hybridization (HCR), and Immunohistochemistry. We found that sturgeon's endodermal cells formed the Archenteron (primitive gut) as frog and bichir. However, these cells continued to proliferate lateroventrally to encompass a massive amount of yolk mass to give rise "yolk inside the gut." Cross-species

comparison revealed that sturgeon retained a unique mode of gut developmental pattern during vertebrate evolution, which is not conserved with any vertebrates including those that retained holoblastic or evolved meroblastic cleavage pattern.

In conclusion, our current findings suggest that sturgeon embryo development represents a distinct transition from holoblastic to meroblastic cleavage, as well as a distinct archaic mode of gut-endoderm development.

Czech summary

Rýhování embrya obratlovců je buď holoblastické (úplné) nebo meroblastické (částečné). Holoblastické rýhování je považováno za původní u obratlovců a vyskytuje se u obojživelníků, savců a chrupavčitých ryb. Meroblastické rýhování se v linii obratlovců vyvinulo pětkrát, včetně sliznatek, příčnoústých, latimérií, kostnatých ryb a amniot. Při holoblastickém rýhování (jako u embryí *Xenopus laevis*) přispívá každá blastomera k jedné ze zárodečných linií. Naopak při meroblastickém způsobu rýhování (jako u kostnatých a amniot – včetně ptáků a plazů) se na tvorbě zárodečných vrstev podílí pouze animální pól. K přechodu z holoblastického na meroblastický typ dochází obvykle zvětšením velikosti vajíčka ve srovnání se stavem ancestrální linie. Například embrya několika druhů žab a nekostnatých ryb se rýhovala holoblasticky, ale vzhledem ke zvětšené velikosti vajíčka a objemu žloutku je vegetativní pól považován za neslučitelný s buněčným dělením a má pozměněný způsob rýhování a tvorby zárodečných vrstev.

Jeseteři (*Acipenser*) jsou označováni za živoucí fosilie a patří do linie paprskoploutví, kteří se vyvinuli asi před 200 miliony let. Jejich jikry jsou 2× větší než jikry *X. laevis*. Navzdory rozdílné velikosti si jejich embrya zachovávají téměř stejné vlastnosti jako embrya *X. laevis*. Nicméně vegetativní blastomery jeseterů jsou větší a dělí se pomaleji než u *X. laevis*. Byla vyslovena domněnka, že vegetativní blastomery jeseterů jsou extraembryonální jako žloutek kostnatých ryb (dánio pruhované) a žloutkové buňky bichirů – nejstarší divergentní žijící skupiny paprskoploutvích ryb, mihulí (*Petromyzontidae*) – zachovalé linie bezčelistnatých ryb a žáby – *Eleutherodactylus coqui*. Kromě toho byl dosud nedostatečně prozkoumán způsob vývoje střeva jeseterů a jeho evoluční konzervace. V této studii jsme proto mapovali vývoj vegetativních blastomer a střev jeseterů a porovnávali je s jinými taxony.

Nejprve jsme pro vývoj robustní techniky specifické inhibice blastomer embryí jeseterů použili polynenasycené aldehydy odvozené od rozsivek, 2, 4-dekadienal (DD; modelový aldehyd pro experimentální studie). Embryím jeseterů jsme aplikovali optimalizované množství DD (0,01 v/v) a následně je ozařovali viditelným světlem (91,15–44,86 W m²). Pozoruhodné je, že DD plus světlo, a nikoliv samotná injekce DD nebo ozáření světlem, mohou inhibovat rýhování. Kromě toho qPCR-tomografie odhalila, že lokalizace maternální mRNA zůstává u částečně se rýhujících embryích ve srovnání s normálními v ose animálního-vegetativního pólu konstantní.

Ve druhé studii jsme pokračovali v mapování vývoje vegetativních blastomer jeseterů. Zjistili jsme, že z těchto blastomer vznikají primordiální zárodečné buňky (PGC) a zbytek blastomer tvořily vegetativní žloutkové buňky. Histologie plastických řezů odhalila, že jádra vegetativních žloutkových buněk se během vývoje embryí výrazně zmenšovala. Když bylo rýhování vegetativního pólu inhibováno, embryogeneze pokračovala, aniž by se vytvořily vegetativní žloutkové buňky. Acelulární žloutková hmota byla podobná jako u moderních kostnatých ryb (např. dánií). RT-qPCR a pulz BrdU navíc odhalily, že žloutkové buňky se po MBT stávají transkripčně neaktivními. Naše výsledky zde naznačují, že meroblastické rýhování paprskoploutvích se vyvinulo fúzí vegetativních blastomer, což je paralelní s blízce příbuznou skupinou, např. kostlínů (*Lepisosteidae*), která se vyvinula přibližně před 57 miliony let.

Nakonec jsme pokračovali ve sledování vývoje střeva jeseterů a jeho srovnání s dalšími taxony včetně holoblastických (*X. laevis*, bichir a myš) a meroblastických (kuře, kostlín a dánio) zástupců. K tomuto účelu jsme použili histologii, *in-situ* hybridizaci (HCR) a imunohistochemii. Zjistili jsme, že endodermální buňky jeseterů tvoří archenteron (primitivní střevo) jako u žab a bichirů. Tyto buňky však pokračovaly v lateroventrální proliferaci, aby obklopily obrovské množství žloutkové hmoty a daly vzniknout "žloutku uvnitř střeva". Mezdruhové srovnání ukázalo, že jeseteři si během evoluce obratlovců zachovali jedinečný způsob vývoje střeva,

který se nezachoval u žádného obratlovce včetně těch, kteří si zachovali holoblastické nebo se u nich vyvinulo meroblastické rýhování.

Závěrem lze říci, že naše současná zjištění naznačují, že vývoj embrya jeseterů představuje odlišný přechod od holoblastického k meroblastickému šrýhování a také odlišný archaický způsob vývoje střevního endodermu.

Acknowledgments

My heartfelt gratitude goes to my thesis advisor, Assoc. Prof. Martin Pšenička. The door to Martin office was always open whenever I ran into a trouble spot or had a question about my research or writing. He consistently let me do my own research while directing me in the right direction when he thought I needed it. My studies and research work would not have been this smooth without favorable living and working conditions in the laboratory of germ cell. I would also like to thank my lab members and fellow students for providing me with a warm and friendly environment in which to work during my research, particularly Roman Franěk, Tomáš Tichopád, Fučíková Michaela and Xuan Xie, as well as other lab mates. Beside our research, the university administration and international students' office staff has always helped me whenever required. I would like to thank the administration staff for all their help and support.

No words are enough to thank my parents without whose blessings I would not achieve this in my life. My brothers and sisters have always been the pillars of strength for me, especially my elder brother Syed Shabeer Hassan Rashdi, who has been my guiding star since forever. This accomplishment would not have been possible without his unfailing support and continuous encouragement throughout my life and through the process of researching and writing this thesis. A special mention goes to the little kids in my family, who has always rejuvenated me with their talks, when I was tired and exhausted of my studies and research work. I am very thankful to all my friends who have supported me along the way. A special acknowledgement goes to my best friend and elder sister Dr. Rehana Shahnawaz.

I am also thankful for the financial support from following research funding agencies.

- Czech Science Foundation (20-23836S).
- Grant Agency of the University of South Bohemia (019/2021/Z).
- Grant Agency of the University of South Bohemia (036/2020/Z).
- Ministry of Education, Youth and Sports of the Czech Republic project CENAKVA (LM2018099).
- Biodiversity (CZ.02.1.01/0.0/0.0/16_025/0007370).

List of publications

Peer-reviewed journals with IF

- Franěk, R., Cheng, Y., Fučíková, M., Kašpar, V., Xie, X., **Shah, M.A.**, Linhart, O., Šauman, I., Pšenička, M., 2022. Who is the best surrogate for germ stem cell transplantation in fish? *Aquaculture* 549: 737759. (IF 2021 = 5.135)
- Raza, S.H., Abdelnour, S.A., Alotaibi, M.A., AlGabbani, Q., Naiel, M.A., Shokrollahi, B., Noreldin, A.E., Jahejo, A.R., **Shah, M.A.**, Alagawany, M., Zan, L., 2022. MicroRNAs mediated environmental stress responses and toxicity signs in teleost fish species. *Aquaculture* 546: 737310. (IF 2021 = 5.135)
- Shah, M.A.**, Iegorova, V., Rodina, M., Franěk, R., Tichopád, T., Pšenička, M., Saito, T., 2022. Blastomeres derived from the vegetal pole provide extra-embryonic nutrition to sturgeon (*Acipenser*) embryos: transition from holoblastic to meroblastic cleavage. *Aquaculture* 551: 737899. (IF 2021 = 5.135)
- Franěk, R., Kašpar, V., **Shah, M.A.**, Gela, D., Pšenička, M., 2021. Production of common carp donor-derived offspring from goldfish surrogate broodstock. *Aquaculture* 534: 736252. (IF 2021 = 5.135)
- Shah, M.A., Saito, T., Šindelka, R., Iegorova, V., Rodina, M., Baloch, A.R., Franěk, R., Tichopád, T., Pšenička, M., 2021. Novel technique for definite blastomere inhibition and distribution of maternal RNA in sterlet *Acipenser ruthenus* embryo. *Fisheries Science* 87: 71–83. (IF 2021 = 2.148)
- Xie, X., Tichopád, T., Kislik, G., Langerová, L., Abaffy, P., Šindelka, R., Franěk, R., Fučíková, M., Steinbach, C., **Shah, M.A.**, Šauman, I., Pšenička, M., 2021. Isolation and characterization of highly pure type A spermatogonia from sterlet (*Acipenser ruthenus*) using flow-cytometric cell sorting. *Frontiers in Cell and Developmental Biology* 9: 772625. (IF 2021 = 6.081).
- Baloch, A.R., Fučíková, M., Rodina, M., Metscher, B., Tichopád, T., **Shah, M.A.**, Franěk, R., Pšenička, M., 2019. Delivery of iron oxide nanoparticles into primordial germ cells in sturgeon. *Biomolecules* 9: 333. (IF 2019 = 4.082)

Abstracts and conference proceedings

- Shah, M.A.**, Pšenička, M., 2019. The development of a novel technique for partial cleavage inhibition on sturgeon embryo model. 7th International Workshop on the Biology of Fish Gametes 2019, Rennes, France.

Training and supervision plan during study	
Name	Mujahid Ali Shah
Research department	2019–2022 – Laboratory of Germ Cell of FFPW
Supervisor	Assoc. Prof. Pšenička Martin
Period	21 st January 2019 until 15 th September 2022
Ph.D. courses	Year
Applied hydrobiology	2019
Pond aquaculture	2020
Biostatistics	2020
Basic of scientific communication	2020
Ichthyology and fish taxonomy	2021
English language	2021
Scientific seminars	Year
Seminar days of RIFCH and FFPW	2019
	2020
	2021
	2022
International conferences	Year
Shah, M.A., Pšenička, M., 2019. The development of a novel technique for partial cleavage inhibition on sturgeon embryo model. 7th International Workshop on the Biology of Fish Gametes 2019, Rennes, France.	2019
Foreign stays during Ph.D. study at RIFCH and FFPW	Year
South Ehime Fisheries Research Institute, Ehime University, Japan. 1–32, 10, 2019	2019
Institute of Animal Science, Department of Ichthyology and Biotechnology in Aquaculture, Warsaw University of Life Science, Poland. 8. 11. 21 – 8. 1. 2022	2021
Pedagogical activities	Year
Consultation of thesis Ph.D. student Rigolin Nayak	2020–
Teaching of 90 hour on microinjection and microscopy, Plastic section histology	2022

Curriculum vitae**PERSONAL INFORMATION**

Name: Mujahid Ali
Surname: Shah
Title: M.Sc.
Born: 20th March 1993
Nationality: Pakistan
Languages: English and Urdu
Contact: mshah@frov.jcu.cz, mujahidalishah512@gmail.com

**RESEARCH INTEREST**

Developmental biology, Genetic and reproduction

EDUCATION

2019 – present Ph.D. Zootechnics (Fisheries), Faculty of Fisheries and Protection of Waters, University of South Bohemia, Czech Republic.
 2016–2018 M.Sc. Biology (Animal genetics, Breeding and reproduction), School of Life Science and Engineering, Southwest University of Science and Technology, Mianyang 621010, Sichuan, China.
 2011–2016 DVM (Doctor of Veterinary Medicine), Sindh Agriculture University Tandojam, Sindh-Pakistan.

PROFESSIONAL EXPERIENCE

6–8/2016 Work as a veterinary practitioner at private clinic, T. jam, Sindh, Pakistan
 6–7/2014 Teaching biology at private education centre, T. jam, Sindh, Pakistan

COMPLETED COURSES

Applied hydrobiology, Pond aquaculture, Biostatistics Basic of scientific communication, Ichthyology and Fish taxonomy, English language

RESEARCH STAY AND COLLABORATIONS

1. 10 – 31. 10. 2019 South Ehime Fisheries Research Institute, Ehime University, Japan.
 8. 11 – 8. 1. 2022 Institute of Animal Science, Department of Ichthyology and Biotechnology in Aquaculture, Warsaw University of Life Science, Poland.